Unclassified **NEA/NSC/DOC(2013)7**

Organisation de Coopération et de Développement Économiques
Organisation for Economic Co-operation and Development **30-May-2013**

English - Or. English

NUCLEAR ENERGY AGENCY
NUCLEAR SCIENCE COMMITTEE

NEA/NSC/DOC(2013)7
Unclassified

Benchmarks for uncertainty analysis in modelling (UAM) for the design, operation and safety analysis of LWRs

Volume I: Specification and Support Data for Neutronics Cases (Phase I)

JT03340502

English - Or. English

NUCLEAR ENERGY AGENCY

NUCLEAR SCIENCE COMMITTEE
NEA COMMITTEE ON SAFETY OF NUCLEAR INSTALLATIONS

BENCHMARKS FOR UNCERTAINTY ANALYSIS IN MODELLING (UAM) FOR THE DESIGN, OPERATION AND SAFETY ANALYSIS OF LWRs

Volume I: Specification and Support Data for Neutronics Cases (Phase I)

Version 2.1 (Final Specifications)

K. Ivanov, M. Avramova, S. Kamerow

I. Kodeli, E. Sartori, E. Ivanov, O. Cabellos

May 2013

OECD Nuclear Energy Agency

Foreword

In recent years there has been an increasing demand from nuclear research, industry, safety and regulation for best-estimate predictions to be provided with their confidence bounds. Consequently an "in-depth" discussion on "Uncertainty Analysis in Modelling" was organised at the 2005 OECD/NEA Nuclear Science Committee (NSC) meeting, which led to a proposal for launching an Expert Group on "Uncertainty Analysis in Modelling" and endorsing the organisation of a workshop with the aim of defining future actions and a programme of work.

As a result the NEA/OECD Uncertainty Analysis in Modelling (UAM) workshop took place in Pisa, Italy on April 28-29, 2006. The major outcome of the workshop was to prepare a benchmark work programme with steps (exercises) that would be needed to define the uncertainty and modelling tasks. The other proposals made during the meeting were to be incorporated under the different steps (exercises) within the overall benchmark framework for the development of uncertainty analysis methodologies for multi-physics (coupled) and multi-scale simulations.

Following the results of the UAM-2006 workshop, the OECD/NEA NSC at its June 2006 meeting endorsed the creation of an Expert Group on Uncertainty Analysis methods in Modelling (EGUAM) under the auspices of the Working Party on Scientific Issues in Reactor Systems (WPRS). Since the Expert Group addresses multi-scale/multi-physics aspects of uncertainty analysis, it works in close co-ordination with the benchmark groups on coupled neutronics/thermal-hydraulics simulations and on coupled core-plant problems. It also co-ordinates its activities with the Group on Analysis and Management of Accidents (GAMA) of the Committee on Safety of Nuclear Installations (CSNI). The Expert Group has the following mandate:

1. To elaborate a state-of-the-art report on current status and needs of sensitivity and uncertainty analysis (SA/UA) in modelling, with emphasis on multi-physics (coupled) and multi-scale simulations.
2. To identify the opportunities for international co-operation in the uncertainty analysis area that would benefit from co-ordination by the NEA/NSC.
3. To create a roadmap along with a schedule and organisation for the development and validation of methods and codes required for uncertainty analysis including the benchmarks adequate to meet those goals.

The NEA/NSC has endorsed this activity to be undertaken with the Pennsylvania State University (PSU) as the main co-ordinator and host with the assistance of the Scientific Board. The NSC/NEA has renewed and updated the mandate of the EGUAM at the beginning of February 2011. The expert group will provide advice to the WPRS and the nuclear community on the scientific development needs (data and methods, validation experiments, scenario studies) of sensitivity and uncertainty methodology for modelling of different reactor systems and scenarios.

The main activity will be focused on uncertainties in modelling LWR transients. In this context the objectives will be:

a) To determine modelling uncertainties for reactor systems under steady-state and transient conditions, quantifying the impact of uncertainties for each type of calculation in the multi-physics analysis, i.e.
    a. neutronics calculations;
    b. thermal hydraulics modelling;
    c. fuel behaviour.
b) For each of these types of calculation the major sources of uncertainty will be determined, arising from:
    a. data (e.g. nuclear data, geometry, materials);

   b. numerical methods;
   c. physical models;

c) To develop and test methods for combining the above sources of uncertainty for each type of calculation so as to yield uncertainty assessment for the coupled multi-physics analyses;
d) To develop a benchmark framework, which combines information from available integral facility and NPP experimental data with analytical and numerical benchmarking;
e) Where available, experimental data will be used to test the individual types of calculation as well coupled multi-physics simulations.

To summarise, in addition to LWR best-estimate calculations for design and safety analysis, the modelling aspects of Uncertainty Analysis (UA) and Sensitivity Analysis (SA) are to be further developed and validated on scientific grounds in support of their performance. There is a need for efficient and powerful UA and SA methods suitable for such complex coupled multi-physics and multi-scale simulations. The proposed benchmark sequence will address this need by integrating the expertise in reactor physics, thermal-hydraulics and reactor system modelling as well as uncertainty and sensitivity analysis, and will contribute to the development and assessment of advanced/optimised uncertainty methods for use in best-estimate reactor simulations. Such an effort can be undertaken within the framework of a programme of international co-operation that would benefit from the co-ordination of the NEA/NSC and from interfacing with the CSNI activities. More information can be found at: http://www.oecd-nea.org/science/wprs/egrsltb/UAM/.

Version 2.0 of the Volume I: Specification and Support Data for Neutronics Cases (Phase I) of the OECD LWR UAM benchmark is based on Version 1.0 (issued in December 2007) and incorporates suggestions and corrections proposed by the benchmark participants at the following meetings:

- UAM-2 workshop, held in Garching, Germany, 2-4 April 2008;
- UAM-3 workshop, held in Pennsylvania, USA, 29 April-1 May 2009;
- UAM-4 workshop, held in Pisa, Italy, 14-16 April 2010;
- UAM-5 workshop, held in Stockholm, Sweden, 13-15 April 2011.

The information in this document is subject to future changes in anticipation of new releases of covariance data libraries, new findings or modelling tools. For reference purposes, the information and suggestions from each workshop are only added to the previous Version 1.0 without significant deletions of text from the earlier version.

This publication (Version 2.1) has incorporated the following changes from the previously released specifications (Version 2.0).

- Figure 11 (GEN-III Type 3): In the legend of the figure, the enrichment of the UOX fuel rods (white) has been changed from 4.2% to 3.2% in order to match the figure's caption which had correctly stated the enrichment as 3.2%. The position of the two Gd pins (orange) has been changed in order to achieve assembly symmetry. Horizontal nomenclature has been updated in order to avoid the use of the letters “I” and “O” and confusion with the numbers “1” and “0”.

- Figure 26: The position of the bottom-most right-hand-side control rod bank 1 has been corrected in order to achieve core symmetry.

Acknowledgements

The authors would like to thank the ORNL team - Cecil V. Parks, Stephen M. Bowman, Mark L. Williams, Jess C. Gehin; James R. Felty from DOE and J Blair Briggs from INL for arranging the release of the SCALE 5.1 and SCALE 6.0 covariance libraries for the purposes of the OECD LWR UAM benchmark. Their support and help in establishing and carrying out this benchmark are invaluable.

We wish to acknowledge here the special contributions provided by Alain Santamarina and Claire Vaglio-Gaudard from CEA on the PWR Generation III assembly and core models: UOX core and MOX core specifications.

Special appreciation goes to the report reviewers, which are the members the Scientific Board of UAM Expert Group:

Scientific Board and Technical Committee

Name	***Organisation***	***Country***	***Role***
Kostadin IVANOV	PSU	USA	Co-ordination and host
Thomas DOWNAR	U-Michigan	USA	Member
Yassin HASSAN	Texas A&M	USA	Member
Mark WILLIAMS	ORNL	USA	Member
Martin ZIMMERMANN	PSI	Switzerland	Member
Akitoshi HOTTA	TEPSYS	Japan	Member
Francesco D'AURIA	U-Pisa	Italy	Member
Tomasz KOZLOWSKI	U-Illinois	USA	Chair of EGUAM, NSC
Sören KLIEM	HZDR	Germany	Member
Andreas PAUTZ	GRS	Germany	Member
Eric ROYER	CEA	France	Member
Hideaki UTSUNO	JNES	Japan	Member
Maria AVRAMOVA	PSU	USA	Member
Ivo KODELI	IJS	Slovenia	Member
Enrico SARTORI	Consultant	France	Member
Jim GULLIFORD	OECD/NEA		Secretariat

The authors wish to express their sincere appreciation for the outstanding support offered by Professor F. D'Auria (U-Pisa), Dr. S. Langenbuch (GRS), and E. Royer (CEA) by preparing a document on the expected impact and benefits of the OECD LWR UAM benchmark activity for LWR safety and licensing Technology Relevance of the "Uncertainty Analysis In Modelling" Project for Nuclear Reactor Safety, NEA/NSC/DOC (2007)15.

This publication is dedicated to the memory of Professor José María Aragonés Beltrán and graduate student Sophia Kamerow. Professor José Aragonés was Full Professor and Chair in Nuclear Physics, Professor of Mechanical Engineering in the Department of Nuclear Engineering (DIN), College of Industrial Engineering (ETSI-Industriales), Polytechnic University of Madrid (UPM). He was Head of the R&D Group for Nuclear Analysis at the UPM, Delegate for Spain in the OECD/NEA Nuclear Science Committee, Member of the International Academy of Nuclear Energy (INEA), Member of the Scientific Council of the Directorate on Nuclear Energy (DEN) of CEA, France, and Executive Committee member in European Projects: NURESIM and NURISP. He has contributed and supported strongly the development of OECD/NEA coupled code and uncertainty analysis benchmarks.

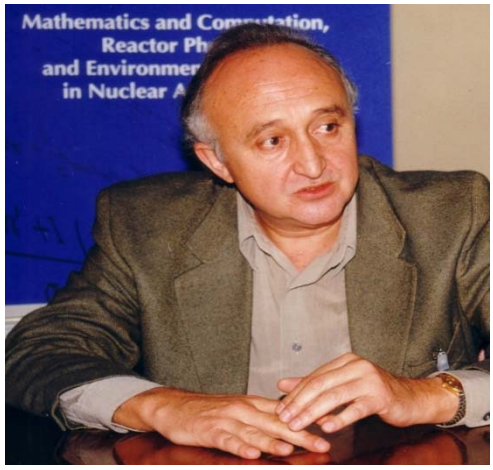

José María Aragonés Beltrán
1947-2010

Sophia Kamerow was a graduate student at Nuclear Engineering Programme at the Pennsylvania State University (PSU), US. She completed both her BS and MS degrees at PSU and she was on her way to obtain a PhD in Nuclear Engineering at PSU. She was the graduate student working on the Phase I of the OECD LWR UAM benchmark activity and she has contributed to both preparing the Specifiaction on Phase I and the analysis of reference and partcipants'results submitted for the different exercises of Phase I.

Sophia Kamerow
1967-2011

TABLE OF CONTENTS

FOREWORD 3
ACKNOWLEDGEMENTS 5
LIST OF FIGURES 9
LIST OF TABLES 11
CHAPTER 1: INTRODUCTION 12
1.1 OBJECTIVE 12
1.2 DEFINITION OF BENCHMARK PHASES AND EXERCISES 13
1.3 CONTENT OF THIS DOCUMENT 14
CHAPTER 2: DEFINITION OF EXERCISE I-1: CELL PHYSICS 16
2.1 STATUS OF NUCLEAR DATA COVARIANCE INFORMATION 16
2.2 MULTI-GROUP PROCESSING OF NUCLEAR AND COVARIANCE DATA 21
2.3 COVARIANCE DATA AND TOOLS DISTRIBUTED FOR THE UAM PHASE I PROJECT 23
2.4 TEST PROBLEMS 29
CHAPTER 3: DEFINITION OF EXERCISE I-2: LATTICE PHYSICS 37
3.1 DISCUSSION OF INPUT, PROPAGATED, AND OUTPUT UNCERTAINTIES 37
3.2 TEST PROBLEMS 40
CHAPTER 4: DEFINITION OF EXERCISE I-3: CORE PHYSICS 54
4.1 DISCUSSION OF INPUT, PROPAGATED AND OUTPUT UNCERTAINTIES 54
4.2 TEST PROBLEMS 55
CHAPTER 5: REQUESTED OUTPUT 79
5.1 INTRODUCTION 79
5.2 RESULTS FOR EXERCISE I-1 79
5.3 RESULTS FOR EXERCISE I-2 81
CHAPTER 6: CONCLUSIONS 89
REFERENCES 91
APPENDIX I: LIST OF NUCLIDES WITH COVARIANCE INFORMATION IN 44GROUPV5COV SET 95
APPENDIX II: LIST OF NUCLIDES WITH COVARIANCE INFORMATION IN 44GROUPV6COV SET 96
APPENDIX III: LIST OF NUCLIDES WITH COVARIANCE INFORMATION IN 44GROUPV5REC SET 97
APPENDIX IV: LIST OF NUCLIDES WITH COVARIANCE INFORMATION IN 44GROUPV6REC SET 99
APPENDIX V: THE 44-GROUP STRUCTURE 101

APPENDIX VI: ANGELO AND LAMBDA DESCRIPTION 102
APPENDIX VII: PERTURBATION THEORY AND KINETIC PARAMETERS UNCERTAINTY PROPAGATION 109
APPENDIX VIII: PWR BURN-UP PIN-CELL BENCHMARK 124

List of Figures

1: Calculation of one-group effective cross-section uncertainty 30
2: Depiction of 44-group covariance matrix, weighting factor matrices and, uncertainty matrix 30
3: Configuration of PB-2 BWR unit cell 31
4: Configuration of TMI-1PWR unit cell 32
5: Configuration of Kozloduy-6 VVER-1 000 unit cell 32
6: PB-2 assembly design - Type 2 initial fuel and lattice 41
7: PB-2 assembly design - Type 2 initial lattice 42
8: Control rod blade model and characteristics for PB-2 43
9: TMI-1 assembly design and data 44
10: Kozloduy-6 VVER-100 assembly design and data 45
11: GEN-III Assembly descriptions 48
12: PB-2 radial reflector model – dimensions and material compositions 49
13: TMI radial reflector model – dimensions and material compositions 50
14: Kozloduy-6 radial reflector model – dimensions and material compositions 50
15: Color-set configuration for PB-2 51
16: Color-set configuration for TMI-1 51
17: Color-set configuration for Kozloduy-6 52
18: PB-2 reactor core cross-sectional view 56
19: PB-2 initial core loading 57
20: PB-2 assembly design - Type 1 initial fuel 58
21: PB-2 assembly design - Type 2 initial fuel 58
22: PB-2 assembly design - Type 3 initial fuel 59
23: PB-2 - axial variation of the fuel composition 60
24: Elevation of core components for PB-2 61
25: PB-2 - core orificing and TIP system arrangement 62
26: TMI-1 reactor core cross-sectional view and characteristics 63
27: TMI-1 – definition of fuel assembly types 64
28: TMI-1 assembly design with 8 Gd pins 65
29: Kozloduy-6 reactor core cross-sectional view and characteristics 66
30: Kozloduy-6 – control rod arrangement 67
31: Kozloduy-6 – core loading 68
32: GEN-III UOX core 71
33: GEN-III MOX core 72
34: Vertical cut of benchmark models for SNEAK 7A and SNEAK 7B assemblies [66] 74
35: SNEAK 7A R-Z Model [66] 74
36: SNEAK 7B R-Z Model [66] 75
37: SNEAK 7A 3D heterogeneous model [66] 76
38: SNEAK 7B 3D heterogeneous model [66] 77
39: Output sample of Exercise 1 80
40: Sample output for core power distribution associate uncertainties 82
41: Form for radial power distribution for PB-2 BWR results 84
42: Form for axial power distribution for PB-2 BWR results 84
43: Form for radial power distribution for TMI-1 PWR results 86
44: Form for axial power distribution for TMI-1 PWR results 86
45: Form for radial power distribution for Kozloduy-6 results 88
46: Form for axial power distribution for Kozloduy-6 results 88

A.1: The SNEAK 7A U matrices for group-wise ^{238}U and ^{239}Pu fission for Λ_{eff} analysis 113
A.2: The SNEAK 7A U matrices for group-wise ^{238}U and ^{239}Pu capture for Λ_{eff} analysis 113
A.3: The SNEAK 7A U matrices for group-wise $^{\mathbf{238}}U$ and $^{\mathbf{239}}Pu$ fission spectra for β_{eff} analysis..... 114
A.4: The SNEAK 7A U matrices for group-wise ^{238}U and ^{239}Pu nu-bar for Λ_{eff} analysis..... 114
A.5: The SNEAK 7B U matrices for group-wise ^{238}U and ^{239}Pu fission for Λ_{eff} analysis..... 115
A.6: The SNEAK 7B U matrices for group-wise ^{238}U and ^{239}Pu capture for Λ_{eff} analysis..... 115
A.7: The SNEAK 7B U matrices for group-wise ^{238}U and ^{239}Pu nu-bar for Λ_{eff} analysis..... 116
A.8: The SNEAK 7B U matrices for group-wise ^{238}U and ^{239}Pu fission spectra for Λ_{eff} analysis 116
A.9: The χ-covariance for $^{\mathbf{239}}Pu$ (a) and $^{\mathbf{238}}U$ (b) 118
A.10: The sensitivity to χ for ^{239}Pu, ^{238}U in SNEAK 7A and for ^{235}U in a thermal reactor 119
A.11: The Configuration of unit-cell..... 125

List of Tables

1: Number of materials and cross-sections with covariances of neutron cross-sections 19
2: Nuclides and materials present in TMI-1 PWR core calculations 19
3: Nuclides and materials present in PB-2 BWR core calculations 20
4: Nuclides and materials present in Kozloduy-6 VVER-1 000 core calculations 20
5: Priority list of important nuclides 20
6: Number of nuclides and energy groups in the available multi-group covariance matrices 22
7: The nuclides or materials (in ZA order) for which covariance data are provided in ZZ-SCALE5.1/COVA-44G 26
8: The nuclides or materials (in ZA order) for which covariance data are provided in ZZ-SCALE6/COVA-44G 27
9: Weight percent information from natural concentrations 33
10: Summary of critical configuration specifications 34
11: Specifications for KRITZ-2:1 LEU critical experiment 34
12: Specifications for KRITZ-2:13 LEU critical experiment 34
13: Specification for KRITZ-2.19 LEU critical experiment 35
14: Linear thermal expansion coefficients 38
15: PB-2 fuel assembly data 40
16: Additional TMI-1 assembly data 44
17: Kozloduy-6 assembly composition data 46
18: GEN-III unit cell information and operating conditions 46
19: Fuel and cladding composition data for GEN-III assemblies 47
20: PB-2 initial core loading information 57
21: TMI-1 composition of BP material 65
22: UOX/MOX core design 69
23: Zircaloy/He composition for the upper axial reflector 69
24: Stainless steel composition for the reflector 70
25: The materials for SNEAK 7A R-Z model, 10^{24} cm^{-3} [49] 75
26: The materials for SNEAK 7B R-Z model, 10^{24} cm^{-3} [49] 76
27: Atomic densities for SNEAK 7A rods, 10^{24} cm^{-3} [49] 77
28: Atomic densities for SNEAK 7B 3D homogenised model, 10^{24} cm^{-3} [49] 78
A.1: The main contributors to Λ_{eff} uncertainty for SNEAK 7A 114
A.2: The main contributors in Λ_{eff} uncertainty for SNEAK 7B 116
A.3: The main contributors in Λ_{eff} uncertainty for SNEAK 7A and 7B 117
A.4: Effective delayed neutron fraction uncertainty by variations of fission spectra, % 120
A.5: Effective delayed neutron fraction uncertainty by variations of fission balance, % 120
A.6: Benchmark data and expected due to cross-section errors 120
A.7: Sensitivity in beta-eff relative to the nuclear data 122
A.8: SNEAK-7A - Uncertainty (in %) in β_{eff} based on the covariance data from the JENDL-4 evaluation 122
A.9: SNEAK-7A - Uncertainty (in %) in β_{eff} based on the covariance data from the SCALE-6 library 123
A.10: Hot Full Power (HFP) conditions for fuel pin-cell test problem 124
A.11: Configuration of pin-cell test problem 124
A.12: Simplified operating history data for benchmark problem pin-cell calculation and specific power 125
A.13: Initial MCNP input 126
A.14: TRITON/SCALE input 127
A.15: SERPENT input 128
A.16: Benchmark nuclides 132

Chapter 1: Introduction

In addition to the establishment of light water reactor (LWR) best-estimate calculations for design and safety analysis, understanding uncertainties is important for introducing appropriate design margins and deciding where additional efforts should be undertaken to reduce uncertainties. The need of uncertainty evaluations for LWR best-estimate calculations was discussed and addressed within the framework of the CRISSUE-S international European Union (EU) Project [1] along with the identification of sources of uncertainties in coupled neutronics/thermal-hydraulics simulations. For this reason, the modelling aspects of Uncertainty Analysis (UA) and Sensitivity Analysis (SA) are to be further developed and validated on scientific grounds in support of their performance. In line with recent meetings the international expert community in reactor physics, thermal-hydraulics, and uncertainty and sensitivity analysis, has decided that a first step in this direction is to define an OECD benchmark for Uncertainty Analysis in Modelling (UAM) for design, operation, and safety analysis of LWRs [2] [3] [4]. The expected impact and benefits of the OECD LWR UAM benchmark activity for LWR safety and licensing are summarised in [5]. This benchmark project is challenging and responds to needs of estimating confidence bounds for results from simulations and analysis in real applications.

Reference LWR systems and scenarios for coupled code analysis are defined to study the uncertainty effects for all stages of the system calculations. Measured data from plant operation are available for the chosen scenarios. The existing OECD/NEA/NSC coupled code transient benchmarks – such as BWR Turbine Trip (TT) [6], PWR Main Steam Line Break (MSLB) [7], VVER-1 000 (V 1 000) Coolant Transients (CT) [8], BWR Full Bundle Test (BFBT) [9], PWR Sub-channel and Bundle Test (PSBT) [10] are used as part of the framework for adding uncertainty analysis methodologies in the best-estimate modelling for design and operation of LWRs. Such an approach facilitates the benchmark activities since many organisations have already developed input decks and tested their codes on the above-mentioned coupled code benchmarks. From these OECD LWR transient benchmark problems, the Peach Bottom 2 (PB-2) BWR Turbine Trip (TT) is proposed as the first reference system-scenario, although provisions are made to address the other LWR systems and scenarios such as TMI-1 PWR MSLB, PWR-RIA-ATWS, BWR-CRDA-ATWS (with boron modelling), VVER-1 000 CT, etc. The Peach Bottom 2 BWR Turbine Trip Benchmark is well documented not only in the OECD/NEA/NRC BWR TT benchmark specifications [6] but also in a series of EPRI [11] [12] and PECo reports [13], which include design, operation, and measured steady-state and transient neutronics and thermal-hydraulics data. The fuel cycle depletion, steady-state and transient measured data, available at the integral parameter level and the local distribution level, are very important features of the Peach Bottom 2 BWR Turbine Trip. Integration with the OECD/NEA/NRC BWR BFBT and PSBT benchmarks and the uncertainty analysis exercises performed in their framework will be made. The integration of the PB-2 BWR turbine trip will also be extended to the on-going NEA/CSNI BEMUSE-3 benchmark through the NEA internal co-operation between the NSC and CSNI Committees.

1.1 Objective

The proposed technical approach is to establish a benchmark for uncertainty analysis in best-estimate modelling and coupled multi-physics and multi-scale LWR analysis, using as bases a series of well-defined problems with complete sets of input specifications and reference experimental data. The objective is to determine the uncertainty in LWR system calculations at all stages of coupled reactor physics/thermal hydraulics calculation. The full chain of uncertainty propagation from basic data, engineering uncertainties, across different scales (multi-scale), and physics phenomena (multi-physics) is tested on a number of benchmark exercises for which experimental data is available and for which the power plant details have been released.

The principal objectives are: a) to subdivide the complex system/scenario into several steps or exercises, each of which can contribute to the total uncertainty of the final coupled system calculation, b) to identify input, output and assumptions for each step, c) to calculate the resulting uncertainty in each step; d) to propagate the uncertainties in an integral systems simulation for which high-quality plant experimental data exist for the total assessment of the overall computer code uncertainty. As part of this effort, the development and assessment of different methods or techniques to account for the uncertainties in the calculations will be investigated and reported to the participants.

In summary, the objective of the proposed work is to define, co-ordinate, conduct, and report an international benchmark for uncertainty analysis in best-estimate coupled code calculations for design, operation, and safety analysis of LWRs. The title of this benchmark is: "OECD UAM LWR Benchmark".

The experimental data are used as much as possible (two "interactions" with "known" experimental data are indicated above but others can be added). The benchmark team identifies Input (I), Output (O) or target of the analysis, as well as provides guidance on assumptions for each step and propagated uncertainty parameters (U). The uncertainty from one step should be propagated to the others (as much as feasible and realistic).

1.2 Definition of benchmark phases and exercises

The above-described approach is based on the introduction of 9 steps (exercises), which allows for developing a benchmark framework which mixes information from the available integral facility and NPP experimental data with analytical and numerical benchmarking. Such an approach compares and assesses current and new uncertainty methods on representative applications and simultaneously benefits from different methodologies to arrive at recommendations and guidelines. These 9 steps (exercises) are carried out in 3 phases as follows:

Phase I (Neutronics Phase)

- Exercise I-1: "Cell Physics" focused on the derivation of the multi-group microscopic cross-section libraries and their uncertainties.
- Exercise I-2: "Lattice Physics" focused on the derivation of the few-group macroscopic cross-section libraries and their uncertainties.
- Exercise I-3: "Core Physics" focused on the core steady-state stand-alone neutronics calculations and their uncertainties.

Phase II (Core Phase)

- Exercise II-1: "Fuel Physics": Fuel thermal properties relevant to steady-state and transient performance.
- Exercise II-2: "Time-Dependent Neutroncs": Neutron kinetics and fuel depletion stand-alone performance.
- Exercise II-3: "Bundle Thermal-Hydraulics": Thermal-hydraulic fuel bundle performance.

Phase III (System Phase)

- Exercise III-1: "Core Multi-Physics" - Coupled neutronics/thermal-hydraulics core performance (coupled steady-state, coupled depletion, and coupled core transient with boundary conditions).
- Exercise III-2: "System Thermal-Hydraulics" - Thermal-hydraulics system performance.
- Exercise III-3: "Coupled Core-System" - Coupled neutronics kinetics thermal-hydraulic core/thermal-hydraulic system performance.

- Exercise III-4: “Comparison of Best Estimate Plus Uncertainty (BEPU) vs. Conservative Calculations”.

1.3 Content of this document

Separate specifications will be prepared for each phase in order to allow participation in the full phase or only in a subset of the exercises. Boundary conditions and necessary input information are provided by the benchmark team. The intention is to follow the calculation scheme for coupled calculations for LWR design and safety analysis established in the nuclear power generation industry and regulation. This specification document covers Phase I, which includes the first 3 exercises (neutronics) as follows:

Chapter 2 of this document provides the definition of Exercise I-1.

Chapter 3 provides the definition of Exercise I-2.

Chapter 4 provides the definition of Exercise I-3.

Chapter 5 specifies the requested output for the three exercises.

Chapter 6 provides summary and conclusions.

This phase is focused on understanding uncertainties in prediction of key reactor core parameters associated with LWR stand-alone neutronics core simulation. Such uncertainties occur due to input data uncertainties, modelling errors, and numerical approximations. Input data for core neutronics calculations primarily include the lattice averaged few group cross-sections. Three main LWR types are selected, based on previous benchmark experience and available data:

- PWR (TMI-1)
- BWR (Peach Bottom-2)
- VVER-1 000 (Kozloduy-6, Kalinin-3)

Representative designs for Generation 3 PWR (GEN-III) are added to Phase I in order to address the modelling issues and the likely increased prediction uncertainties related to the designs of GEN-III LWR currently being built, both with UOX and MOX fuels [14].

The SNEAK (fast core) problem) [15] is added as an optional test case to Exercise I-3 since it has a unique set of experimental data for β_{eff} uncertainties and can be used as an example on how to calculate uncertainty in β_{eff}. The two high-quality reactor physics benchmark experiments, SNEAK-7A & 7B (Karlsruhe Fast Critical Facility) are part of the International Reactor Physics Benchmark Experiments (IRPhE) database. The objectives of adding the SNEAK test problem to Exercise I-3 are as follows:

- The PWR, BWR and VVER cases are very similar in spectrum; a fast reactor case based on a well-evaluated experiment would broaden the verification of methods for Phase I of UAM and is a link to reactors of a next generation.
- Fast reactor benchmarks are proposed to test and compare state-of-the-art cross-section sensitivity and uncertainty codes.
- The benchmark provides a unique set of experimental data on delayed neutrons effective fraction; it could be useful in analysis of components of a β_{eff} uncertainty.
- The analysis of the experimental set could bring a better comprehension on validity of covariance matrices to be applied.

In principle, the sources of Input (I) uncertainties in computer code simulations are identified as:

- uncertainties of input data;

- model limitations;
- approximations in the numerical solution;
- nodalisation;
- homogenisation approaches;
- imperfect knowledge of boundary and initial conditions.

For each exercise it is important to identify which new input uncertainties are taken into account and which input uncertainties are propagated from the previous exercise. In Phase I of the benchmark the input uncertainties are specified as follows: best-estimate values for input parameters supplemented by the variance-covariance matrices (utilised for cross-section uncertainties), and for other input uncertainties – probability distribution functions (PDF) and associated parameters. Other important parameters to be defined are the Output (O) uncertainties and propagated Uncertainty parameters (U) for each exercise. This task is directly related to the objective of each exercise. The Output (O) uncertainties are for specified output parameters for each exercise, used to test (evaluate) the utilised uncertainty method. The propagated Uncertainty parameters (U) are output parameters, which are selected to be propagated further through the follow-up exercises in order to calculate the overall resulting uncertainty. The Phase I of the benchmark adopts the following approach. For Output (O) uncertainties – requested is the best-estimate value of the parameter with associated uncertainties where the associated uncertainties are in terms of standard deviation. For propagated Uncertainty parameters (U) – requested is the best-estimate value of the parameter with associated uncertainties where the associated uncertainties are variance-covariance matrices.

Sometimes simple measures of propagation of uncertainties are necessary to allow for comparative analysis – such a simple measure is the concept of "one group effective cross-section uncertainties".

As a source of their cross-section data the participants can use the Nuclear Data Libraries (NDL), which are normally used in conjunction with their lattice physics codes. The three major libraries (ENDF, JEFF and JENDL) are possible candidates. For cross-section covariance data the 44-group covariance library from SCALE-6.0[1] is proposed. In addition to the covariance matrices, a utility programme for interpolating or collapsing from a given group structure to another one is provided for participants' use. Participants can choose any energy multi-group structure according to the input requirements of their lattice code to be utilised. For cross-section generation any type of lattice solver can be used. For core calculations the established two-group energy structure for LWR analyses is proposed as the major part of the benchmark activities. However, provisions are made for utilisation of other few-group structures if the participants want to investigate them. The Monte-Carlo method will provide reference solutions for the test problems of each Exercise of Phase I.

[1] The covariance data libraries for the recent release SCALE-6.1 are the same as for SCALE-6.0

Chapter 2: Definition of Exercise I-1: cell physics

The Exercise I-1 is entitled "Cell Physics", and is focused on derivation of the multi-group microscopic cross-section libraries. Its objective is to address the uncertainties due to the basic nuclear data as well as the impact of processing the nuclear and covariance data, selection of multi-group structure, and self-shielding treatment. The intention for Exercise I-1 is to propagate the uncertainties in evaluated Nuclear Data Libraries – NDL – (microscopic pointwise cross-sections) into multi-group microscopic cross-sections used as an input by their lattice physics codes. The participants can use any of the major NDLs such as Evaluated Nuclear Data Files (ENDF) [16] [17] [18], Joint European Fission and Fusion files (JEFF) [19] [20], Japanese Evaluated Nuclear Data Library (JENDL) [21], and TALYS-based Evaluated Nuclear Data Library (TENDL)-2008 [22]. The evaluation of nuclear data induced uncertainty is possible by the use of nuclear data covariance information. The development of nuclear data covariance files is in progress in the major NDLs. For the purposes of the OECD LWR UAM benchmark the availability of covariance data is important for all relevant nuclides (actinides, fission products, absorbers and burnable poisons, structural materials, etc.), present in the reactor core and reflector regions of LWRs, covering the entire energy range of interest (from 0 to 10 MeV), and for all relevant reaction cross-section types.

2.1 Status of nuclear data covariance information

In the major NDLs standards and formats are in place to permit the communication of estimated uncertainties in the evaluated cross-section data. The evaluation of nuclear data induced uncertainty is possible by the use of nuclear covariance data. By including the uncertainty or covariance information, the analyst can propagate cross-section data uncertainties through sensitivity studies to the final calculated quantities of interest. The covariance data files provide the estimated variance for the individual data as well as any correlations that may exist. Availability of covariance evaluations is very limited in the NDLs; however, nuclear data covariance files for some additional materials are being developed for major NDLs. The uncertainty evaluations are developed utilising information from experimental cross-section data, integral data (critical assemblies), and nuclear models and theory. The covariance information in the NDLs is given with respect to pointwise cross-section data and/or with respect to resonance parameters. Methods to approximate uncertainty data have also been used to cover nuclides for which covariance data in NDLs were not available thus producing a rather complete set of "low-fidelity" covariance data. These are not included in the official NDLs, but this approximate set of data is distributed for sensitivity and uncertainty applications with codes such as SCALE.

As mentioned above the evaluated nuclear data (α) are determined from experiments with uncertainty, which means that different values of $\hat{\alpha}$ are possible, with varying degrees of probability, p[$\hat{\alpha}$]d$\hat{\alpha}$. The following definitions are introduced:

- Evaluated data, α=expected value of $\hat{\alpha}$: $\alpha \to E[\hat{\alpha}] = \int_{\hat{\alpha}} \hat{\alpha} p(\hat{\alpha}) d\hat{\alpha}$
- Variance in evaluated data $\mathrm{Var}(\alpha) \equiv E[\Delta\alpha^2] = E[(\hat{\alpha} - \alpha)^2]$
- Standard deviation $\sigma_\alpha \equiv \sqrt{Var(\alpha)}$
- Covariance in two data parameters $(\alpha_1,\alpha_2) \equiv \mathrm{Cov}(\alpha_1,\alpha_2) = E[\Delta\alpha_1,\Delta\alpha_2]$

$\mathrm{Cov}(\alpha_1,\alpha_2) = (\sigma_{\alpha_1} c_{1.2} \sigma_{\alpha_2})$ Where the correlation coefficient = $C_{1,2} \in [-1,1]$

- Covaiance matrix $\equiv C_{\alpha\alpha} = \begin{bmatrix} \mathrm{Var}(\alpha_1) & \mathrm{Cov}(\alpha_1,\alpha_2) & \mathrm{Cov}(\alpha_1,\alpha_3) \\ \mathrm{Cov}(\alpha_2,\alpha_1) & \mathrm{Var}(\alpha_2) & \mathrm{Cov}(\alpha_2,\alpha_3) \\ \mathrm{Cov}(\alpha_3,\alpha_1) & \mathrm{Cov}(\alpha_3,\alpha_2) & \mathrm{Var}(\alpha_3) \end{bmatrix}$

The uncertainty information in the evaluated libraries is included in files called “covariance files” (files for nuclear variance and covariance data) within the ENDF-6 formalism. The following covariance files are defined:

- Data covariances obtained from parameter covariances and sensitivities (MF30);
- Data covariances for number of neutrons per fission (MF31);
- Data covariances for resonance parameters (MF32);
- Data covariances for reaction cross-sections (MF33);
- Data covariances for angular distributions (MF34);
- Data covariances for energy distributions (MF35);
- Data covariances for radionuclide production yields (MF39);
- Data covariances for radionuclide production cross-sections (MF40).

To propagate nuclear data uncertainties in reactor core calculation files MF31, MF32, and MF33 are the only data currently available within ENDF/B and other NDL’s. For example, for each isotope and type of reaction, quantities in MF33 are the covariances of the expected cross-section values, providing a measure of the accuracy and correlations of the evaluated cross-sections. Please note that the MF33 uncertainties often refer to the *complete* uncertainties in evaluated cross-sections, not just uncertainties in the MF3 data. For example, uncertainties in the resonance range of a cross-section may be described by file 33 whenever file 32 data is not present. The following information is needed for processing uncertainties into the form of full covariance matrices:

- Stored quantities in MF3 (or MF 10) - expected value of a physical quantity:

$$\langle x \rangle = \int x \; f(x)\, dx \qquad (1)$$

Where $f(x)$ is the density function averaged over all variables other than x.

- Stored quantities in MF33 - relative and absolute covariances of the 2nd degree moments of the joint density function:

$$\mathrm{Cov}(\mathrm{x},\mathrm{y}) = \iint \left(x - \langle x \rangle\right)\left(y - \langle y \rangle\right) f(x,y)\, dx\, dy \qquad (2)$$

Where $f(x,y)$ is the density function averaged over all variables other than x and y. Please note that when $x = y$ then $\mathrm{Cov}(\mathrm{x},\mathrm{y}) = \mathrm{Cov}(\mathrm{x},\mathrm{x}) = \mathrm{Var}(\mathrm{x})$. In this way the uncertainties are presented in terms of variances and covariances (variance-covariance matrices).

The reasons for existing correlations in nuclear data uncertainties are:

- Energy correlations as a result of:
  -physics;
  -systematic experimental uncertainties;
  -random experimental uncertainties;

- Reaction correlations as a result of:
  - combining or subtracting two reactions to obtain another;
- Material correlations as a result of:
  - nuclear data is measured as ratio to data for some standard materials.

The total covariance matrix for a given energy-dependent cross-section (by isotope and type of reaction) is made up of the contribution of single covariance matrices, each one defining a type of correlation (between energy intervals or correlation with a different cross-section).

Review of the compilation, processing and analysis of uncertainty data for neutron induced reactions available in the most recent different internationally distributed nuclear data libraries have been performed for the purposes of the UAM LWR benchmark activities. The latest evaluated nuclear data files available from the NEA/OECD and NNDC-BNL are:

1) JENDL-3.3 (2002). The number of nuclides in this NDL is 337 and the covered incident neutron energy range is from 10^{-5} eve to 20 MeV. In JENDL-3.3, covariances are included for 20 nuclides. The physical quantities for which covariance's are deduced are cross-sections, resolved and unresolved resonance parameters, the first order Legendre-polynomial coefficient for the angular distribution of elastically scattered neutrons, and fission neutron spectra. Covariances were estimated on the basis of the same methods that were adopted in the JENDL-3.3 evaluation.
2) JEFF-3.1.1 (2009). The number of nuclides in this NDL is 381. The covariances are provided for 46 nuclides, and only for cross-sections. JEFF-3.1.1is the current European NDL (JEFF Report No.22) and was released in 2009.
3) ENDF/B-VI.8 (2001) and ENDF/B-VII.0 (2006). The latest version of this NDL has 393 nuclides. The official version of ENDF/B-VII.0 was released at the end of 2006. The ENDF.B-VII library contains 14 sub-libraries (2 - new, 7 - many improvements and updates, 5 - unchanged). It is the largest library - it contains data for 393 materials (390 isotopes plus 3 elements). There are major improvements in the ENDF.B-VII library as compared to the previous versions/releases:
   - significant advances are made in evaluation of actinide cross-sections;
   - fission products are completely updated;
   - Includes resonances (resolved and unresolved) in modern representation.

With regard to neutron cross-section covariances (uncertainties plus correlation matrix) in the ENDF/B-VII library there is a drastic reduction compared to ENDF-B-VI.8 since the later covariances were from the 1970s and mostly produced for ENDF/B-V. It was decided to keep only quality covariances and 90% of covariances were removed. Only partial covariances for 13 materials were migrated to ENDF/B-VII from ENDF/B-VI, and new covariances for 9 materials were added. The new covariances are for Gd isotopes, and this new evaluation includes unresolved resonances.

The covariance vision for the ENDF/B-VII as reported by BNL is as follows:

- produce crude but reasonable covariances for all materials in ENDF/B-VII.0;
- improve all covariances – and release VII.1 version;
- Quality results – release VII.2.

When the first step is completed and made available it can be used for the purpose of the OECD LWR UAM benchmark. This will be low-fidelity covariances and covariance matrices available for all materials in ENDF/B-VII.0 at any temperature, in a tabulated form or MF33 format. The delay in preparing the complete covariance data for the ENDF/B-VII is caused by the following reasons:

- large multi-dimensional data representations are needed;

- methods to evaluate the covariances are not well established;
- covariance data for resonance parameters need special care.

The same applies to the new versions of JEFF, JENDL and TENDL – JEFF-4.0, JENDL-4.0 and TENDL-2009. When these NDLs supplemented by complete covariance data are made available they can be used for the purpose of the OECD LWR UAM benchmark.

The new BNL-LANL approach is utilised with covariances for the entire energy range: the fast neutron region is based on EMPIRE (BNL) [23] [24] and KALMAN (LANL) using both theoretical and experimental uncertainties, while the thermal and resonance regions are based on ATLAS (BNL) [25] and KALMAN. The SAMMY code (ORNL) [26] [27] is being used to generate resonance-parameter covariance matrices in the resolved and unresolved resonance regions for selected materials, while a simple "integral approximation" will be used to generate low-fidelity uncertainties in the thermal and resonance ranges for most of the other materials. The "integral approximation" uses uncertainties in integral measurements of thermal cross-sections and resonance integrals to approximate differential data uncertainties [28].

Table 1 shows the total number of materials and cross-section reactions with neutron cross-section covariance data in the recent versions of the major evaluated nuclear data files.

Table 1: Number of materials and cross-sections with covariances of neutron cross-sections

Data files	Number of materials	Number of cross-sections
ENDF/B-VI.8	44	400
JEFF-3.1	34	350
JENDL-3.3	20	160
TENDL-2008	From F-19 to Po-209	all

The covariance data in the major data files are scarce in terms of materials (including actinides) and types of covariance matrices available. They contain uncertainty information only for few isotopes and reactions and usually for different number and different isotopes in different files. For isotopes not included, usually their covariances are assumed to be zero, which will result in the underestimation of core parameters uncertainties. For example the list of nuclides and materials present in LWR reactor cores of interest to this benchmark are given in Table 2 through Table 4. These nuclides can be ranked according to their importance regarding the multiplication factor predictions. An example of such priority list of the most important nuclides for LWR calculations is given in Table 5. (Please note that the nuclides are not listed in the order of their importance.)

In conclusion, the status of available covariance data in the major NDLs is such that it cannot support the objectives of the OECD LWR UAM benchmark. Once the more complete covariance data containing low-fidelity covariances that supplement available NDL evaluations available for all required materials are ready, they can be used for the purposes of this benchmark within the framework of Exercise I-1.

Table 2: Nuclides and materials present in TMI-1 PWR core calculations

H-1	B-10	B-11	C-0	O-16	Al-27	Si-0	Cr-0
Mn-0	Fe-0	Ni-0	Cu-63	Kr-83	Rh-103	Rh-105	Ag-107
Ag-109	Cd-113	In-115	I-135	Xe-131	Cs-133	Cs-134	Cs-135
Nd-143	Nd-145	Pm-147	Pm-148	Pm-148(m)	Pm-149	Sm-147	Sm-149
Sm-150	Sm-151	Sm-152	Eu-153	Eu-154	Eu-155	Gd-153	Gd-155
U-234	U-235	U-236	U-238	U-239	Np-237	Np-239	Pu-238
Pu-239	Pu-240	Pu-241	Pu-242	Am-241	Am-242(m)	Am-243	Cm-242
LFP1[2]	LFP2[3]	Zr-2[4]	Zr-4[5]	SS[6]			

[2] Lumped fission products group 1

Table 3: Nuclides and materials present in PB-2 BWR core calculations

H-1	B-10	B-11	C-0	O-16	Kr-83	Rh-103	Rh-105
Ag-109	I-135	Xe-131	Xe-135	Cs-133	Cs-134	Cs-135	Nd-143
Nd-145	Nd-147	Pm-147	Pm-148	Pm-148(m)	Pm-149	Sm-147	Sm-148
Sm-149	Sm-150	Sm-151	Sm-152	Eu-153	Eu-154	Eu-155	Gd-154
Gd-155	Gd-156	Gd-157	Gd-158	Gd-160	U-234	U-235	U-236
U-238	U-239	Np-237	Np-239	Pu-238	Pu-239	Pu-240	Pu-241
Pu-242	Am-241	Am-242(m)	Am-243	Cm-242	Cm-244	Cm-245	Cm-246
Cm-247	LFP1	LFP2	Inc-718[7]	Zr-4	SS		

Table 4: Nuclides and materials present in Kozloduy-6 VVER-1 000 core calculations

H-1	B-10	B-11	C-0	N-14	O-16	Al-27	Si-0
P-31	S-0	Ti-0	Cr-0	Mn-55	Fe-0	Ni-0	Br-81
Kr-82	Kr-83	Kr-84	Kr-85	Kr-86	Sr-89	Sr-90	Y-89
Zr-0	Zr-91	Zr-93	Zr-95	Zr-96	Y-90	Nb-93	Nb-95
Mo-95	Mo-96	Mo-97	Mo-98	Mo-99	Mo-100	Tc-99	Ru-100
Ru-101	Ru-102	Ru-104	Ru-105	Ru-106	Rh-103	Rh-105	Pd-104
Pd-105	Pd-106	Pd-107	Pd-108	Ag-109	Ag-110(m)	Ag-111	Cd-110
Cd-111	Cd-113	In-115	Sb-0	Sb-125	Sb-127	Te-123	Te-127(m)
Te-129(m)	I-127	I-129	I-131	I-135	Xe-128	Xe-130	Xe-131
Xe-132	Xe-133	Xe-134	Xe-135	Xe-136	Cs-133	Cs-134	Cs-135
Cs-136	Cs-137	Ba-134	Ba-137	Ba-140	La-139	La-140	Ce-140
Ce-141	Ce-142	Ce-143	Ce-144	Pr-141	Pr-143	Nd-142	Nd-143
Nd-144	Nd-145	Nd-146	Nd-147	Nd-148	Nd-150	Pm-147	Pm-148
Pm-148(m)	Pm-149	Pm-151	Sm-147	Sm-148	Sm-149	Sm-150	Sm-151
Sm-152	Sm-153	Sm-154	Eu-151	Eu-153	Eu-154	Eu-155	Eu-156
Eu-157	Gd-154	Gd-155	Gd-156	Gd-157	Gd-158	Gd-160	Tb-159
Tb-160	Tb-161	Dy-160	Dy-160	Dy-161	Dy-162	Dy-164	Ho-165
Hf-174	Hf-176	Hf-177	Hf-178	Hf-179	Hf-180	Ta-181	Ta-182
U-235	U-236	U-237	U-238	Np-237	Pu-238	Pu-239	Pu-240
Pu-241	Pu-242	Am-241	Am-242(m)	Am-243	Cm-242	Cm-243	Cm-244
Cm-245	Cm-246	Cm-247	Cm-248	Bk-249	Cf-249	Cf-250	Cf-251
Cf-252							

Table 5: Priority list of important nuclides

H-1	B-10	B-11	O-16	Zr-91	Zr-93	Zr-96	Rh-103	Xe-135
Sm-149	Gd-155	Gd-157	U-234	U-235	U-236	U-237	U-238	Np-237
Np-239	Pu-238	Pu-239	Pu-240	Pu-241	Pu-242	Am-241	Am-242(m)	Am-243
Cm-242	Cm-244	Cm-245						

[3] Lumped fission products group 2

[4] Zircaloy-2

[5] Zircaloy-4

[6] Stainless Steel

[7] Inconel-718

2.2 Multi-group processing of nuclear and covariance data

Prior to using the covariance information in applications, a processing method/code must be used to convert the energy-dependent covariance information to a multi-group format. Within the framework of Exercise I-1 the participants can use/develop their own processing methods or utilise available tools/codes at NEA/OECD and RSICC/ORNL to process the cross-section data and associated covariance data (group-wise covariance matrices) for the multi-group libraries utilised as input in their lattice physics codes.

The data from the evaluated nuclear data files usually are processed with codes such as NJOY. The multi-group structures should correspond to the structure of input libraries in the utilised lattice physics codes. For example some of the input multi-group structures utilised for LWR analysis in lattice-physics codes are:

- CASMO-4 [29] input libraries – 40 and 70 groups;
- HELIOS [30] input libraries – 47 and 190 groups;
- APOLLO-2 [31] input libraries - 172 and 281 groups;
- TRITON [32] – 44 and 238 groups.

Uncertainties are inevitably introduced into the broad-group cross-sections due to approximations in the grouping procedure. The dominant uncertainty is generally with regard to the energy weighting function used to average the pointwise or fine-group data within a single broad group. Intelligent selection of the weighting functions can reduce such uncertainties. Sensitivity studies using different group structures can help to identify uncertainties introduced with the choice of given multi-group structures. Detailed knowledge of the specific application is needed to prepare adequate group constants. One rigorous way to determine the optimum energy mesh for LWR applications is described in [31]. Continuous energy Monte Carlo solutions can be used to guide and inform multi-group library generation and use.

The SCALE system provides a rigorous mechanism for multi-group cross-section processing using the continuous energy solver CENTRM [33] for self-shielding in the resolved resonance and thermal regions for appropriately weighting multi-group cross-sections using a continuous energy spectrum. The CENTRM module used for cross-section processing within SCALE performs an ultra-fine energy grid (typically 30 000-70 000 energy points) transport calculation using ENDF-based point data to generate effectively continuous energy neutron flux solutions in the resonance and thermal ranges. This is used to weight the multi-group cross-sections to be used in subsequent transport calculations. There is also a special sensitivity version of CENTRM that computes pointwise flux derivatives for evaluating implicit sensitivities associated with perturbations in resonance self-shielding.

The judicious selection of the energy group structure can also help to reduce the sensitivity of the computed responses to the weighting function, at least for a selected set of problems.

The covariance data can be processed in multi-group form. For example MF33 data are structured to be processed to yield the multi-group covariance matrices. There are several procedures to process covariances:

- ERRORR/COVR modules of NJOY [34] – can process ENDF Files 31, 32, 33 (not capable of processing Reich-Moore covariance data). Processed data are in COVFILS format.
- ERRORJ [35, 36] – can process the covariance for cross-sections including resonance parameters (Files 31, 32, 33, 34 and 35). It was recently integrated into the NJOY processing system. Processed data are generated in COVFILS format.
- PUFF-IV [37] – a multi-group covariance processing code. The PUFF-IV has the capability to process the uncertainty information in ENDF (Files 31, 32, 33) and generate the desired multi-group correlation matrix. Processed data are in COVERX format.

- SAMMY [38] - an R-matrix tool for analysis of cross-section data in the resolved and unresolved resonance regions. SAMMY code can be used to generate a resonance-parameter covariance matrix in the resolved and unresolved resonance regions. The evaluated data files with covariance data are then processed with ERRORJ to generate multi-group covariance data for reactor applications. REFIT [39] is an alternative code to SAMMY with equivalent features.

In principle the covariance matrices can be now self-shielded in the same way as the cross-sections, although in practice this is rarely done. The impact of this treatment on the obtained covariance matrices and their dependence on energy group structure needs to be studied. The uncertainty can be self-shielded using Bondarenko factors, in the same way that the cross-sections are processed in the NJOY module GROUPR.

The ORNL's TSUNAMI system uses a completely different approach to address the impact of self-shielding in sensitivity analysis. Rather than modifying the covariance data, the sensitivity coefficients are modified to include the "implicit effects" of perturbations in the group cross-sections caused by perturbations in self-shielding. Implicit effects account for the impact of resonance self-shielding on sensitivity coefficients and uncertainty evaluations [40]. This allows the use of unshielded covariance data. Treatment of implicit effects is a standard part of the TSUNAMI analysis, and has been shown to be a significant sensitivity component in some cases [41].

Reducing the number of energy groups leads to a reduction in the amount of information contained in the covariance matrices. The pointwise cross-sections and associated Covariance Matrix (CM) are averaged using an energy dependent flux to give multi-group cross-sections and associated CMs. The integrations used in the averaging process are usually evaluated using numerical integration schemes – any such schemes have an uncertainty associated with them.

Several multi-group covariance matrices have been developed and used for different applications. There are multi-group covariance matrices for major isotopes of interest in reactor core calculations based on a compilation of the available uncertainty data as shown in Table 6:

Table 6: Number of nuclides and energy groups in the available multi-group covariance matrices

Name	Number of nuclides	Number of energy groups
ANL	42	17
NEA/OECD	31	15
SCALE5.1/ORNL	299	44
SCALE6.0/ORNL	401	44

- The multi-group ANL cross-section covariance matrix [42] was developed based on a simple "educated guess" for uncertainties and the simplest estimate for the correlation matrix. They found that the nuclear data uncertainties are significant for only a few parameters – k_{eff} for thermal systems at EOC due to high burn-up; burn-up reactivity swing and related isotopic density variations during core depletion. In the ANL covariance matrix the uncertainty values are given in an "energy band" consistent with multi-group structures used for deterministic calculations of both thermal and fast reactors. The ANL covariance matrix has been used with the ERANOS software based on generalised perturbation method for core calculations of GEN-IV design core models and very high burn-up PWR core model.
- The NEA covariance matrix is extracting relevant covariance data from current evaluations in major data files and processing them in a multi-group structure. The name is NEA-1 730: ZZ-COV-15GROUP. ZZ-COV-15GROUP is a 15-group (which can be expanded to a desired multi-group structure) cross-section covariance matrix library presenting a general overview of the available data. The origin of this covariance matrix is from ENDF/B-V, /B-VI.8, JENDL-3.3, JEFF-3.0, IRDF-2002 and IAEA. It has been used with the cross-section sensitivity/uncertainty

(S/U) SUSD3D software available from OECD/NEA for propagation in core/experiment calculations.

- There are several evaluations of multi-group uncertainty libraries (44 groups) provided in the ORNL SCALE code package. These evaluations were generated by the multi-group preparation code PUFF-4, which processes the ENDF/B covariance data. These have been used by both TSUNAMI and TRITION. There are several different evaluations of multi-group uncertainty libraries (44 groups) provided in the ORNL SCALE code package. As can be seen in Tables 7 and 8**,** the nuclide covariance data in SCALE 5.1 and SCALE-6.0 are the most complete – it is a collection of all covariance data produced over the last few decades and critically reviewed for the most important nuclides. It is in 44 groups and can be expanded or reduced to the participants' multi-group structures. For these reasons it was decided initially at the OECD UAM-1 workshop to utilise the nuclide multi-group covariance data in SCALE 5.1 for the purposes of Exercise I-1. Since in 2009, the improved/extended SCALE-6.0 covariance library became available it was decided at the OECD UAM-3 workshop that this library would be used for Exercise I-1. The details of such utilisation are given in Section 2.3.

History and description of SCALE covariance libraries are given below:

- The first covariance libraries were released in SCALE-5.0. These were the ones entitled, 44GROUPV5COV and 44GROUPANLCOV. They are now obsolete.
- In SCALE-5.1 the above covariance libraries were replaced by 4 COV libraries:
  - 44GROUPV5COV contains only covariances contained in ENDF/B-V;
  - 44GROUPV5REC contains ENDF/B-V covariances supplemented by other data sources (as described for 44GROUPV6REC below);
  - 44GROUPV6COV contains only covariances contained in ENDF/B-VI;
  - 44GROUPV6REC was the initially recommended covariance library based on several sources, including evaluated data files END/B-VI, ENDF/B-V, JENDL, and JEF. Data missing from all evaluated data files were represented by the "integral approximation" described above, for the resonance and thermal energy ranges only. This approximation was used for 299 materials – see Table 7: The nuclides or materials (in ZA order) for which covariance data are provided in ZZ-SCALE5.1/COVA-44G.
- The SCALE-5.1 recommended covariance library was updated and transformed into the SCALE-6.0 library. The data in the SCALE-6 library have been assembled from a variety of sources, including high-fidelity covariance evaluations from ENDF/B-VII, ENDF/-VI, and JENDL-3.3, as well approximate uncertainties obtained from a collaborative project performed by Brookhaven National Laboratory, Los Alamos National Laboratory, and Oak Ridge National Laboratory. It includes recent high-fidelity ENDF/B-VII uncertainty evaluations for the nuclides ^{235}U, ^{238}U, ^{239}Pu, ^{232}Th, and Gd isotopes. Approximate uncertainties span the full energy range of 0-20 MeV. Approximate uncertainties included for inelastic scattering and (n, 2n), as well as capture, fission, and elastic scattering reaction cross-section and number of neutrons per fission. Table 8 shows the nuclides with covariance data in ZZ-SCALE6/COVA-44G.

2.3 Covariance data and tools distributed for the UAM Phase I project

The package distributed to UAM Phase I participants consists of the following items distributed in 2 parts:

1) Cross-section relative covariance libraries:

- A set of four cross-section covariance libraries [43] [44] from the SCALE-5.1 and SCALE-6.0 [45] package and their documentation[8]. These libraries are in 44 energy groups in the original and the processed forms for user convenience.

2) Tools for handling and transforming the cross-section covariance data:

- ANGELO- a code to transform these covariance data libraries into a user specified energy group-structure for the BOXR, COVFIL and COVERX formats [46] [47];
- LAMBDA - a programme for verifying the mathematical properties of the covariance data [46] [47].

3) In addition, it is recommended to use modules of the NJOY system (COVR) [34], [35] for plotting of the matrices and transformation to BOXR format. Utility routines of the ERRORJ [36] code package can be useful for COVERX files handling and conversion to COVFILS format (NJOY and ERRORJ can be obtained separately).

2.3.1 The cross-section relative covariance data sets

According to the SCALE 5.1 manual [44], a total of four cross-section relative covariance libraries have been released:

- 44GROUPV5COV, Basic ENDF/B-V Covariance Library
- 44GROUPV5REC, Recommended ENDF/B-V Covariance Library
- 44GROUPV6COV, Basic ENDF/B-VI Covariance Library
- 44GROUPV6REC. Recommended ENDF/B-V Covariance Library

These libraries correspond to the basic ENDF/B-V cross-section set, basic ENDF/B-VI set of cross-sections, and two recommended sets that include the version V and VI sets plus a large number of nuclides for which covariance information is included, based on integral uncertainty data. Each of these sets contains cross-section covariance information in the SCALE 44 neutron energy group structure. It is envisaged to apply the covariance libraries to their respective ENDF/B-based cross-section libraries, (i.e. the V5 libraries to the version V cross-section libraries and the V6 libraries to the version VI cross-section libraries). In addition, there are two covariance sets for each ENDF/B version, corresponding to a *basic* set with only the materials included in the ENDF/B formal release and a *recommended* set with covariance information for most cross-section materials on the cross-section library. The *basic* sets do not include substitutions and additions for nuclides with bad or missing covariance data such that they are useable in their present form. The *recommended* sets, while efforts were made to include covariance for every material, include most but not all of the materials present on the cross section library.

In the report [43], tables are given with the missing data clearly identified. The files contain the covariance data for the following reactions or parameters: total, elastic, inelastic, (n, 2n), fission, χ, (n,γ), (n,p), (n,d), (n,t), (n,^{3}He), (n,α), and ν-bar.

In parentheses is the total number of the different relative covariance matrices in the four libraries for each nuclide. In Appendices I-IV the list of nuclides and the origin of the covariance data are provided for each library. The 44-energy-groups structure is described in Appendix V.

[8] These libraries have been released through the SCALE-6.0 package and are thus subject to US Export control. In order to obtain a copy, users must fill in the corresponding forms that can be obtained from the OECD/NEA Data Bank programs@oecd-nea.org or directly from RSICC pdc@ornl.gov. Those who have a SCALE-6.0 license do not need a new license for these data.

Some of the covariance data cover only the thermal and resonance region (based on Mughabghab (BNL) thermal and resonance integral uncertainty evaluation – this represents a large fraction of the covariance data). It is a collection of all covariance data produced over the last decades in which the most important nuclides have been critically reviewed.

The SCALE-6.0 covariance library data corresponds also to 44-group relative uncertainties assembled from a variety of sources, including evaluations from ENDF/B-VII, ENDF/B-VI, JENDL-3.3, and more than 300 approximated uncertainties from a collaborative project performed by Brookhaven National Laboratory (BNL), Los Alamos National Laboratory (LANL), and Oak Ridge National Laboratory (ORNL). The current SCALE covariance library spans the full energy range of the multi-group cross-section libraries, while the approximate uncertainty data in SCALE 5.1 did not extend above 5 keV. More than 100 new materials have also been added to the covariance library.

It is assumed that the same relative (rather than absolute) uncertainties can be applied to all cross-section libraries, even if these are not strictly consistent with the nuclear data evaluations. Only energy is fully correlated in the SCALE 6.0 44-group covariance library. There are no real cross-reaction and cross-nuclide correlations. Participants are expected to address problem-specific resonance self-shielding effects when performing sensitivity and uncertainty analysis.

- The library includes evaluated covariances obtained from ENDF/B-VII, ENDF/B-VI, and JENDL-3.3 for more than 50 materials.

- Among the materials in the SCALE library with covariances taken from high-fidelity nuclear data evaluations are the following:

  - ENDF/B-VII evaluations *(includes both VII.0 and pre-release covariances proposed for VII.1):* Au, ^{209}Bi, ^{59}Co, ^{152,154,155,156}Gd, ^{191,193}I, ^{7}Li, ^{23}Na, ^{93}Nb, ^{58}Ni, ^{99}Tc, ^{232}Th, ^{48}Ti, ^{239}Pu, ^{233,235,238}U, V

  - ENDF/B-VI evaluations: Al, ^{241}Am, ^{10}B, ^{12}C, ^{50,52,53,54}Cr, ^{63,65}Cu, ^{54,56,57}Fe, In, ^{55}Mn, ^{60,61,62,64}Ni, ^{206,207,208}Pb, ^{242}Pu, ^{28,29}Si

  - JENDL-3.3 evaluations: ^{11}B, ^{1}H, ^{16}O, ^{240,241}Pu

- At the other end of the spectrum from high fidelity data, “low-fidelity” (lo-fi) covariances (BLO data) are defined to be those that are estimated independently of a specific data evaluation. The approximate covariance data in SCALE are based on results from a collaborative project funded by the Department of Energy Nuclear Criticality Safety Programme to generate low-fidelity covariances over the energy range from 10^{-5} eV to 20 MeV for materials without covariances in ENDF/B-VII.0. Nuclear data experts at BNL, LANL, and ORNL devised simple procedures to estimate data uncertainties in the absence of high-fidelity covariance evaluations. The result of this project is a set of covariance data in the ENDF/B file 33 formats that can be processed into multi-group covariances.

Table 7: The nuclides or materials (in ZA order) for which covariance data are provided in ZZ-SCALE5.1/COVA-44G

H-1(10)	H-2(3)	H-3(2)	He-3(2)	He-4	Li-6(2)	Li-7(3)	Be-9(2)
B-10(3)	B-11(2)	C-0(6)	N-14(2)	N-15	O-16(3)	O-17	F-19(3)
Na-23(3)	Mg-0	Al-27(2)	Si-0(3)	Si-28	Si-29	Si-29	Si-30
P-31	S-0	S-32	Cl-0	K-0	Ca-0	Sc-45(2)	Ti-0
V-0(2)	Cr-0(2)	Cr-50	Cr-52	Cr-53	Cr-54	Mn-55(3)	Fe-0(2)
Fe-54	Fe-56	Fe-57	Fe-58	Co-59(3)	Ni-0(2)	Ni-58	Ni-60
Ni-61	Ni-62	Ni-64	Cu-0	Cu-63	Cu-65	Ga-0	Ge-72
Ge-73	Ge-74	Ge-76	As-75	Se-74	Se-76	Se-77	Se-78
Se-80	Se-82	Br-79	Br-81	Kr-78	Kr-80	Kr-82	Kr-83
Kr-84	Kr-85	Kr-86	Rb-85	Rb-87	Sr-84	Sr-86	Sr-87
Sr-88	Sr-89	Sr-90	Y-89	Y-89	Y-90	Y-91	Zr-0
Zr-90	Zr-91	Zr-92	Zr-93	Zr-94	Zr-96	Nb-93	Nb-93
Nb-94	Nb-95	Mo-0	Mo-94	Mo-95	Mo-96	Mo-97	Tc-99
Ru-96	Ru-99	Ru-100	Ru-101	Ru-102	Ru-104	Ru-105	Ru-106
Rh-103	Rh-105	Pd-102	Pd-104	Pd-105	Pd-106	Pd-107	Pd-108
Pd-110	Ag-107	Ag-109	Ag-111	Cd-0	Cd-106	Cd-108	Cd-110
Cd-111	Cd-112	Cd-113	Cd-114	Cd-116	In-0	In-113	In-115
Sn-112	Sn-114	Sn-115	Sn-116	Sn-117	Sn-118	Sn-119	Sn-120
Sn-122	Sn-124	Sb-121	Sb-123	Sb-124	Te-120	Te-122	Te-123
Te-124	Te-125	Te-126	Te-127(m)	Te-128	Te-130	I-127	I-129
I-130	I-131	Xe-124	Xe-126	Xe-128	Xe-129	Xe-130	Xe-131
Xe-132	Xe-133	Xe-134	Xe-135	Xe-136	Cs-133	Cs-134	Cs-135
Cs-137	Ba-134	Ba-135	Ba-136	Ba-137	Ba-138	Ba-140	La-139
La-140	Ce-140	Ce-141	Ce-142	Ce-143	Ce-144	Pr-141	Pr-142
Pr-143	Nd-142	Nd-143	Nd-144	Nd-145	Nd-146	Nd-147	Nd-148
Nd-150	Pm-147	Pm-148	Pm-148(m)	Pm-149	Sm-144	Sm-147	Sm-148
Sm-149	Sm-150	Sm-151	Sm-152	Sm-153	Sm-154	Eu-151	Eu-152
Eu-153	Eu-154	Eu-155	Gd-152	Gd-154	Gd-155	Gd-156	Gd-157
Gd-158	Gd-160	Tb-159	Tb-160	Dy-160	Dy-161	Dy-162	Dy-163
Dy-164	Ho-165	Er-166	Er-167	Lu-175	Lu-176	Hf-0	Hf-174
Hf-176	Hf-177	Hf-178	Hf-179	Hf-180	Ta-181	Ta-182	W-0
W-182	W-183	W-184	W-186	Re-185(2)	Re-187(2)	Au-197(3)	Pb-0(2)
Pb-206	Pb-207	Pb-208	Bi-209(2)	Th-230	Th-232(4)	Pa-231	Pa-233(3)
U-232	U-233	U-234	U-235	U-235(6)	U-236	U-237	U-238(4)
Np-237(2)	Pu-0	Pu-238(7)	Pu-239(9)	Pu-240(10)	Pu-241(11)	Pu-242(3)	Pu-243
Pu-244	Am-241(4)	Am-242	Am-242(m)	Am-243	Cm-242	Cm-243	Cm-244
Cm-245	Cm-246	Cm-247	Cm-248	Bk-249	Cf-249	Cf-250	Cf-251
Cf-252(3)	Cf-253	Es-253					

Table 8: The nuclides or materials (in ZA order) for which covariance data are provided in ZZ-SCALE6/COVA-44G

H-1	**H-ZrH**	**H-poly**	**H-freegas**	H-2	**H2-freegas**	H-3	He-3
He-4	Li-6	Li-7	**Be-7**	Be-9	**Be-bound**	B-10	B-11
C-0	**C-graphite**	N-14	N-15	O-16	O-17	F-19	Na-23
Mg-0	**Mg-24**	**Mg-25**	**Mg-26**	Al-27	Si-0	Si-28	Si-29
Si-30	P-31	S-0	S-32	**S-34**	**S-36**	Cl-0	**Cl-35**
Cl-37	**Ar-36**	**Ar-38**	**Ar-40**	K-0	**K-39**	**K-40**	**K-41**
Ca-0	**Ca-40**	**Ca-42**	**Ca-43**	**Ca-44**	**Ca-46**	**Ca-48**	Sc-45
Ti-0	**Ti-46**	**Ti-47**	**Ti-48**	**Ti-49**	**Ti-50**	V-0	Cr-50
Cr-52	Cr-53	Cr-54	Mn-55	Fe-0	Fe-54	Fe-56	Fe-57
Fe-58	**Co-58**	**Co-58(m)**	Co-59	Ni-58	**Ni-59**	Ni-60	Ni-61
Ni-62	Ni-64	Cu-63	Cu-65	Ga-0	**Ga-69**	**Ga-71**	**Ge-70**
Ge-72	Ge-73	Ge-74	Ge-76	**As-74**	As-75	Se-74	Se-76
Se-77	Se-78	**Se-79**	Se-80	Se-82	Br-79	Br-81	Kr-78
Kr-80	Kr-82	Kr-83	Kr-84	Kr-85	Kr-86	Rb-85	**Rb-86**
Rb-87	Sr-84	Sr-86	Sr-87	Sr-88	Sr-89	Sr-90	Y-89
Y-90	Y-91	Zr-0	Zr-90	Zr-91	Zr-92	Zr-93	Zr-94
Zr-95	Zr-96	Nb-93	Nb-94	Nb-95	Mo-0	**Mo-92**	Mo-94
Mo-95	Mo-96	Mo-97	**Mo-98**	**Mo-99**	**Mo-100**	Tc-99	Ru-96
Ru-98	Ru-99	Ru-100	Ru-101	Ru-102	**Ru-103**	Ru-104	Ru-105
Ru-106	Rh-103	Rh-105	Pd-102	Pd-104	Pd-105	Pd-106	Pd-107
Pd-108	Pd-110	Ag-107	Ag-109	Ag-111	Cd-0	Cd-106	Cd-108
Cd-110	Cd-111	Cd-112	Cd-113	Cd-114	**Cd-115(m)**	Cd-116	In-0
In-113	In-115	Sn-112	**Sn-113**	Sn-114	Sn-115	Sn-116	Sn-117
Sn-118	Sn-119	Sn-120	Sn-122	**Sn-123**	Sn-124	**Sn-125**	Sb-121
Sb-123	Sb-124	**Sb-125**	**Sb-126**	Te-120	Te-122	Te-123	Te-124
Te-125	Te-126	Te-127(m)	Te-128	**Te-129(m)**	Te-130	I-127	I-129
I-130	I-131	**I-135**	**Xe-123**	Xe-124	Xe-126	Xe-128	Xe-129
Xe-130	Xe-131	Xe-132	Xe-133	Xe-134	Xe-135	Xe-136	Cs-133
Cs-134	Cs-135	**Cs-136**	Cs-137	**Ba-130**	**Ba-132**	**Ba-133**	Ba-135
Ba-136	Ba-137	Ba-138	Ba-140	**La-138**	La-139	La-140	**Ce-136**
Ce-138	**Ce-139**	Ce-140	Ce-141	Ce-142	Ce-143	Ce-144	Pr-141
Pr-142	Pr-143	Nd-142	Nd-143	Nd-144	Nd-145	Nd-146	Nd-147
Nd-148	Nd-150	Pm-147	Pm-148	Pm-148(m)	Pm-149	**Pm-151**	Sm-144
Sm-147	Sm-148	Sm-149	Sm-150	Sm-151	Sm-152	Sm-153	Sm-154
Eu-151	Eu-152	Eu-153	Eu-154	Eu-155	**Eu-156**	**Eu-157**	Gd-152
Gd-153	Gd-154	Gd-155	Gd-156	Gd-157	Gd-158	Gd-160	Tb-159
Tb-160	**Dy-156**	**Dy-158**	Dy-160	Dy-161	Dy-162	Dy-163	Dy-164
Ho-165	**Er-162**	**Er-164**	Er-166	Er-167	**Er-168**	**Er-170**	Lu-175
Lu-176	Hf-0	Hf-174	Hf-176	Hf-177	Hf-178	Hf-179	Hf-180
Ta-181	Ta-182	W-0	W-182	W-183	W-184	W-186	Re-185
Re-187	**Ir-191**	**Ir-193**	Au-197	**Hg-196**	**Hg-198**	**Hg-199**	**Hg-200**
Hg-201	**Hg-202**	**Hg-204**	**Pb-204**	Pb-206	Pb-207	Pb-208	Bi-209
Ac-225	**Ac-226**	**Ac-227**	**Th-227**	**Th-228**	**Th-229**	Th-230	Th-232
Th-233	**Th-234**	Pa-231	**Pa-232**	Pa-233	U-232	U-233	U-234
U-235	U-235(6)	U-236	U-237	U-238	**U-239**	**U-240**	**U-241**
Np-235	**Np-236**	Np-237	**Np-238**	**Pu-236**	**Pu-237**	Pu-238	Pu-239
Pu-240	Pu-241	Pu-242	Pu-243	Pu-244	**Pu-246**	Am-241	Am-242
Am-242(m)	Am-243	**Am-244**	**Cm-241**	Cm-242	Cm-243	Cm-244	Cm-245
Cm-246	Cm-247	Cm-248	**Cm-249**	**Cm-250**	Bk-249	**Bk-250**	Cf-249
Cf-250	Cf-251	Cf-252	Cf-253	**Cf-254**	Es-253	**Es-254**	**Es-255**
Fm-255							

In bold: added nuclides / materials

These libraries will be delivered in the original SCALE COVERX format. A slightly modified routine EDITCVX from the code ERRORJ [36] was used to subdivide the original libraries into separate COVERX format files for each nuclide or material. This allows for "cleaning-up" the files removing zero covariances, and in particular easier handling and faster ANGELO runs. Although it is in principle possible to process both the original and the separated COVERX files with the ANGELO and LAMBDA codes, the use of separate files is recommended.

Following a request from the UAM (Uncertainty Analysis in Modelling) Expert Group, the authorisation was granted by the SCALE management and DOE to use the group cross-section covariance data now distributed with SCALE-5.1 and SCALE-6.0 for the purpose of the Phase I (Neutronics Phase) benchmark study and in connection with other codes.

2.3.2 Tools for handling and transforming the cross-section relative covariance data

The code ANGELO [45] [46] is designed for the interpolation of the multi-group covariance matrices from the original to a user defined energy structure which is also distributed for the convenience of the users. The algorithm used in the ANGELO code is relatively simple; therefore the interpolations involving the energy group structures which are very different from the original one (such as large difference in the number of energy groups) are to be avoided as they may not be accurate. ANGELO does not carry out cross-section and flux weighting; therefore the interpolations to group structures which differ significantly from the original should be avoided (especially if the number of groups is reduced considerably). Still, the procedure tends to be conservative. The interpolation procedure was found to give reliable results if the number of groups changed by up to a factor of 4. In this range the procedure can therefore be considered as an adequate and easy-to-use alternative to more rigorous methods, like the ERRORR module of NJOY. Several input formats are available for the covariance files: BOXR, COVERX and several flexible text file formats. The output format is COVFILS (recommended) and different binary formats. The COVFILS format is native of NJOY [34] [35], which allows using the NJOY module COVR to perform covariance plotting and output formatting operations, such as transformation to the compact BOXR format. The utility programmes of ERRORJ can be also used to convert COVFILS format to COVERX. The input description is provided in Appendix VI.

LAMBDA [46], [47] is a programme used to verify some mathematical properties and the physical consistency of the data and the interpolation procedure, in particular the positive definiteness of the multi-group covariance matrices. The trace and the number of positive, negative, and zero eigenvalues are calculated and the matrix is classified on this basis. The correlation matrix is tested to determine if any element exceeds unity. This quality verification is highly recommended before using the covariance information to data consistency analyses with integral experiments and to data adjustment. Accepted input formats are BOXR and COVERX. The input description is provided in Appendix VI.

Initially ANGELO-LAMBDA with the corresponding library ZZ-SCALE5.1/COVA-44G was distributed to the participants of the OECD UAM benchmark. These utility programmes for interpolation and mathematical verification of the matrices were extended to handle the 44-group covariances available in SCALE-5.1 for the work carried out within the Expert Group on UAM. Next, the updated ANGELO-LAMBDA with the corresponding library ZZ-SCALE6/COVA-44G was distributed among the OECD UAM benchmark participants. These utility programmes for interpolation and mathematical verification of the matrices were extended to handle the 44-group covariances available in SCALE-6.0 again for the work carried out within the expert group on UAM.

The SCALE library is based on a 44-group structure. For other group structures, NEA/OECD has provided the tools for handling and transforming the cross-section covariance in a consistent way (ANGELO and LAMBDA – last update: 5 February 2010). ANGELO2.3 code is used for interpolation of covariance matrices to user defined energy group structure; only file-33 covariance matrices can be treated. (Cross-correlations between reactions are treated correctly but not cross-correlations between nuclides). The advantages are easy to use and are a fast alternative to NJOY processing while the disadvantages are

that no flux or cross-section weighting is involved. Please note that the processing of fission spectra covariances by ANGELO code may not preserve the normalisation of the matrix (zero-sum rule), therefore the use of constrained sensitivity method as coded in SAGEP and SUSD3D is mandatory to determine the corresponding uncertainties. LAMBDA2.3 code is used for verification of mathematical properties of covariance matrices.

2.4 Test problems

Nuclear data uncertainties in the evaluated NDLs obtained from analysis of experimental differential data and nuclear models are stored as variance and covariance data. Within the framework of Exercise I-1, the covariance data library is processed in a multi-group format. To propagate the uncertainty, the final multi-group cross-section libraries and associated uncertainties should be consistent with the requirements of the intended lattice physics codes.

Evaluation of covariance matrices to be used in the analysis

The variance and covariance data used should be evaluated prior to the propagation of uncertainty. In the analysis of uncertainty, covariance matrices provide the framework on which the evaluation of uncertainty is based. The outcome of the uncertainty calculations is directly affected by the quality of the covariance matrices.

Equation 3, below, provides a technique with which participants can evaluate the covariance matrices used in their analyses. The effective uncertainty will provide an overview of a "size of the covariance matrix" and will enable participants to evaluate different covariance matrices.

- Participants are required to identify five nuclide reactions that contribute the most to the uncertainty in k_{inf}. For comparison purposes a simple measure of propagation of uncertainties, a one-group effective uncertainty for each nuclide reaction, is requested. These one-group effective uncertainties can be calculated using the following Equation 3 or Equation 4:

  $$\text{One-group effective cross-section uncertainty } (\Delta^2) = \sum \Delta^2_g \quad (3)$$
  $$= \sum \alpha_{x,g} \bullet \text{cov}\,(x, y)_g \bullet \alpha_{y,g}$$

  where

$\Delta^2 = \sum \Delta^2_g$	summation of Δ^2_g from energy group 1 to group G
$\Delta^2_g = \alpha_{x,g} \bullet \text{cov}\,(x_g, y_g) \bullet \alpha_{y,g}$	each group uncertainty is weighted by x reaction and y reaction
$\alpha_{x,g} = \sigma_{g,x}[\varphi_{g,x}/\varphi_T] / \sigma_x$	weighting factor based on data from x reaction
$\alpha_{y,g} = \sigma_{g,y}[\varphi_{g,y}/\varphi_T] / \sigma_y$	weighting factor based on data from y reaction
cov (x,y) =	relative covariance matrix between reaction type x and reaction type y
$\sigma_{x,g}$, $\sigma_{y,g}$ =	flux averaged multi-group effective cross-sections
σ_x , σ_y =	flux averaged one-group effective cross-sections
x =	neutron reaction type
y =	neutron reaction type
φ_g =	group flux
φ_T =	summation of group fluxes

  Suggestions were made regarding the weighting factor, the calculation of α based on light water reactor spectrum should be used in lieu of the above calculation which is based on group flux ratio. The suggested spectra are given below. These spectra are based on energy of the neutrons rather than group fluxes. Thus, in the calculation of α, the group flux [φ (E)] is replaced with ω (E).

  For 10^{-5} eV <E < 0.125 eV, use $\omega(E) = C_1 E e^{-E/kT}$ (Maxwellian Thermal Spectrum)

For 0.125 eV <E < 820.8 keV, use ω (E) = C_2/E (Slowing-Down Spectrum)

For 820.8 keV < E< 20 MeV, use ω (E) = $C_3\sqrt{E}\ e^{-E/1.273}$ (Fission Spectrum)

Where

C_1 = 9498.4 [ev^{-2}]

C_2 = 1

C_3 = 2.5625 [$Mev^{-1.5}$]

Figures 1 and 2 illustrate the one-group effective cross-section uncertainty calculation procedure using as example a 44-group covariance matrix weighted by reaction x and reaction y.

Figure 1: Calculation of one-group effective cross-section uncertainty

$$\Delta^2_1 = [\alpha_{x,1} \bullet \mathrm{cov}(x_1,y_1) \bullet \alpha_{y,1}] + [\alpha_{x,2} \bullet \mathrm{cov}(x_2,y_1) \bullet \alpha_{y,1}] + \ldots\ldots\ldots\ldots [\alpha_{x,44} \bullet \mathrm{cov}(x_{44},y_1) \bullet \alpha_{y,1}]$$

$$\Delta^2_2 = [\alpha_{x,1} \bullet \mathrm{cov}(x_1,y_2) \bullet \alpha_{y,2}] + [\alpha_{x,2} \bullet \mathrm{cov}(x_2,y_2) \bullet \alpha_{y,2}] + \ldots\ldots\ldots\ldots [\alpha_{x,44} \bullet \mathrm{cov}(x_{44},y_2) \bullet \alpha_{y,2}]$$

$$\bullet$$

$$\bullet$$

$$\bullet$$

$$\Delta^2_{44} = [\alpha_{x,1} \bullet \mathrm{cov}(x_1,y_{44}) \bullet \alpha_{y,44}] + [\alpha_{x,2} \bullet \mathrm{cov}(x_2,y_{44}) \bullet \alpha_{y,44}] + \ldots\ldots\ldots [\alpha_{x,44} \bullet \mathrm{cov}(x_{44},y_{44}) \bullet \alpha_{y,44}]$$

$$\Delta^2_{\mathrm{effective}} = \Delta^2_1 + \Delta^2_2 + \Delta^2_3 + \ldots\ldots\ldots\ldots\ldots\ldots\ldots\ldots\ldots\ldots\ldots\ldots\ldots\ldots + \Delta^2_{44}$$

In cases, where reaction x and reaction y are the same, i.e. ^{235}U (n, fission) and ^{235}U (n, fission), then the weighting factor matrix of one reaction is a transpose of the same weighting factor matrix.

One-group effective cross-section uncertainty (Δ^2) $= \sum \Delta^2_g$

$= \sum \alpha_{x,g}{}^T \bullet \mathrm{cov}(x, x)_g \bullet \alpha_{x,g}$

$= \sum [\alpha_g]^T \bullet [\mathrm{cov}(x, x)_g] \bullet [\alpha_g]$ (4)

Figure 2: Depiction of 44-group covariance matrix, weighting factor matrices and, uncertainty matrix

	α_{x1}	α_{x2}	•	•	•	•	•	•	α_{x44}	
α_{y1}	$\mathrm{cov}(x_1,y_1)$	$\mathrm{cov}(x_2,y_1)$	•	•	•	•	•	•		Δ^2_1
αy_2	$\mathrm{cov}(x_1,y_2)$	$\mathrm{cov}(x_2,y_2)$								Δ^2_2
•	•		•							•
•	•			•						•
•	•				•					•
•	•					•				•
•	•						•			•
•	•							•		•
α_{y44}	$\mathrm{cov}(x_1,y_{44})$								$\mathrm{cov}(x_{44},y_{44})$	Δ^2_{44}

In each matrix, the variances are identified by the diagonal values inside the matrix. If the weighting factor (α) is set to 1 the calculation will yield a flat-weighted one-group effective uncertainty that will be used for future comparisons.

Analysis of LWR pin-cell models

In order to perform a comparative analysis of the multi-group cross-section, uncertainty data obtained after processing test problems are devised or utilised from the previously defined benchmarks (participants can select which test problem to analyse):

- Two-dimensional fuel pin-cell test problems representative of BWR PB-2 [6], PWR TMI-1 [7], and Kozloduy-6 VVER-1000 [8]. The specifications of these three test problems are given subsequently in Figure 1 through Figure 3. The figures include geometry and material specifications. Concerning boundary conditions, participants should apply the following type of boundary conditions in this case:
  - For a "*cylindrical pin-cell*" model, reflective boundary conditions are utilised at the center-line boundary while white boundary conditions are applicable at the peripheries of the cell-model;
  - For a "*square pin-cell*" model, reflective boundary conditions on all surfaces are applied.

  Each pin-cell model should be analysed at Hot Full Power conditions (HFP) as well as Hot Zero Power (HZP) conditions.

  Figures 3, 4 and 5 provide the configuration and operating conditions of the test problems:

Figure 3: Configuration of PB-2 BWR unit cell

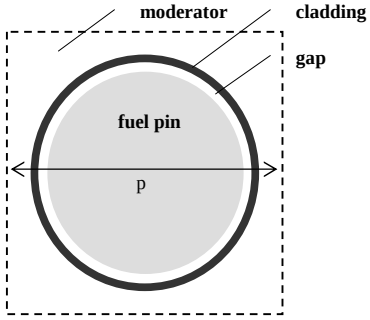

p – pitch of the unit cell

Parameter	Value
Unit cell pitch, [mm]	18.75
Fuel pellet diameter, [mm]	12.1158
Fuel pellet material	UO_2
Fuel density, [g/cm^3]	10.42
Fuel enrichment, [w/o]	2.93
Cladding outside diameter, [mm]	14.3002
Cladding thickness, [mm]	0.9398
Cladding material	Zircaloy-2
Cladding density, [g/cm^3]	6.55
Gap material	He
Moderator material	H_2O

Parameter / Reactor condition	HZP	HFP
Fuel temperature, [K]	552.833	900
Cladding temperature, [K]	552.833	600
Moderator (coolant) temperature, [K]	552.833	557
Moderator (coolant) density, [kg/m^3]	753.978	460.72
Reactor power ,[MWt]	3.293	3 293
Void fraction (%)	-	40

Figure 4: Configuration of TMI-1PWR unit cell

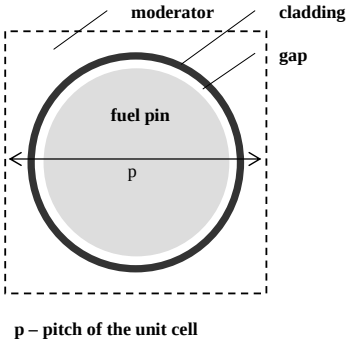

Parameter	Value
Unit cell pitch, [mm]	14.427
Fuel pellet diameter, [mm]	9.391
Fuel pellet material	UO_2
Fuel density, [g/cm^3]	10.283
Fuel enrichment, w/o	4.85
Cladding outside diameter, [mm]	10.928
Cladding thickness, [mm]	0.673
Cladding material	Zircaloy-4
Cladding density, [g/cm^3]	6.55
Gap material	He
Moderator material	H_2O

Parameter / Reactor condition	HZP	HFP
Fuel temperature, [K]	551	900
Cladding temperature, [K]	551	600
Moderator (coolant) temperature, [K]	551	562
Moderator (coolant) density, [kg/m^3]	766	748.4
Reactor power ,[MWt]	2.772	2 772

Figure 5: Configuration of Kozloduy-6 VVER-1 000 unit cell

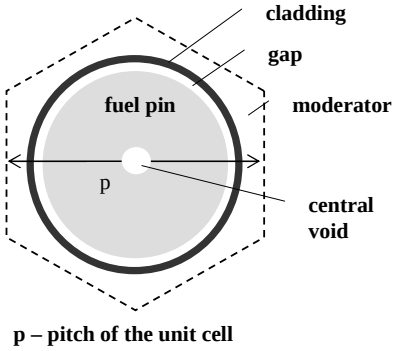

Parameter	Value
Unit cell pitch, [mm]	12.75
Fuel pellet diameter, [mm]	7.56
Fuel pellet material	UO_2
Fuel density, [g/cm^3]	10.4
Fuel enrichment, [w/o]	3.3
Central void diameter, [mm]	1.4
Central void material	dry air
Cladding outside diameter, [mm]	9.1
Cladding thickness, [mm]	0.69
Cladding material	Zr +1% Nb
Cladding density, [g/cm^3]	n/a
Gap material	He
Moderator material	H_2O

Parameter / Reactor condition	HZP	HFP
Fuel temperature, [K]	552.15	900
Cladding temperature, [K]	552.15	600
Moderator (coolant) temperature, [K]	552.15	560
Moderator (coolant) density, [kg/m^3]	767	752.5
Reactor power ,[MWt]	3.000	3 000

Please note that the ^{234}U atom density is equal to 0.0054 wt% for the three unit cells and for the Kozloduy-6 VVER-1 000 unit cell the air composition of central void is 79% nitrogen and 21% oxygen. Additional information for zircaloy, inconel, and stainless-steel is provided in Table 9:

Table 9: Weight percent information from natural concentrations

Nuclide	ID	Zirc-2	Zirc-4	Zirlo
O	8 000	0.125	0.125	0.125
Cr	24 000	0.100	0.100	0.100
Fe	26 000	0.135	0.210	0.210
Ni	28 000	0.055	0.000	0.000
Zr	40 000	98.135	98.115	97.115
Nb	41 000	0.000	0.000	1.000
Sn	50 000	1.450	1.450	1.450
Nuclide	**ID**	**SS-347**	**Inconel-718**	**Inconel-750**
Al	13 000	0.000	0.000	0.980
Si	14 000	0.510	0.350	0.000
Cr	24 000	17.400	18.960	20.140
Mn	25 000	1.990	0.870	0.990
Fe	26 000	68.350	27.930	8.880
Ni	28 000	11.700	51.190	69.020

To enhance the differences between the three cell cases (PWR, BWR and VVER) for the Exercise I-1, the HFP case of the BWR is defined to be analysed at 40% void fraction (with a corresponding moderator density (ρ) of 460.72 kg/m^3) instead of 0%. Hence the PWR and BWR cases are for square pitch but with different spectra, while the VVER case is for triangular pitch. The PWR MOX pin cell case at HFP conditions is also added to Exercise I-1. It is based on the information and conditions provided in Figures 11 and 12 of Chapter 3. The MOX 9.8% Pu composition is selected as a test case to be analysed in Exercise I-1.

For each test problem, k_{eff} (k_∞), and its associated uncertainties based on the multi-group covariance matrices available are requested. The uncertainty in k_{eff} should be presented in terms of [%k] and not [%Δk/k]. In addition, the top five contributors of the uncertainty in k_{eff} are also requested in order to identify neutron-nuclide reactions that contribute to most of the uncertainties. Further, one-group effective uncertainties are also requested for comparison purposes as some manipulations of the covariance matrices are required prior to criticality analysis. Participants are encouraged to submit the one-group effective uncertainties, one-group effective variances, and un-weighted one-group effective uncertainties of the top five nuclide contributors identified in the previous section of this exercise.

In addition, the microscopic absorption cross-section and its uncertainties for both ^{235}U and ^{238}U are requested as well as the microscopic fission cross-section and its uncertainties for both ^{235}U and ^{238}U.

Validation of the calculated uncertainties against the experimental values

- Fuel pin-cell test problems from the KRITZ-2 LEU critical experiments [48] [49], see Table 10: the KRITZ-2:1 and KRITZ-2:13 experiments at two different temperatures and two boron concentrations are selected for the purposes of the OECD LWR UAM benchmark since their rod pitch sizes are similar to those of lattices present in the PB-2 and TMI-1 cores. For this exercise, the pin-cell should be modelled with no boron present. Tables 11 and 12 provide the information needed to perform the KRITZ-2:1 and KRITZ-2.13 pin-cell analysis. An additional test problem

from the KRITZ-2:19 with MOX fuel is also included as a test case and its specification is shown in Table 13. Further information on specifications and results are available in [49].

Table 10: Summary of critical configuration specifications

Experiment	**KRITZ-2:1**		**KRITZ-2:13**		**KRITZ-2:19**	
Fuel	UO_2, 1.86 wt.% ^{235}U		UO_2, 1.86 wt.% ^{235}U		MOx, 1.5 wt.% PuO_2 91.41 at.% ^{239}Pu	
Fuel pellet diameter (mm)	10.58		10.58		9.45	
Clad outer diameter (mm)	12.25		12.25		10.79	
Rod pitch (mm)	14.85		16.35		18.00	
Number of fuel rods	44 x 44		40 x 40		25 x 24	
Temperature (°C)	19.7	248.5	22.1	243.0	21.1	235.9
Boron concentration (ppm)	217.9	26.2	451.9	280.1	4.8	5.2
Water height (mm)	652.8	1055.2	961.7	1109.6	665.6	1000.1

Table 11: Specifications for KRITZ-2:1 LEU critical experiment

KRITZ-2:1 Experiments	**Cold**	**Hot**
Temperature (˚C)	19.7	248.5
Fuel material	UO_2	UO_2
Fuel enrichment	1.86 w/o ^{235}U	1.86 w/o ^{235}U
Fuel pellet density (g/cm^3)	10.145	10.06879
Fuel pellet diameter (mm)	10.58	10.6066
Cladding material	Zircaloy-2	Zircaloy-2
Cladding density (g/cm^3)	6.50600	6.47484
Cladding outer diameter (mm)	12.25	12.2696
Cladding thickness (mm)	0.74	0.7412
Fuel pitch (mm)	14.85	14.9112
Fuel pitch type	square	square

Table 12: Specifications for KRITZ-2:13 LEU critical experiment

KRITZ-2:13 Experiments	**Cold**	**Hot**
Temperature (˚C)	22.1	243.0
Fuel material	UO_2	UO_2
Fuel enrichment	1.86 w/o ^{235}U	1.86 w/o ^{235}U
Fuel pellet density (g/cm^3)	10.145	10.07140
Fuel pellet diameter (mm)	10.58	10.6057
Cladding material	Zircaloy-2	Zircaloy-2
Cladding density (g/cm^3)	6.50600	6.47591
Cladding outer diameter (mm)	12.25	12.2689
Cladding thickness (mm)	0.74	0.7411
Fuel pitch (mm)	16.35	16.4150
Fuel pitch type	Square	Square

Table 13: Specification for KRITZ-2.19 LEU critical experiment

KRITZ-2:19 Experiments	Cold	Hot
Temperature (˚C)	21.1	235.9
Fuel material	MOX	MOX
Fuel enrichment	1.5 w/o PuO_2	1.5 w/o PuO_2
Fuel pellet density (g/cm^3)	9.58	9.55126
Fuel pellet diameter (mm)	9.45	9.4642
Cladding material	Zircaloy-2	Zircaloy-2
Cladding density (g/cm^3)	6.506	6.47674
Cladding outer diameter (mm)	10.79	10.8062
Cladding thickness (mm)	0.67	0.671
Moderator material	water	water
Fuel pitch (mm)	0.99793	0.81909
Fuel pitch type	square	square

VVER physics experiments [49[9]] [59[10]] performed at the critical facility of the Russian Research Center "Kurchatov Institute" (RRC KI) are selected for the purposes of the OECD LWR UAM benchmark since their rod pitch sizes are similar to those of lattices present in the Kozloduy-6 and Kalinin-3 cores. Their information can be found in the above-mentioned references.

For each test problem, k_{eff} (k_∞), and its associated uncertainties based on the multi-group covariance matrices available are requested. The uncertainty in k_{eff} should be presented in terms of [%k] and not [%Δk/k]. In addition, the top five neutron-nuclide contributors of the uncertainty in k_{eff} are also requested in order to identify neutron-nuclide reactions that contribute to most of the uncertainties. Further, one-group effective uncertainties are also requested for comparison purposes as some manipulations of the covariance matrices are required prior to criticality analysis.

In addition, the microscopic absorption cross-section and its uncertainties for both ^{235}U and ^{238}U are requested as well as the microscopic fission cross-section and its uncertainties for both ^{235}U and ^{238}U.

One of the objectives of the benchmark is to provide recommendations for physical and numerical models suitable for reactor physics and uncertainty analysis. For that purpose, participants will be requested to provide information about the models they use. If necessary, clusters of models/approaches can be defined for a more consistent comparison of the results. Continuous energy Monte Carlo (MCNP5) solutions with converged eigenvalue and fission source distributions will be provided for each test problem. The statistical uncertainties in the reference Monte Carlo calculations will be evaluated by the benchmark team. The reference solutions with Monte-Carlo simulations are very valuable and several calculations with different nuclear data libraries will be provided in order to assess the effect of the evaluated nuclear data on well-defined problems.

In the calculations of the above-described test problems the participants have to utilise their multi-group cross-section libraries (input to their lattice physics codes) and associated uncertainties. They can utilise their own Sensitivity/Uncertainty (S/U) tools to propagate cross-section uncertainties to calculate quantities of interest in nuclear analysis or the ones available at NEA/OECD – such as SUSD3D [50] – and TSUNAMI [41] at ORNL.

The objective of Exercise I-1 is to address the uncertainties due to the basic nuclear data as well as the impact of processing the nuclear and covariance data with a primary focus on the microscopic cross-sections and their uncertainties. Within Exercise I-1 the uncertainties in evaluated NDLs are propagated

[9] PFacility-VVER-EXP-001

[10] LEU-COMP-THERM-061

into multi-group microscopic cross-sections used as an input by their lattice physics codes. The output uncertainties of Exercise I-1 are input uncertainties in Exercise I-2.

Extension to Exercise I (I-1) denoted as I-1b (PWR curnup pin-cell benchmark) was introduced in order to address the uncertainties in the *depletion calculation* due to the basic nuclear data as well as the impact of processing the nuclear and covariance data. The Exercise I-1b is defined in Appendix VIII.

Chapter 3: Definition of Exercise I-2: lattice physics

This exercise includes the propagation of input uncertainties, defined below, through lattice physics calculations to target and output uncertainties in evaluated lattice-averaged (homogenised assembly/node) parameters e.g. few-group homogenised nodal parameters such as cross-sections, assembly discontinuity factors, form functions and k_{inf}. The input uncertainties, which result in uncertainties in prediction of lattice-averaged parameters and which need to be accounted for and propagated, arise from:

- multi-group cross-section uncertainties (multi-group cross-section covariance matrix);
- uncertainties associated with methods and modelling approximations utilised in lattice physics codes;
- fuel/assembly manufacturing uncertainties.

In order to propagate the input uncertainties through lattice physics calculations to determine uncertainties in output lattice-averaged parameters within the framework of Exercise I-2 the utilisation of a lattice physics code is necessary. Participants can use/select their own lattice physics codes in conjunction with their own UA and SA tools for the purposes of this exercise.

3.1 Discussion of input, propagated, and output uncertainties

In the current established calculation scheme for LWR design and safety analysis, multi-group microscopic cross-section libraries are an input to lattice physics calculations. The multi-group cross-section uncertainties (multi-group cross-section covariance matrix) should be obtained by participants as output uncertainties within the framework of Exercise I-1. In Exercise I-2 multi-group cross-section uncertainties are input uncertainties and must be propagated through the lattice physics calculations to few-group cross-section uncertainties (few-group covariance matrix). All cross-section uncertainties are assumed to follow normal Gaussian distributions and only the first and second moments of the uncertainty distributions, i.e. the means and covariances, are to be propagated through the calculations [51] [52]. The propagation of the cross-section uncertainties is the most important part of Exercise I-2.

The other input uncertainties in Exercises I-2 are new uncertainties added during the cross-section generation process. Methodological uncertainties, which are associated with methods and modelling approximations utilised in lattice physics codes, should be assessed. Different transport methods have been utilised in lattice physics codes such as the Collision Probabilities Method (CPM), the Method of Characteristics (MOC), S_n, P_n, etc. Depending on the availability of different methods in the lattice code of choice, the related uncertainties can play a smaller or larger role.

Based on the discussions among the benchmark participants during the UAM-4 workshop, the following topics were discussed and agreed upon:

Diffusion coefficient

The definition of diffusion coefficient is as follows:

$$D = \frac{1}{3\Sigma_{transport}} \qquad (5)$$

Transport cross-section

The definition of transport cross-section is as follows:

$$\sum_{transport} = (\mathbf{1} - \overline{\boldsymbol{\mu}}) \sum_{scattering} - \sum \boldsymbol{a} \qquad (6)$$

where $\overline{\mu} = \frac{2}{3A}$ and A = nuclear mass number

In addition, the energy cut-off point of 0.625 eV should be used for collapsing the cross-section into two energy groups.

Thermal expansion coefficient

In the unit fuel cell, thermal expansion as a result of increasing temperature causes changes in the volume density which, in turn, changes the number density. This temperature effect changes the calculation of the macroscopic cross-sections and should be addressed in the evaluation of the uncertainties. In addition, thermal expansion affects the calculation of the linear power density as the calculation reflects the temperature drop across the fuel element. Table 14 presents linear thermal expansion coefficients for selected materials:

Table 14: Linear thermal expansion coefficients

Material	Temperature (°C)	Linear thermal expansion coefficient [x10^{-6}]/K
Unirradiated UO_2 (95% theoretical density)	540 – 2700	17.5
SS-304	340	17.3
Zircaloy-4	340	6.1

Kinetic parameters

The delayed neutron fraction and decay constants are to be considered in six delayed neutron families (groups). The integral uncertainties are to be evaluated from the literature. The formula for collapsing kinetics parameters and calculating k_{eff} and propagation of their uncertainties is available in Appendix VII. The uncertainties in delayed neutron yield and its distribution in delayed groups are to be evaluated.

The participants are responsible for performing spatial discretisation and angular discretisation convergence studies with their lattice physics codes in order to remove the uncertainties associated with numerical approximations (numerical method uncertainties) and reduce the uncertainties associated with neutron transport method (physics uncertainties) used in lattice physics codes. The method related contribution of uncertainty can be derived from earlier benchmarks conducted within the NEA/OECD.

In the current LWR standard calculation scheme (utilised in industry and regulation) the lattice physics calculations for generation of few-group cross-sections usually apply the following approximations (on which the participants should focus as a second important input uncertainty):

- pin cell homogenisation;
- energy group condensation;
- Assembly homogenisation in single assembly environment.

In order to assess the uncertainties in few-group assembly homogenised cross-sections and other nodal homogenised parameters (Assembly Discontinuity Factors – ADFs, Corner Discontinuity Factors – CDFs, Form Functions) due to utilisation of the above-mentioned approximations, one has to decompose and evaluate the errors of these approximations. Evaluation of the uncertainties introduced with such modelling approximations is important because in some situations these approximations work well and in others they do not. This can be accomplished by designing appropriate 2-D mini-core test problems (color-sets) [53] in addition to 2-D single assembly models with reflective boundary conditions. The latter are the base models for cross-section generation with the exception of reflector cross-sections, which are usually generated in 1-D color-sets. For this reason, 2-D color-set test problems are defined by the benchmark team for this exercise in addition to the single assembly and 1-D color-set models.

The participants should also account for fuel/assembly manufacturing uncertainties such as enrichment, pellet density, cladding dimensions, burnable poison (BP) concentration, and assembly

geometry. Assignment of uncertainty measures in the form of PDFs to all input variables should be considered. For example, the PDFs for pellet dimensions, density, Zr homogenisation for the pin cell, and initial isotopic content can be assumed as normal distributions [54]. For the 2-D TMI-1 PWR assembly model (described below), which utilises the pin cell specifications given in Figure 4, the following manufacturing uncertainties in terms of 3σ are provided in [55] assuming normal distributions for their PDFs:

- fuel density: ± 0.17 g/cm^3;
- fuel pellet diameter: ± 0.013 mm;
- gap thickness: ± 0.024 mm;
- clad thickness: ± 0.025 mm;
- ^{235}U concentration: ± 0.00224 w/o.

For the PB-2 BWR assembly the following are manufacturing uncertainties in terms of 3σ with normal distributions for their PDFs:

- cladding ID: ± 0.04 mm;
- cladding thickness: ± 0.04 mm;
- clad roughness: ± 0.3 μm;
- fuel Pellet OD: ± 0.013 mm;
- fuel density: ± 0.91%;
- pellet roughness: ± 0.5 μm;
- rod fill pressure: ± 0.07 MPa.

For VVER-1 000 assembly cases the following manifacturing uncertainties are selected assuming uniform distributions of their PDFs:

- inner hole diameter - Lower limit (014 cm) and Upper limit (0.17 cm);
- fuel density - Lower limit (10.4 g/cm^3) and Upper limit (10.7 g/cm^3);
- fuel pellet diameter - Lower limit (0.753 cm) and Upper limit (0.756 cm);
- clad inner diameter - Lower limit (0.772 cm) and Upper limit (0.778 cm);
- clad outer diameter - Lower limit (0.905 cm)and Upper limit (0.915 cm);
- ^{235}U concentration (base case: 3.3%) - Lower limit (3.25 %) and Upper limit (3.35 %);
- ^{235}U concentration (base case: 3.0%) - Lower limit (2.95 %) and Upper limit (3.05 %).

The benchmark team will address the propagation of manufacturing, methodological and numerical uncertainties within Exercise I-2 in the final benchmark report on comparative analysis of results for Phase I. The participants are advised to focus mostly on cross-section uncertainty propagation, and if their capabilities and resources allow, to propagate in parallel also with the manifacturing uncertainties in Exercise I-2. The problem with different input uncertainty contributors to be taken into account such as cross-section, manufacturing and modelling uncertainties along with considering inter-parameter correlations of input uncertainties is very challenging.

Within the framework of Exercise I-2 the above-described input uncertainties are propagated through lattice physics calculations to target and output uncertainties in evaluated few (usually two) group lattice-averaged (homogenised assembly/node) parameters. The propagated uncertainties are related to the final few-group lattice-averaged parameters consistent with the input requirements of core simulator codes such as few-group diffusion coefficients, cross-sections, ADFs, CDFs, and kinetics and delayed neutron parameters. In addition to evaluating the above-mentioned few-group uncertainties, the uncertainties of assembly (lattice) based kinetics parameters have to be estimated as propagated uncertainties. With regard to the uncertainty of assembly (lattice) based delayed neutron fractions it should be noted that there are no available covariance matrices for delayed neutron data in evaluated nuclear data files. Relevant publications such as [56] were reviewed in order to collect information based on experiments for the most

important actinides. Based on this information the uncertainty in the calculation of effective neutron fractions for uranium-fuelled thermal spectrum systems was quantified to be ± 3%. Requested for propagated uncertainties are the best-estimate values of the parameter with associated uncertainties where the associated uncertainties are variance-covariance matrices for the few group parameters and for the other parameters (delayed neutron fractions and decay constants) the best-estimate value of the parameter with associated uncertainties where the associated uncertainties are in terms of standard deviation.

The output uncertainties are for specified output parameters for Exercise I-2, used to test (evaluate) the utilised uncertainty method. The output uncertainties for Exercise I-2 include one group effective cross-section uncertainties, k_{inf} (k_{eff}) and associated uncertainties, reaction rates and associated uncertainties, and pin power distribution and associated uncertainties. Requested for these output uncertainties are the best-estimate value of the parameter with associated uncertainties where the associated uncertainties are in terms of standard deviation. The requested "one group effective cross-section uncertainties" are simple measures of evaluation of target uncertainties such few-group cross-section uncertainties. The definition of one group effective cross-section uncertainty is the same as given in Section 2.4.

3.2 Test problems

Different stand-alone neutronics single assembly and mini-core test problems have been designed for the purposes of the Exercise I-2 utilising information from the previous OECD coupled code benchmarks BWR PB-2 [6], PWR TMI-1 [7], and Kozloduy-6 VVER-1 000 [8]. More test cases representative of Generation 3 PWR with a 17×17 fuel lattice (instead of 15×15) at HFP conditions are added based on the specification provided by CEA [14]. The added cases include a PWR MOX assembly case.

- 2-D assembly model with reflective boundary conditions. This is the standard model utilised for fuel assembly cross-section generation in LWR analysis. These problems should be analysed at Hot Zero Power (HZP) conditions as well as Hot Full Power (HFP) conditions as defined in Figures 4, 5 and 6.

  BWR Assembly Model: PB-2 Assembly type 2

  For the BWR single assembly model, assembly type 2 the initial loading of PB-2 plant is chosen for this exercise. The information for the BWR single assembly model is given in Table 16 and Figure 6 through Figure 8. In addition, unit cell information for the BWR test problem is available in Figure 3. For HFP conditions, 40% void with a corresponding moderator density (ρ) of 460.72 kg/m^3) is considered.

Table 15: PB-2 fuel assembly data

Assembly type	2
No. of assemblies, initial core	263
No. of assemblies, Cycle 2	261
Geometry	7×7
Assembly pitch, mm	152.4
Fuel rod pitch, mm	18.75
Fuel rods per assembly	49
Water rods per assembly	0
Burnable poison positions	4
No. of spacer grids	7
Inconel per grid, kg	0.225
Zr-4 per grid, kg	1.183
Spacer width, cm	4.128
Assembly average fuel composition: Gd_2O_3, g	441

UO_2, kg	212.21
Total fuel, kg	212.65

Rod type	Number of rods	Pellet density		Stack density (g/cm^3)	Gd_2O_3 (g)	UO_2 (g)	Stack length (cm)
		UO_2 (g/cm^3)	UO_2+Gd_2O_3 (g/cm^3)				
1	25	10.42	–	10.32	0	4 352	365.76
1s	1	10.42	–	10.32	0	3 935	330.20
2	12	10.42	–	10.32	0	4 352	365.76
3	6	10.42	–	10.32	0	4 352	365.76
4	1	10.42	–	10.32	0	4 352	365.76
5A	3	–	10.29	10.19	129	4 171	365.76
6B	1	10.42	10.29	10.27	54	4 277	365.76

Pellet outer diameter = 1.21158 cm.
Cladding = Zircaloy-2, 1.43002 cm outer diameter × .09398 cm wall thickness, all rods.
Gas plenum length = 40.132 cm.

Figure 6: PB-2 assembly design - Type 2 initial fuel and lattice

Assembly design for Type 2 initial fuel

Rod type	^{235}U (wt.%)	Gd_2O_3 (wt.%)	No. of rods
1	2.93	0	26
2	1.94	0	12
3	1.69	0	6
4	1.33	0	1
5A	2.93	3.0	3
6B	2.93	3.0	1

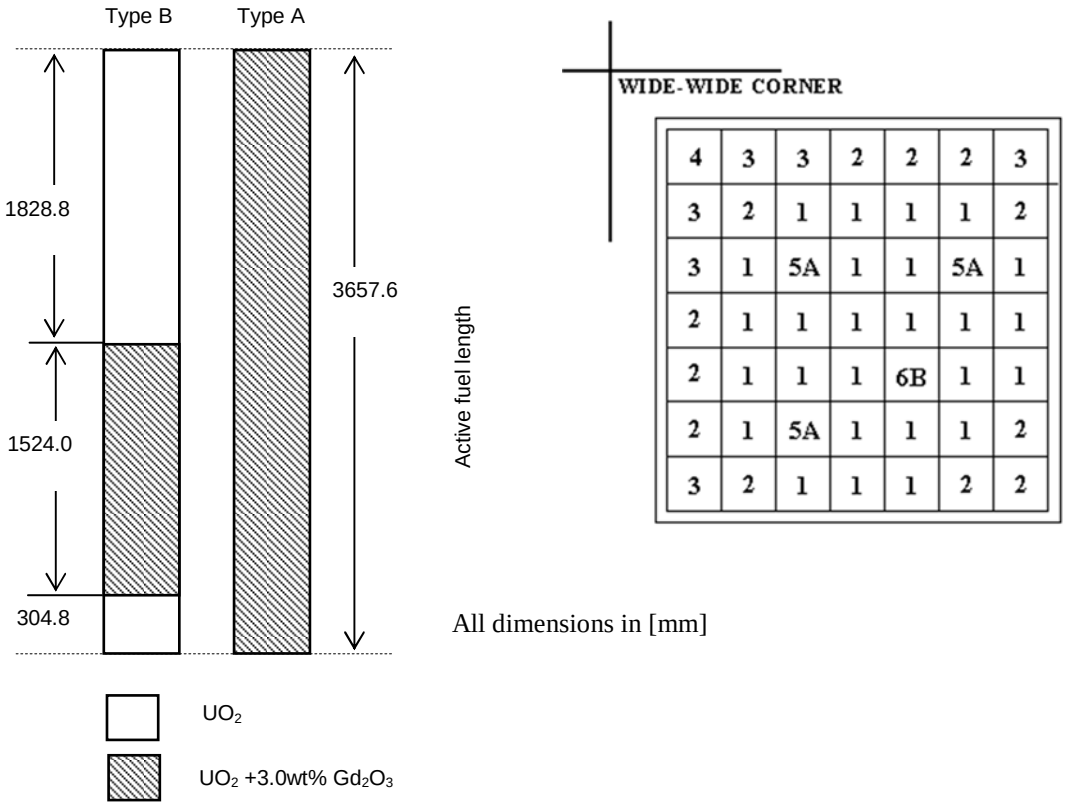

Figure 7: PB-2 assembly design - Type 2 initial lattice

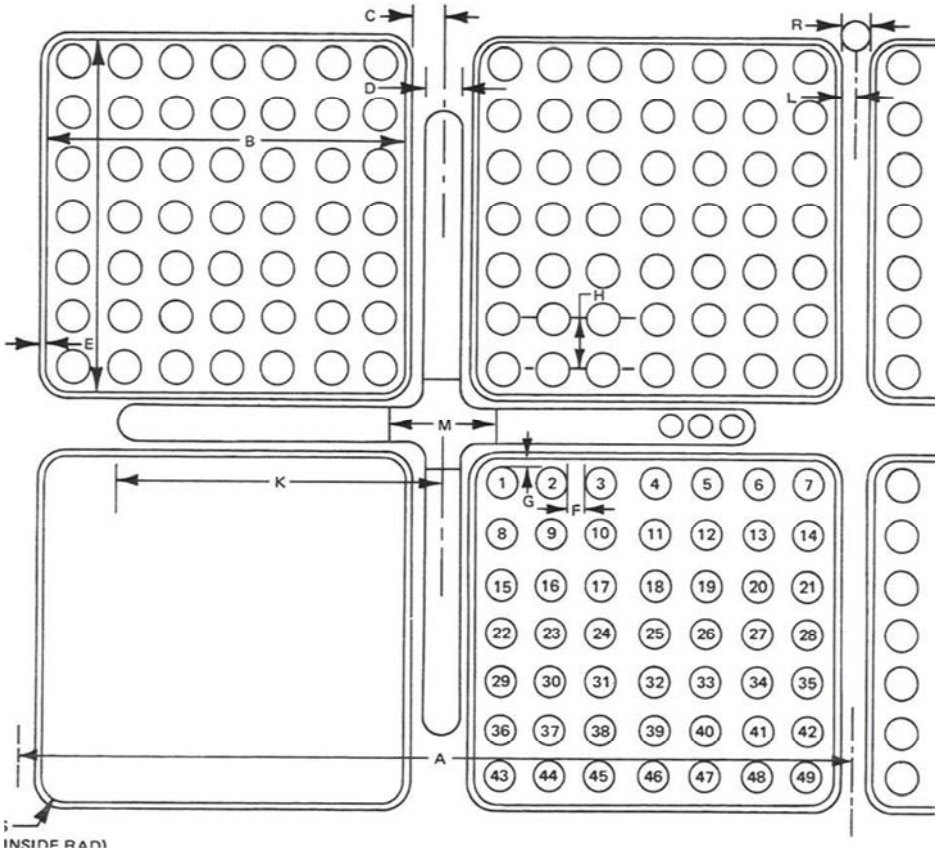

Dim. ID	A	B	C	D	E	F	G	H	I	J
Dim. (cm)	30.48	13.40612	0.9525		0.2032	0.4445	0.36449	1.87452		
Dim. ID	K	L	M	N	O	P	Q	R	S	
Dim. (cm)		0.47498							0.9652	

Figure 8: Control rod blade model and characteristics for PB-2

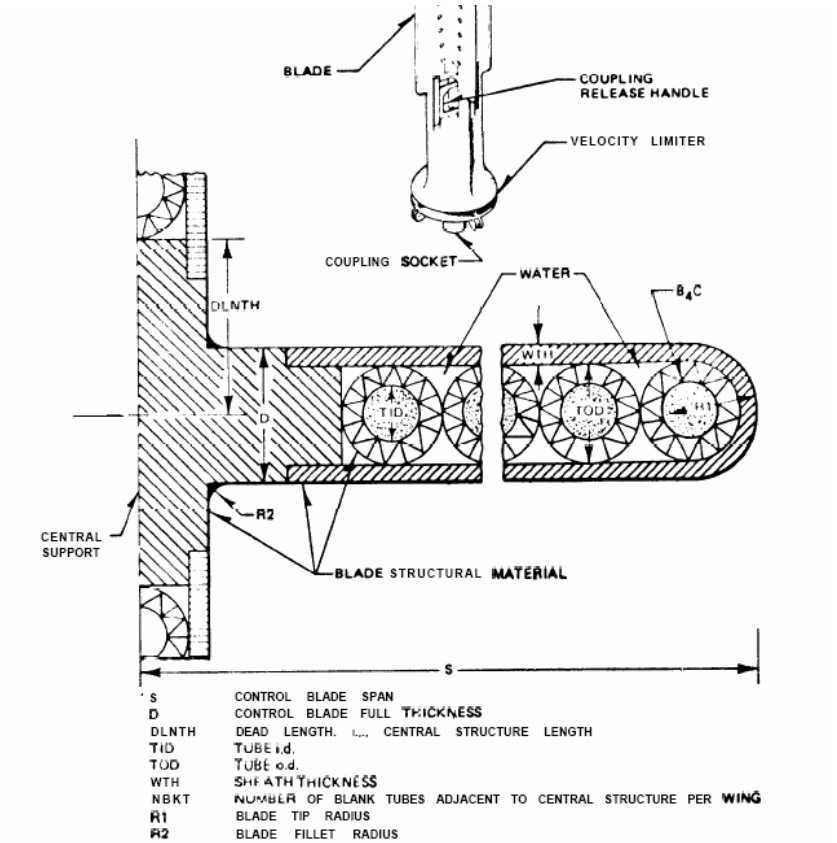

Figure 22. B_4C Control Blade Model (Schematic)

Shape	Cruciform
Pitch, cm	30.48
Stroke, cm	365.76
Control length, cm	363.22
Control material	B_4C granules in Type-304 stainless steel tubes and sheath
Material density	70% of theoretical (2.52 g/cm3)
Number of control material	
Tubes per rod	84
Tube dimensions	0.47752 cm OD by 0.0635 cm wall
Control blade half span, cm	12.3825
Control blade full thickness, cm	0.7925
Control blade tip radius, cm	0.39624
Sheath thickness, cm	0.14224
Central structure wing length, cm	1.98501
Blank tubes per wing	none

PWR Assembly Model: TMI-1

The information for the PWR single assembly model is given in Table 16 and Figure 9, and the PWR fuel pin data is given in Figure 4. There are four gadolinia pins containing integral Gd burnable poisons. The actual mixture of the gadolinia pin is Gd_2O_3+UO_2 with fuel density of 10.144 g/cm^3, the fuel enrichment is 4.12 w/o, and the Gd_2O_3 concentration is 2 wt.%.

Figure 9: TMI-1 assembly design and data

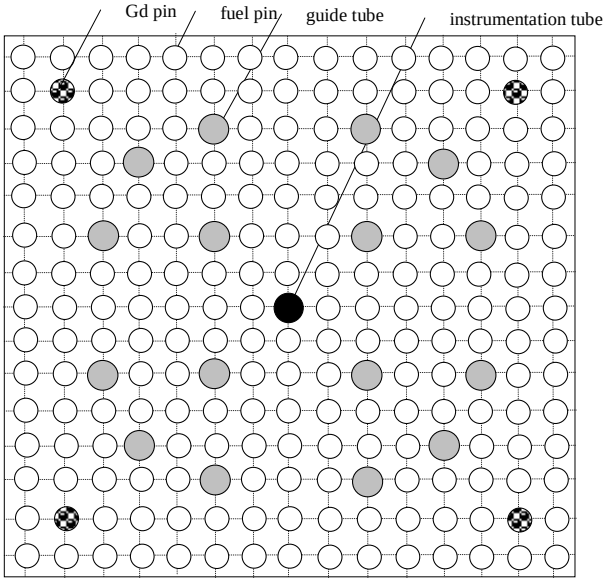

Parameter	Value
Fuel assembly dimensions	15 ×15
Number of fuel rods per FA	208
Number of guide tubes per FA	16
Number of instrumentation tubes per FA	1
Number of Gd pins per FA	4
Fuel rod pitch, mm	14.427
Fuel rod outside diameter, mm	10.922
Fuel pellet diameter, mm	9.390
Cladding thickness, mm	0.673
Guide tube outside diameter, mm	13.462
Guide tube inside diameter, mm	12.649
Instrumentation tube outside diameter, mm	12.522
Instrumentation tube inside diameter, mm	11.201
Fuel assembly pitch, mm	218.110
Gap between fuel assemblies, mm	1.702

Table 16: Additional TMI-1 assembly data

TMI-1 assembly material compositions	
Material	**Composition**
Spacer grids	Zircaloy-4
Central tube	Zircaloy -4
Guide tubes	Zircaloy -4

TMI-1 control rod assembly data	
Item	**Data**
Number of control rods per assembly	16
Outside diameter of control rod, mm	11.2014
Cladding thickness, mm	0.5715
Cladding material	Inconel 625
Absorber material	Ag - 80 %, In - 15%, Cd - 5%
Length of absorber section, mm	3530.6

VVER-1 000 Assembly Model: Kozloduy-6

The information for the VVER single assembly model and compositions data is given in Figure 10 and Table 17.

Figure 10: Kozloduy-6 VVER-100 assembly design and data

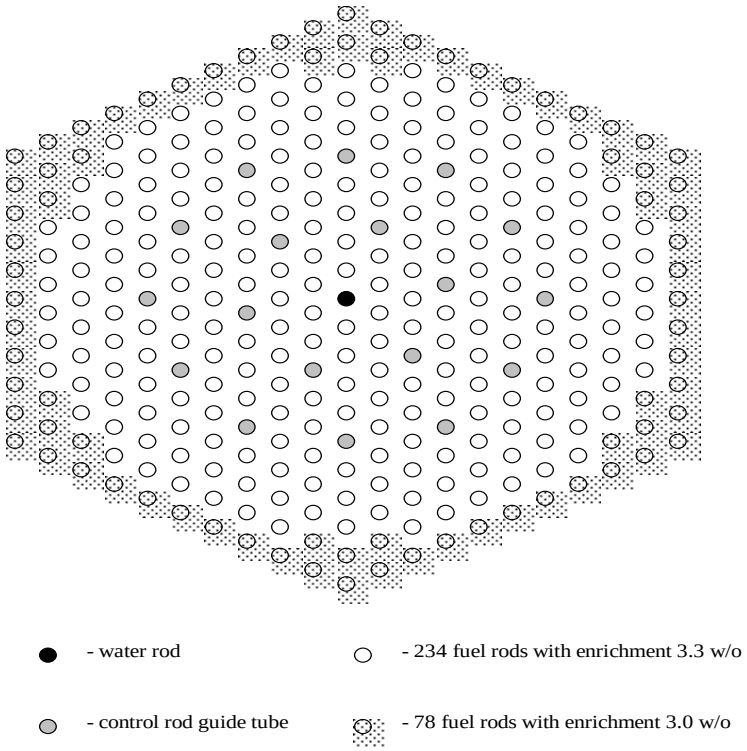

Parameter	Value
Number of fuel rods	312
Number of fuel rods with 3.0 w/o enrichment	78
Number of fuel rods with 3.3 w/o enrichment	234
Number of water rods per FA	1
Number of guide tubes	18
Pellet diameter, mm	7.56
Central void diameter, mm	1.4
Cladding outside diameter, mm	9.1
Cladding thickness, mm	0.69
Fuel rods pitch, mm	12.75
Guide tube outside diameter, mm	12.6
Guide tube inside diameter, mm	11.0
Absorber (control rods) pellet diameter, mm	7.0
Absorber cladding outside diameter, mm	8.2
Water rod outside diameter, mm	11.2
Water rod inside diameter, mm	9.6

Table 17: Kozloduy-6 assembly composition data

Material	Composition
Spacer grids : Steel 08X18H10T; 1.2 % of the FA volume	C - 0.08%, Si-0.8%, Mn-2.0%, Cr-18%, Ni-10%, Ti-0.6%, S-0.02%, P-0.035%, Fe-to 100%
Central tube: E110 Zr + 1% Nb alloy	Zr - 98.722%, Nb - 1.0%, Hf - 0.030%, Fe - 0.050%, Ni - 0.025%, Al - 0.008%, Ti - 0.007%, Si - 0.050%, C - 0.050%, N - 0.007%, O - 0.050%, H - 0.001÷0.002%
Guide tubes: Steel 08X18H10T	C - 0.08%, Si - 0.8%, Mn - 2.0%, Cr - 18%, Ni - 10%, Ti - 0.6%, S - 0.02%, P - 0.035%, Fe - to 100%
Control rods: B_4C	C- 20%, B_{11} - 64.08%, B_{10} - 15.92%

GEN-III Assembly Models [14]

Information for the GEN-III assembly models is provided by Alain Santamarina and Claire Vaglio-Gaudard from CEA and is presented in Tables 18 and 19. There are four assembly types (test cases) available for this exercise.

Table 18: GEN-III unit cell information and operating conditions

Fuel assembly design (HFP conditions)		**HFP conditions for GEN-III fuel pin**	
Parameter	**Value**	**Parameter**	**Value**
Fuel assembly dimensions	17x17	Fuel temperature (K)	900
Number of fuel rods per FA	265	Cladding temperature (K)	610
Number of guide tubes per FA	24	Moderator (coolant) temperature (K)	584
Fuel rod pitch, mm	12.62	Pressure (coolant) (bars)	155
Fuel rod outside diameter, mm	9.487	Reactor power (MWt)	4 250
Fuel pellet diameter (mm)	8.253	Boron concentration (ppm)	1 300
Cladding thickness, mm	0.578	**GEN-III unit cell (HFP conditions)**	
Guide tube outside diameter, mm	12.07	**Parameter**	**Value**
Guide tube inside diameter, mm	11.27	Unit cell pitch (mm)	12.62
Fuel assembly pitch, mm	216.1	Fuel pellet diameter (mm)	8.253
Gap between fuel assemblies, mm	1.560	Cladding outside diameter (mm)	9.487
GEN-III assembly material compositions		Cladding thickness (mm)	0.578
Spacer grids	Zircalloy-4	Cladding material	Zircalloy-4
Central tube	Zircalloy-4	Gap material	He
Guide tubes	Zircalloy-4	Moderator material	H_2O
HZP conditions for GEN-III fuel pin			
Fuel temperature (K)	570	Pressure (coolant) (bars)	155
Cladding temperature (K)	570	Reactor power (MWt)	4.250
Moderator (coolant) temperature (K)	570	Boron concentration (ppm)	1 400

Table 19: Fuel and cladding composition data for GEN-III assemblies

Moderator composition (HFP conditions)	**Isotope**	**10^{24} at/cm^3**	**$UO_2Gd_2O_3$ 2.2% ^{235}U composition**	**Isotope**	**10^{24} at/cm^3**
	H2O	2.340 E-02		U235	4.585E-04
	B10	1.016E-05		U238	2.012E-02
	B11	4.090E-05		O16	4.517E-02
UOx 4.2% ^{235}U composition	Isotope	1024 at/cm3		GD154	5.808E-05
	U235	9.551E-04		GD155	3.952E-04
	U238	2.151E-02		GD156	5.625E-04
	O16	4.493E-02		GD157	4.179E-04
UOx 3.2% ^{235}U composition	Isotope	1024 at/cm3		GD158	6.484E-04
	U235	7.277E-04		GD160	5.834E-04
	U238	2.173E-02	**$UO_2Gd_2O_3$ 1.9% ^{235}U composition**	**Isotope**	**10^{24} at/cm^3**
	O16	4.492E-02		U235	3.960E-04
UOx 2.1% ^{235}U composition	Isotope	1024 at/cm3		U238	2.019E-02
	U235	4.775E-04		O16	4.517E-02
	U238	2.198E-02		GD154	5.808E-05
	O16	4.492E-02		GD155	3.952E-04
				GD156	5.625E-04
				GD157	4.179E-04
				GD158	6.484E-04
				GD160	5.834E-04
MOX 9.8% Pu composition	**Isotope**	**10^{24} at/cm^3**	**MOX 6.5% Pu composition**	**Isotope**	**10^{24} at/cm^3**
	PU238	5.646E-05		PU238	3.750E-05
	PU239	1.226E-03		PU239	8.141E-04
	PU240	5.643E-04		PU240	3.749E-04
	PU241	1.918E-04		PU241	1.274E-04
	PU242	1.755E-04		PU242	1.165E-04
	AM241	2.899E-05		AM241	1.926E-05
	U235	5.349E-05		U235	5.349E-05
	U238	2.080E-02		U238	2.156E-02
	O16	4.620E-02		O16	4.621E-02
MOX 3.7% Pu composition	**Isotope**	**10^{24} at/cm^3**	**Zircalloy-4 composition** (impurities are neglected)	**Isotope**	**10^{24} at/cm^3**
	PU238	2.109E-05		SN116	6.556E-05
	PU239	4.579E-04		SN117	3.433E-05
	PU240	2.108E-04		SN118	1.074E-04
	PU241	7.165E-05		SN119	3.771E-05
	PU242	6.554E-05		SN120	1.420E-04
	AM241	1.083E-05		SN122	1.985E-05
	U235	5.349E-05		SN124	2.442E-05
	U238	2.222E-02		FE56	1.333E-04
	O16	4.622E-02		CR52	6.245E-05
				O16	3.025E-04
				ZR90	2.176E-02
				ZR91	4.692E-03
				ZR92	7.094E-03
				ZR94	7.036E-03
				ZR96	1.110E-03

The assembly descriptions (geometry and materials) are given in Figure 11. The control rods for rodded assembly cases are Ag-In-Cd control rods located in the guide tubes.

Figure 11: GEN-III Assembly descriptions

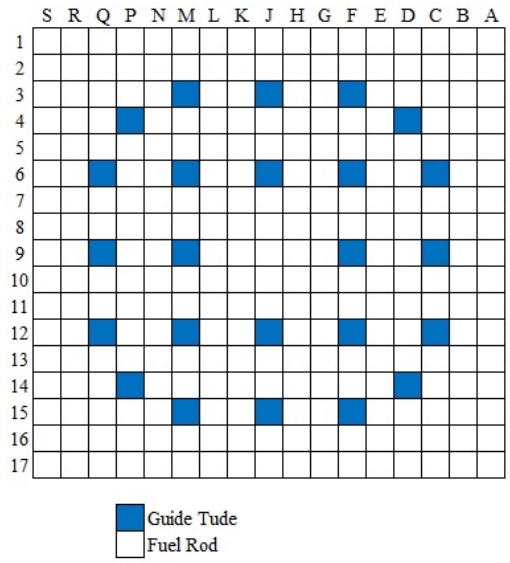

Type 1: UOX 2.1% ^{235}U without UO_2-Gd_2O_3 rods UOX 4.2% ^{235}U assembly without UO_2-Gd_2O_3 rods

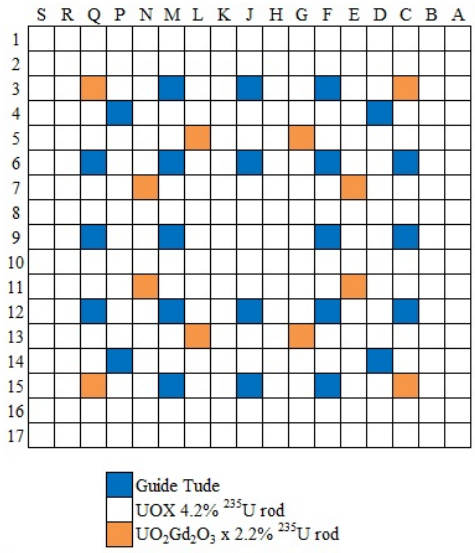

Type 2: UOX 4.2% ^{235}U assembly with 12 UO_2 Gd_2O_3 (2.2% ^{235}U) rods

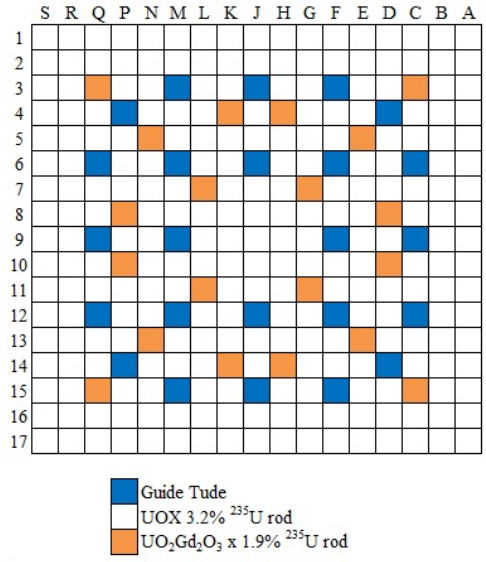

Type 3: UOX 3.2% ^{235}U assembly with 20 UO_2-Gd_2O_3 (1.9% ^{235}U) rods

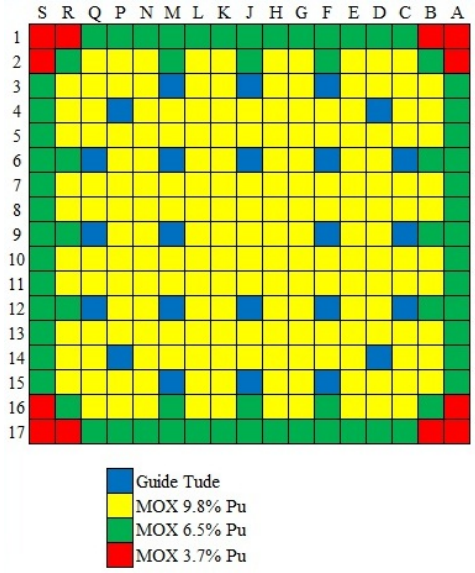

Type 4: MOX assembly (without UO_2-Gd_2O_3 rods)

Based on the agreement, the following output parameters are requested for the specified conditions as a result of the discussions during the UAM-4 workshop:

a) Assembly k_{inf} and associated uncertainties:
   - for HZP of unrodded case;
   - for HZP of rodded case;
   - for HFP of unrodded case;
   - for HFP of rodded case.

b) Homogenised two group cross-sections and associated uncertainties (using 0.625 eV as cut-off point);

c) Covariance matrix for assembly-homogenised two-group cross-sections;

d) Diffusion coefficients (as defined by Equation 5) and associated uncertainties;

e) Two-group pin-cell model uncertainties and two-group assembly model uncertainties to show the effect of homogenisation on the uncertainties;

f) Pin-power distribution and associated uncertainties for:
   - center pin of rodded cases;
   - center pin of unrodded cases
   - corner pin of rodded cases
   - corner pin of unrodded case

- 1-D assembly/reflector model (color set) with reflective boundary conditions on the left boundary and vacuum boundary condition on the right boundary. This is the standard model utilised for reflector cross-section generation in LWR analysis.

The information for the BWR model is given in Figure 12.

Figure 12: PB-2 radial reflector model – dimensions and material compositions

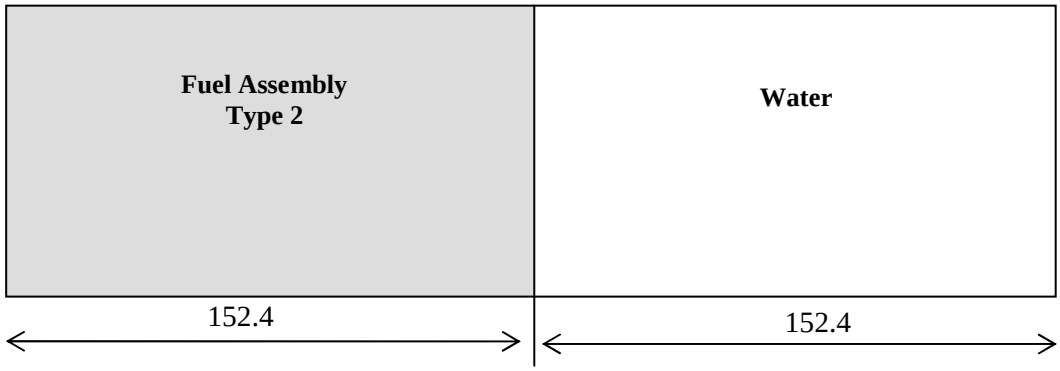

All dimensions in [mm]

Reflector material	Composition
Water (H_2O)	H - 11.19 % ; O - 88.81 %

The information for the PWR model is given in Figure 13.

Figure 13: TMI radial reflector model – dimensions and material compositions

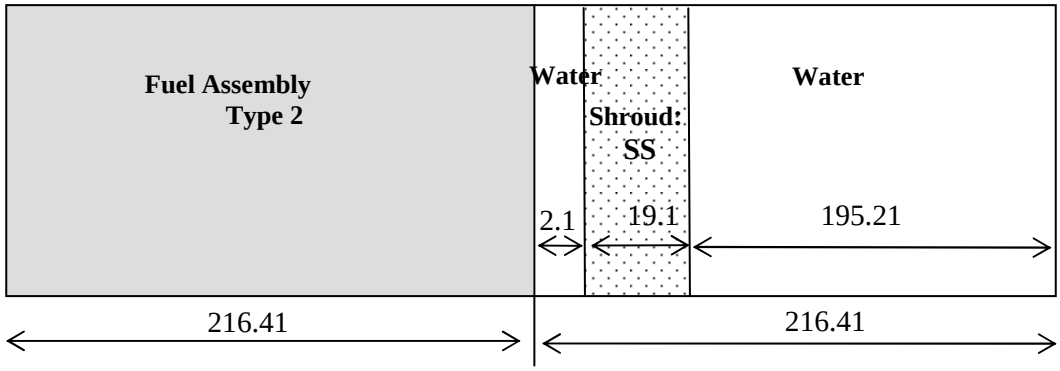

All dimensions in [mm]

Material	Composition
Water (H_2O)	H - 11.19 % ; O - 88.81 %
Shroud (SS)	Stainless steel

The SS is SS304 (Density of 8.03 g/cm3; ^{12}C - 0.08%, ^{55}Mn – 2.00%, ^{31}P – 0.05%, ^{32}S – 0.03%, ^{29}Si - 0.75%, ^{52}Cr – 20.00%, ^{58}Ni – 12.00%, ^{14}N – 0.10%, ^{56}Fe – 64.99%).

The information for the VVER model is given in Figure 14.

Figure 14: Kozloduy-6 radial reflector model – dimensions and material compositions

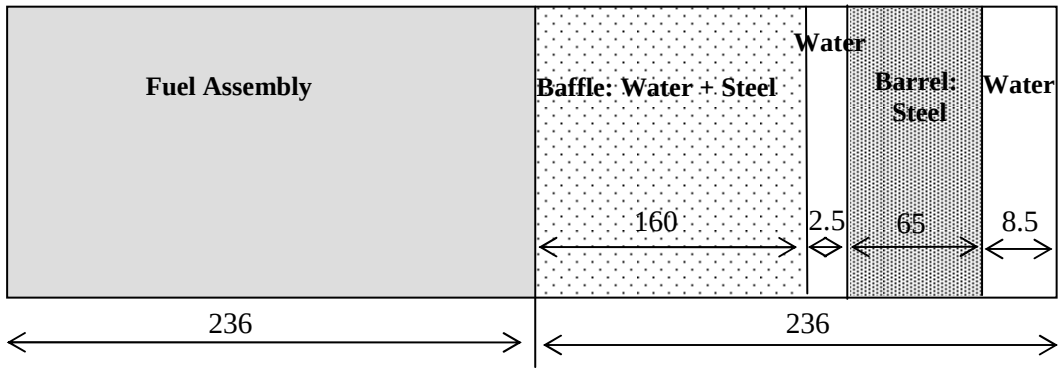

All dimensions in [mm]

Material	Composition
Water (H_2O)	H - 11.19 % ; O - 88.81 %
Barrel: Steel 08X18H10T	C - 0.08%, Si - 0.8%, Mn - 2.0%, Cr - 18%, Ni - 10%, Ti - 0.6%, S - 0.02%, P - 0.035%, Fe - to 100%
Baffle	65.05% - Steel 08X18H10T 34.95% - H_2O

These problems should be analysed at Hot Zero Power (HZP) conditions as well as Hot Full Power (HFP) as defined in Figures 3, 4 and 5. The output uncertainties of the following few-group reflector homogenised parameters will be compared: reflector DFs at the core/reflector interface.

- 2-D assembly color sets (mini-cores). Different mini-core problems were developed involving unrodded and rodded assemblies. Reflective boundary conditions are utilised.

The information for the BWR mini-core is given in Figure 15.

Figure 15: Color-set configuration for PB-2

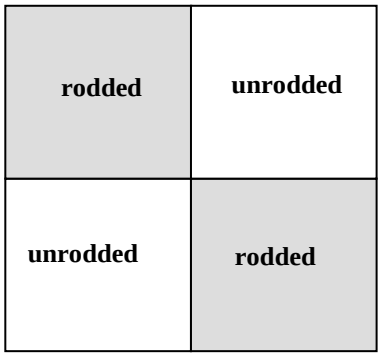

The information for the PWR mini-cores is given in Figure 16.

Figure 16: Color-set configuration for TMI-1

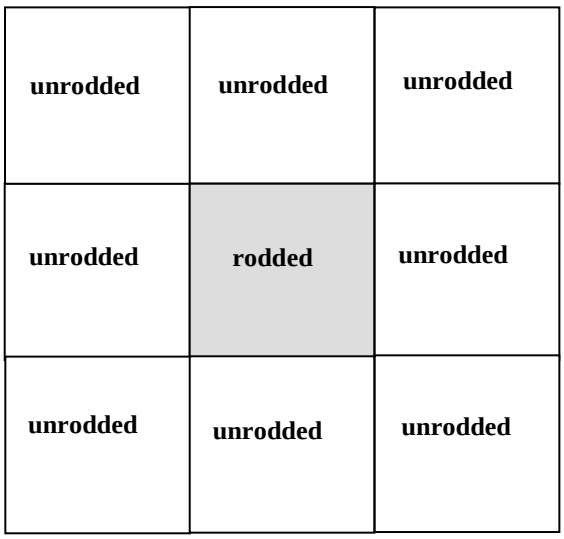

The information for the VVER mini-core is given in Figure 17.

Figure 17: Color-set configuration for Kozloduy-6

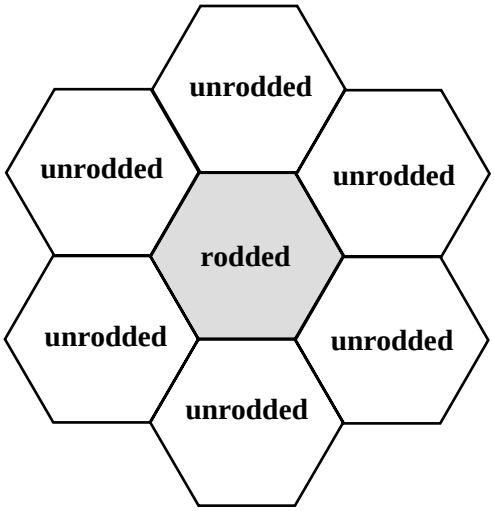

These problems should be analysed at Hot Zero Power (HZP) conditions as well as Hot Full Power (HFP) conditions as defined in Figures 3, 4 and 5.

For each problem the participants should present the mini-core multiplication factors (k_{eff}) and the relative pin powers as well as associated uncertainties due to the few-group cross-section generation process within Exercise I-2.

- It is well known that the available clean core measurements at facilities for thermal systems can be used to assess the performance of nuclear data libraries. That is why the critical configuration (core) test problems from the above-mentioned KRITZ-2 LEU critical experiments [48] [49] - KRITZ-2:1, KRITZ-2:13, KRITZ-2:19 (for which measured data is available) – are also utilised. For each problem the participants have to calculate the configuration multiplication factors (k_{eff}) at "room" and "elevated" temperatures and the relative rod powers of the rods for which the measurements were performed as well as the associated uncertainties. By including the uncertainty or covariance information, the analyst can propagate cross-section data uncertainties through sensitivity studies to the final calculated quantities of interest and compare with the measurement uncertainty.

The KRITZ test problems are also designed as 2-D problems, which utilised experimental axial bucklings to be used for accounting of the axial leakage.

Continuous Monte Carlo (MCNP5) solutions with sufficient statistics to assure not only k_{inf} (k_{eff}) but also fission source convergence will be used as reference solutions for the single assembly and different color-set test problems designed for Exercise I-2. The statistical uncertainties in the reference Monte Carlo calculations will be evaluated by the benchmark team. In addition to the continuous energy multi-group (consistent with the input multi-group structures of the lattice physics codes) MCNP5 cases will be performed in order to show the differences in self-shielding effects.

In the calculations of the above-described test problems the participants can use/select their own lattice physics codes. They can utilise their own Sensitivity/Uncertainty (S/U) tools to propagate cross-section uncertainties to calculate quantities of interest in nuclear analysis or the ones available at NEA/OECD and ORNL.

Exercise I-2 propagates input uncertainties obtained from Exercise I-1 and other input uncertainties added in Exercise I-2. The objective of Exercise I-2 is to obtain uncertainty estimates of k_{inf}, and few group homogenised parameters used in core calculations as a function of the uncertainties discussed above.

The output uncertainties of Exercise I-2 are propagated in Exercises I-3, II-3, III-1 and III-3. The major effort is focused on obtaining uncertainties in two-group homogenised parameters. Provision for few-group (more than two-energy group) homogenised parameters and associated uncertainties with few-group structures selected by participants is made.

Chapter 4: Definition of Exercise I-3: core physics

This exercise consists of core calculations to propagate the input uncertainties to output uncertainties as listed below in evaluated core parameters e.g. core reactivity, power distributions, and rod worth. The input uncertainties, which result in uncertainties in prediction of core parameters and which need to be accounted for and propagated, arise from:

- few-group lattice-averaged (homogenised) cross-section uncertainties;
- approximations in the solution of the transport equation (basic modelling approximations);
- numerical simplifications;
- Variations in geometry.

Understanding the uncertainties in key output reactor core parameters associated with steady-state core simulation is important with regard to introducing appropriate design margins and deciding where efforts should be directed to reduce uncertainties [51]. The propagation of the input uncertainties through core calculations to determine uncertainties in output core parameters within the framework of Exercise I-3 requires utilisation of a core simulator code. Participants can use/select their own core simulator codes in conjunction with their own UA and SA tools for the purposes of this exercise.

4.1 Discussion of input, propagated and output uncertainties

In the current established calculation scheme for LWR design and safety analysis the lattice averaged (homogenised) few-group cross-sections are an input to core calculations. The few-group cross-section uncertainties (few-group covariance matrix) should be obtained by participants as output uncertainties within the framework of Exercise I-2. In Exercise I-3 the few-group cross-section uncertainties are input uncertainties and must be propagated to uncertainties in evaluated stand-alone neutronics core parameters. The propagation of the cross-section uncertainties is the most important part of Exercise I-3. All cross-section uncertainties are assumed to follow normal Gaussian distributions and only the first and second moments of the uncertainty distributions i.e. the means and variances/covariances, are to be propagated through the calculations. If some participants want to take part only in Exercise I-3 (since they have already developed their core models for the benchmark problems discussed below) the benchmark team will provide "reference" input uncertainties (few-group cross-sections supplemented with a few-group covariance matrix). These data will include reference two-group cross-section data and associated variance and covariance matrices for the three representative types of LWRs – TMI-1, PB-2 and VVER-1 000.

The other input uncertainties in Exercises I-3 are new uncertainties added during the core stand-alone calculations. The uncertainties, due to the basic modelling simplifications, include the approximations currently accepted in the nuclear industry and regulation for solving the neutron balance equation. The established standard methodology for core calculation in routine LWR design and safety analysis is based on few-group (mostly two-group) diffusion method. Lately, higher-order transport methods (such as S_n, P_n, SP_n, and MOC methods), finer spatial mesh (usually on pin-cell basis) and more energy groups are being applied to core analysis but they have not reached the maturity to be utilised in the industry and regulation as a routine design and safety analysis approach. The error due to use of the diffusion approximation, and subsequently the uncertainty in core parameters due to the use of the diffusion approximation (diffusion vs. higher order transport approximation) can be accessed from the previous NEA/OECD benchmarks. Uncertainties are also introduced by the choice of the spatial discretisation scheme utilised in the core simulator. The commonly used spatial discretisation schemes are the different types of nodal (finite-volume) methods, finite-difference methods, finite-element methods, etc. The participants are responsible for performing spatial discretisation convergence studies with their core simulator codes in order to remove

the uncertainties associated with numerical approximations (numerical method uncertainties) and reduce the uncertainties associated with the neutron transport method (physics uncertainties) used in core simulator codes.

There are also uncertainties associated with numerical simplifications in core modelling and variations in core geometry which need to be addressed and propagated. The modelling, numerical and geometry variation uncertainties and their propagation in reactor core calculations will be addressed by the benchmark team in the final report on Phase I. The participants are advised to focus mostly on cross-section uncertainty propagation.

Exercise 3 (Core Physics) computes uncertainties at core level. The Output (O) uncertainties are for specified output parameters for Exercise I-3, used to test (evaluate) the utilised uncertainty method. The suggested output parameters to be compared with their associated uncertainties are k_{eff}, assembly power (radial) distribution, axial core averaged power distribution, axial offset, relative pin power distribution and assembly reaction rates for selected fuel assemblies and axial layers (nodes), control rod worth, and core average (point) kinetic parameters. Special attention is required for the relative power distributions, which are correlated to the normalised values. Concerning pin power, the pin power reconstruction is the main technique used today. The uncertainties associated with pin power reconstruction techniques vary depending on selected methods for intra-nodal homogenous power distribution calculation and for treatment of power form functions.

The propagated Uncertainty parameters (U) are for these parameters, which are selected to be propagated further through the follow-up Exercises in order to calculate the overall resulting uncertainty. In Exercise I-3 the target and output uncertainties are the same. For all uncertainty parameters (output and propagated) in this exercise the following are requested: the best-estimate value of the parameter with associated uncertainties where the associated uncertainties are in terms of standard deviation.

4.2 Test problems

Three-dimensional (3-D) light water reactors, two-GEN-III reactors cores with both UOX and MOX fuel compositions and optional fast reactor test problems are defined to be used within Exercise I-3, to assess the stand-alone neutronics core calculations and to determine the output core parameter uncertainties due to the input few-group lattice-averaged cross-section uncertainties, input geometry uncertainties, code modelling approximation uncertainties, and uncertainties due to numerical simplifications.

The PWR, BWR, & VVER cases are very similar in spectrum; a fast reactor case based on a well-evaluated experiment would broaden the verification of methods for Phase I of the UAM benchmark and is a link to reactors of the next generation. Fast reactor benchmarks are proposed to test and compare state-of-the-art cross-section sensitivity and uncertainty codes. It also provides a unique set of experimental data on the delayed neutrons effective fraction. It could also be useful in the analysis of the components of k_{eff} uncertainties. Further, the analysis of the experimental set could bring a better comprehension of the validity of covariance matrices to be applied.

SNEAK (fast reactor core problem) is suggested as an optional test case to the test problems for this exercise since it has a unique set of experimental data for k_{eff} uncertainties and can be used as an example of how to calculate uncertainty in k_{eff}. The two high-quality reactor physics benchmark experiments, SNEAK-7A & 7B (Karlsruhe Fast Critical Facility) are part of the International Reactor Physics Benchmark Experiments (IRPhE) database.

The continuous energy Monte Carlo method is used for reference calculations assuming sufficient statistics, which guarantee that k_{eff} and the fission source convergence. The statistical uncertainties in the reference Monte Carlo calculations will be evaluated by the benchmark team. These test problems are developed and/or utilised on two different levels:

1. HZP core test cases defined for BWR PB-2 [6], PWR TMI-1 [7], and VVER-1 000 [8] based on real plant core data. The boundary conditions are zero flux boundary conditions at radial and axial boundaries of the core models.

   BWR Core Model: PB-2

   The information for the BWR core model is given in Figure 18 through Figure 25. The axial distribution of fuel compositions is given in Figure 23. The participants are advised to divide the active fuel length into 24 equal-distant nodes with a thickness of 15.24 cm each. Top and bottom axial reflectors of the same thickness are added with reflector composition as specified in Figure 12. The control rod positions for the HZP case are provided in [6]. Only fresh fuel assemblies are considered.

Figure 18: PB-2 reactor core cross-sectional view

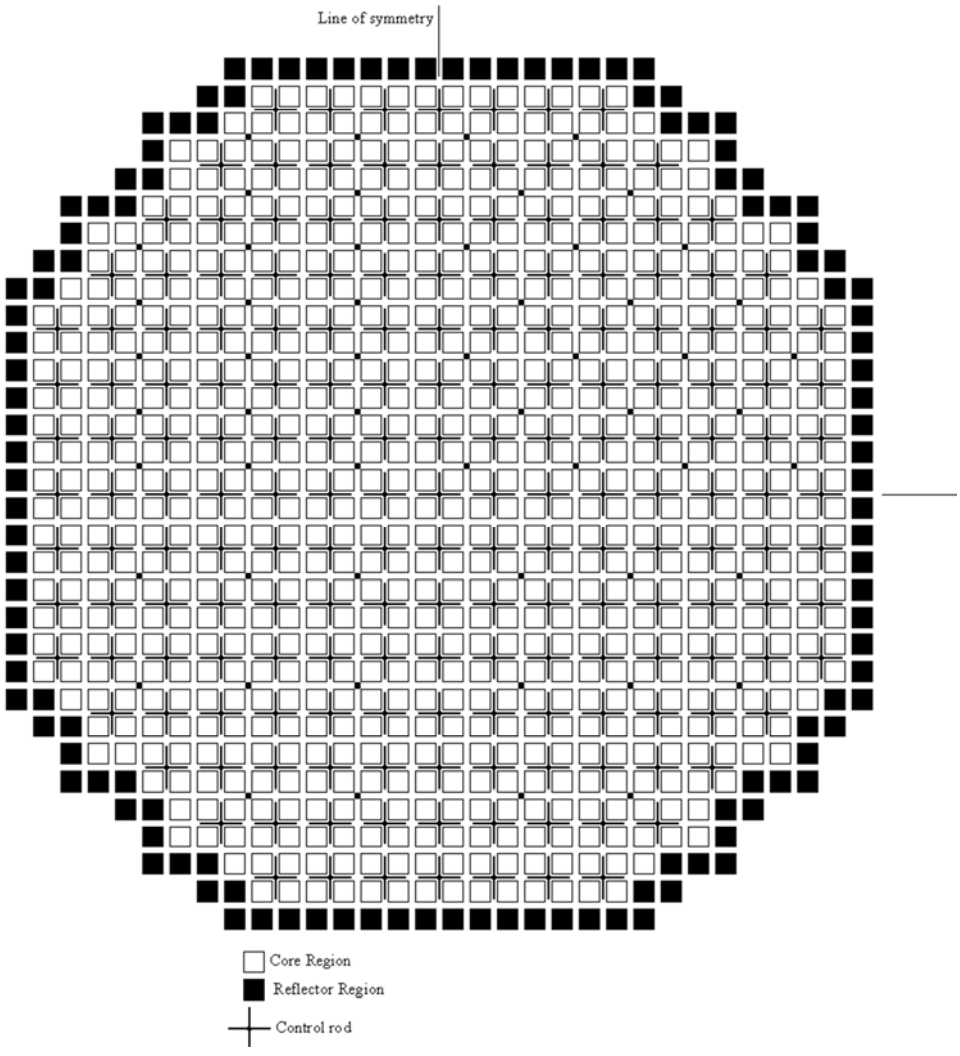

Figure 19: PB-2 initial core loading

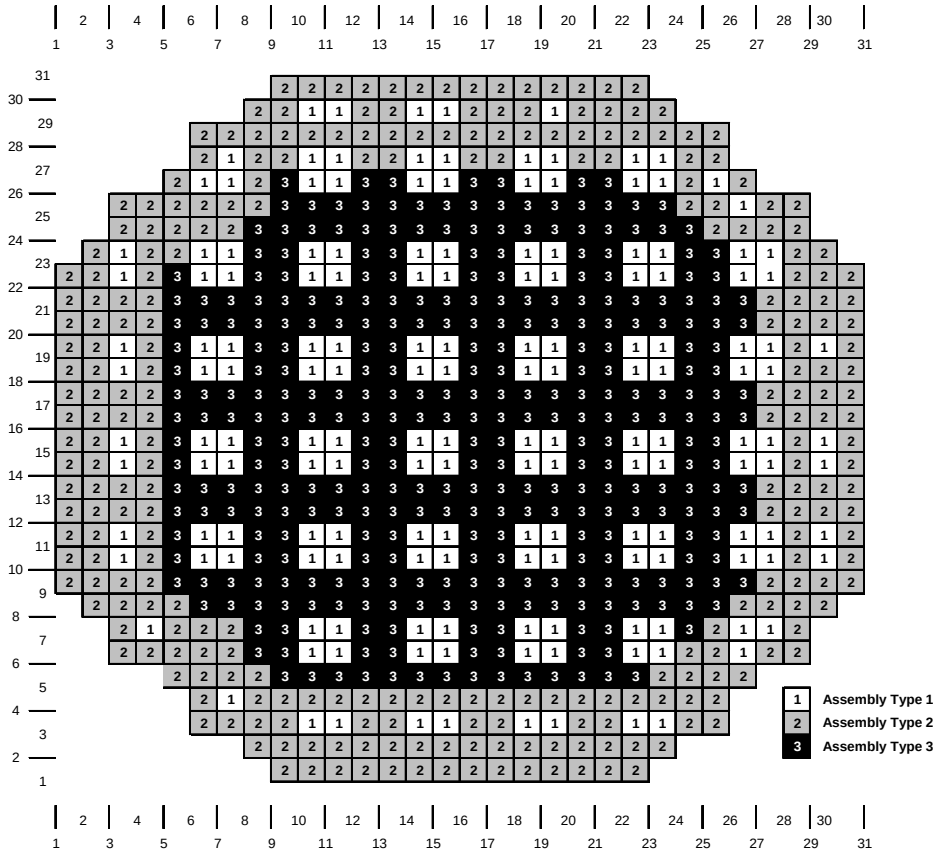

Table 20: PB-2 initial core loading information

	Initial load			Reload	Reload	LTA special
Assembly type	1	2	3	4	5	6
No. of assemblies, initial core	168	263	333	0	0	0
No. of assemblies, Cycle 2	0	261	315	68	116	4
Geometry	7 × 7	7 × 7	7 × 7	8 × 8	8 × 8	8 × 8
Assembly pitch, mm	152.4	152.4	152.4	152.4	152.4	152.4
Fuel rod pitch, mm	18.75	18.75	18.75	16.23	16.23	16.23
Fuel rods per assembly	49	49	49	63	63	62
Water rods per assembly	0	0	0	1	1	2
Burnable poison positions	0	4	5	5	5	5
No. of spacer grids	7	7	7	7	7	7
Inconel per grid, kg	0.225	0.225	0.225	0.225	0.225	0.225
Zr-4 per grid, kg	1.183	1.183	1.183	1.353	1.353	1.353
Spacer width, cm	4.128	4.128	4.128	4.128	4.128	4.128
Assembly average fuel composition:						
Gd_2O_3, g	0	441	547	490	328	313
UO_2, kg	222.44	212.21	212.06	207.78	208.0	207.14
Total fuel, kg	222.44	212.65	212.61	208.27	208.33	207.45

Figure 20: PB-2 assembly design - Type 1 initial fuel

Rod type	Number of rods	Pellet density		Stack density (g/cm^3)	Gd_2O_3 (g)	UO_2 (g)	Stack length (cm)
		UO_2 (g/cm^3)	$UO_2+Gd_2O_3$ (g/cm^3)				
1	31	10.42	-	10.34	0	4548	365.76
2	17	10.42	-	10.34	0	4548	365.76
2s	01	10.42	-	10.34	0	4140	330.2

Pellet outer diameter = 1.23698 cm.
Cladding = Zircaloy-2, 1.43002 cm outer diameter × .08128 cm wall thickness, all rods.
Gas plenum length = 40.64 cm.

Assembly design for Type 1 initial fuel

Rod type	^{23}U (wt.%)	Gd_2O_3 (wt.%)	No. of rods
1	1.33	0	31
2	0.71	0	18

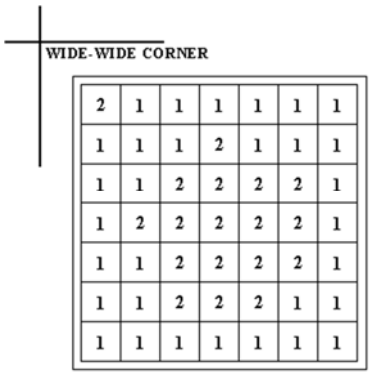

Figure 21: PB-2 assembly design - Type 2 initial fuel

Rod type	Number of rods	Pellet density		Stack density (g/cm^3)	Gd_2O_3 (g)	UO_2 (g)	Stack length (cm)
		UO_2 (g/cm^3)	$UO_2+Gd_2O_3$ (g/cm^3)				
1	25	10.42	–	10.32	0	4 352	365.76
1s	1	10.42	–	10.32	0	3 935	330.20
2	12	10.42	–	10.32	0	4 352	365.76
3	6	10.42	–	10.32	0	4 352	365.76
4	1	10.42	–	10.32	0	4 352	365.76
5A	3	–	10.29	10.19	129	4 171	365.76
6B	1	10.42	10.29	10.27	54	4 277	365.76

Pellet outer diameter = 1.21158 cm.
Cladding = Zircaloy-2, 1.43002 cm outer diameter × .09398 cm wall thickness, all rods.
Gas plenum length = 40.132 cm.

Assembly design for Type 2 initial fuel

Rod type	^{235}U (wt.%)	Gd_2O_3 (wt.%)	No. of rods
1	2.93	0	26
2	1.94	0	12
3	1.69	0	6
4	1.33	0	1
5A	2.93	3.0	3
6B	2.93	3.0	1

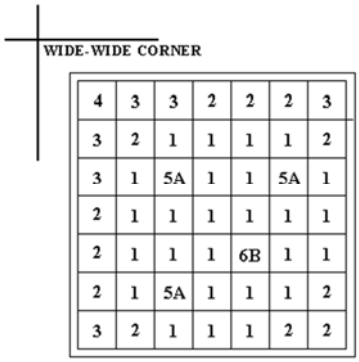

Figure 22: PB-2 assembly design - Type 3 initial fuel

Rod type	Number of rods	Pellet density		Stack density (g/cm^3)	Gd_2O_3 (g)	UO_2 (g)	Stack length (cm)
		UO_2 (g/cm^3)	$UO_2+Gd_2O_3$ (g/cm^3)				
1	26	10.42	–	10.32	0	4 352	365.76
2	11	10.42	–	10.32	0	4 352	365.76
3	6	10.42	–	10.32	0	4 352	365.76
4	1	10.42	–	10.32	0	4 352	365.76
5A	2	–	10.29	10.19	129	4 171	365.76
6C	1	–	10.29	10.19	117	3 771	330.20
7E	1	10.42	10.25	10.28	43	4 292	365.76
8D	1	10.42	10.25	10.19	129	4 172	365.76

Pellet outer diameter = 1.21158 cm.
Cladding = Zircaloy-2, 1.43002 cm outer diameter × .09398 cm wall thickness, all rods.
Gas plenum length = 40.132 cm.

Assembly design for Type 3 initial fuel

Rod type	^{235}U (wt.%)	Gd_2O_3 (wt.%)	No. of rods
1	2.93	0	26
2	1.94	0	11
3	1.69	0	6
4	1.33	0	1
5A	2.93	3.0	2
6C	2.93	3.0	1
7E	2.93	4.0	1
8D	1.94	4.0	1

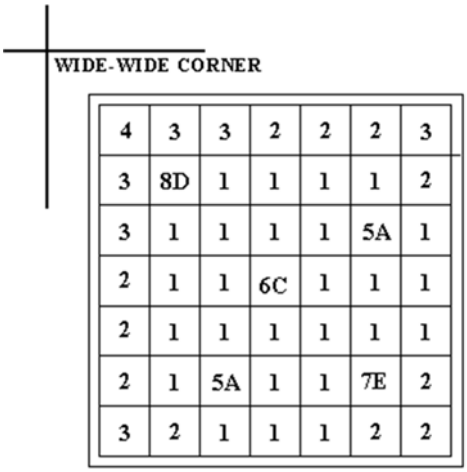

Figure 23: PB-2 - axial variation of the fuel composition

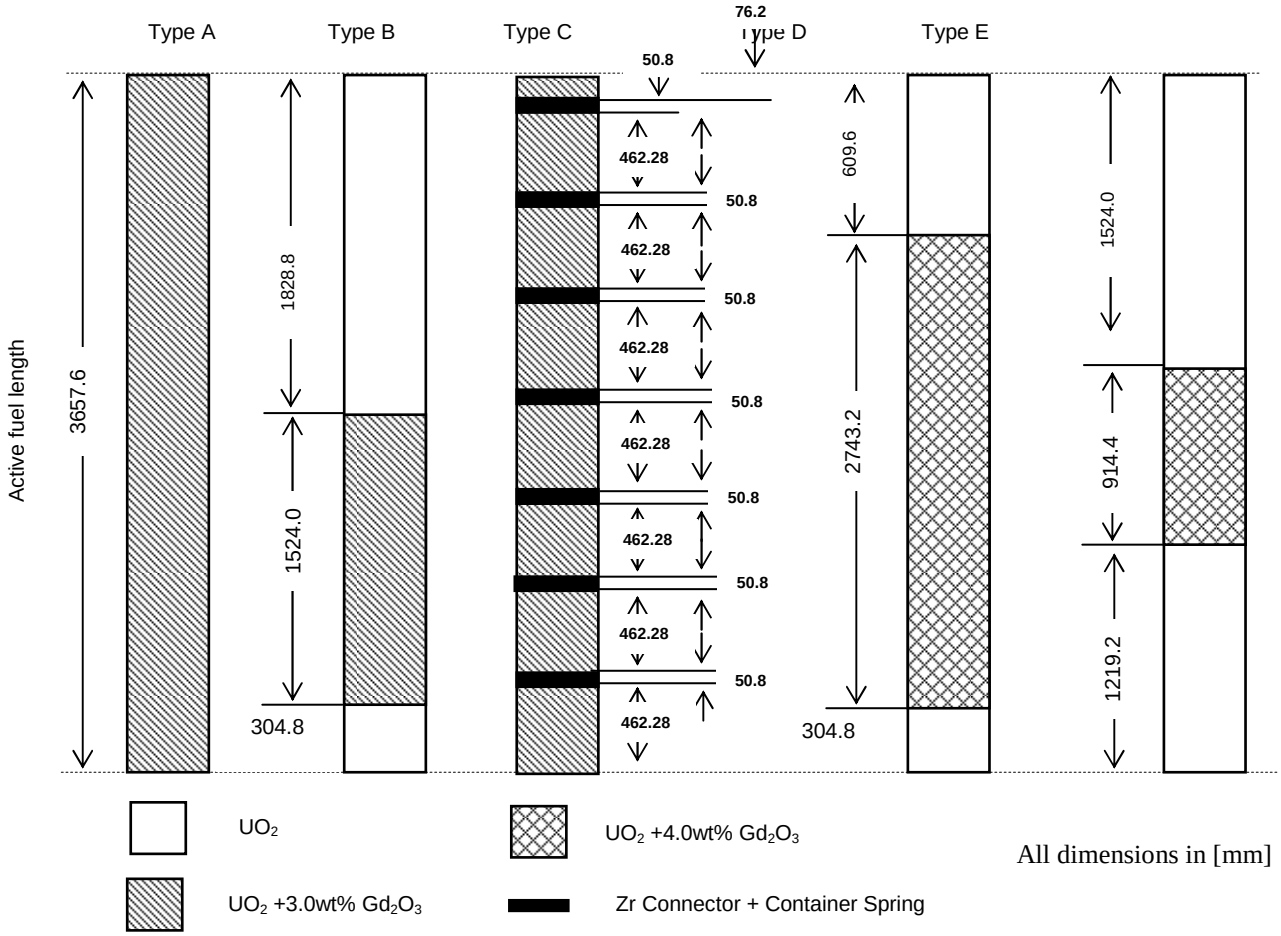

Figure 24: Elevation of core components for PB-2

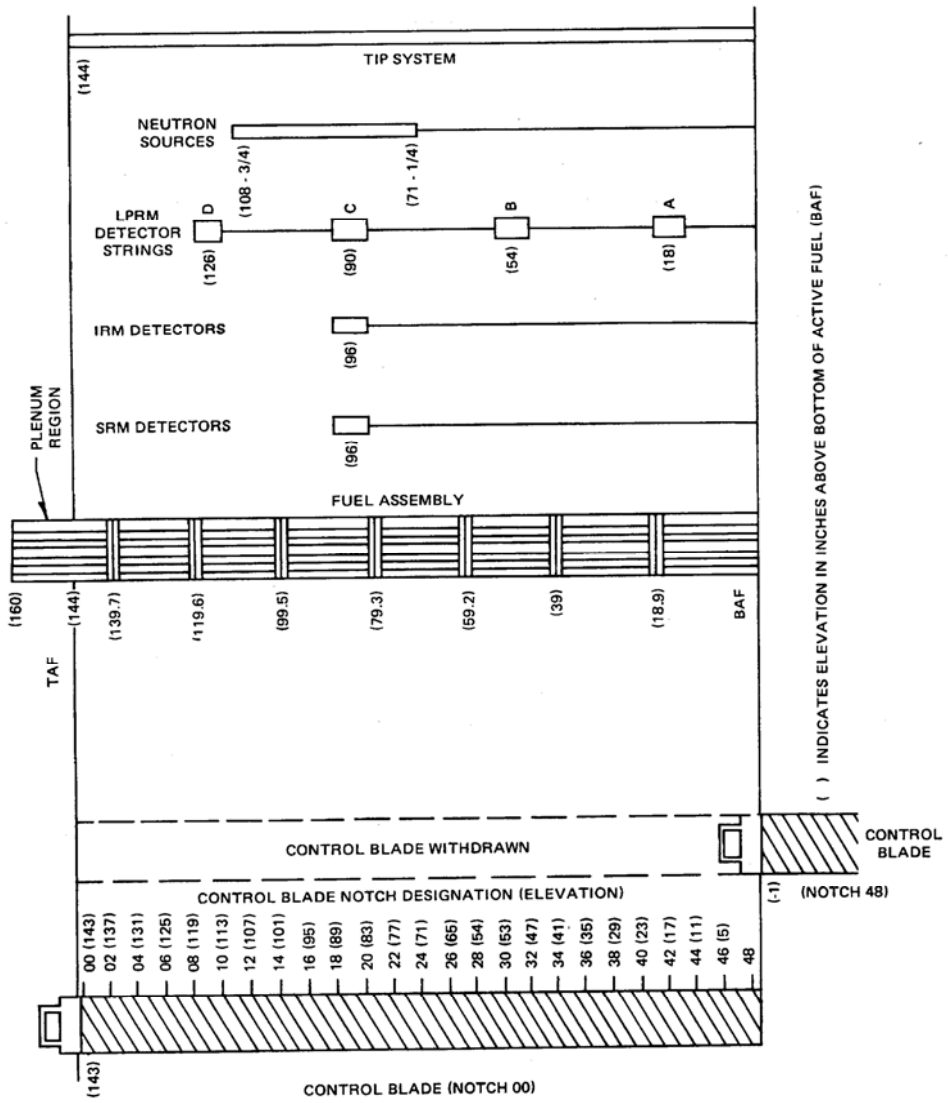

Figure 25: PB-2 - core orificing and TIP system arrangement

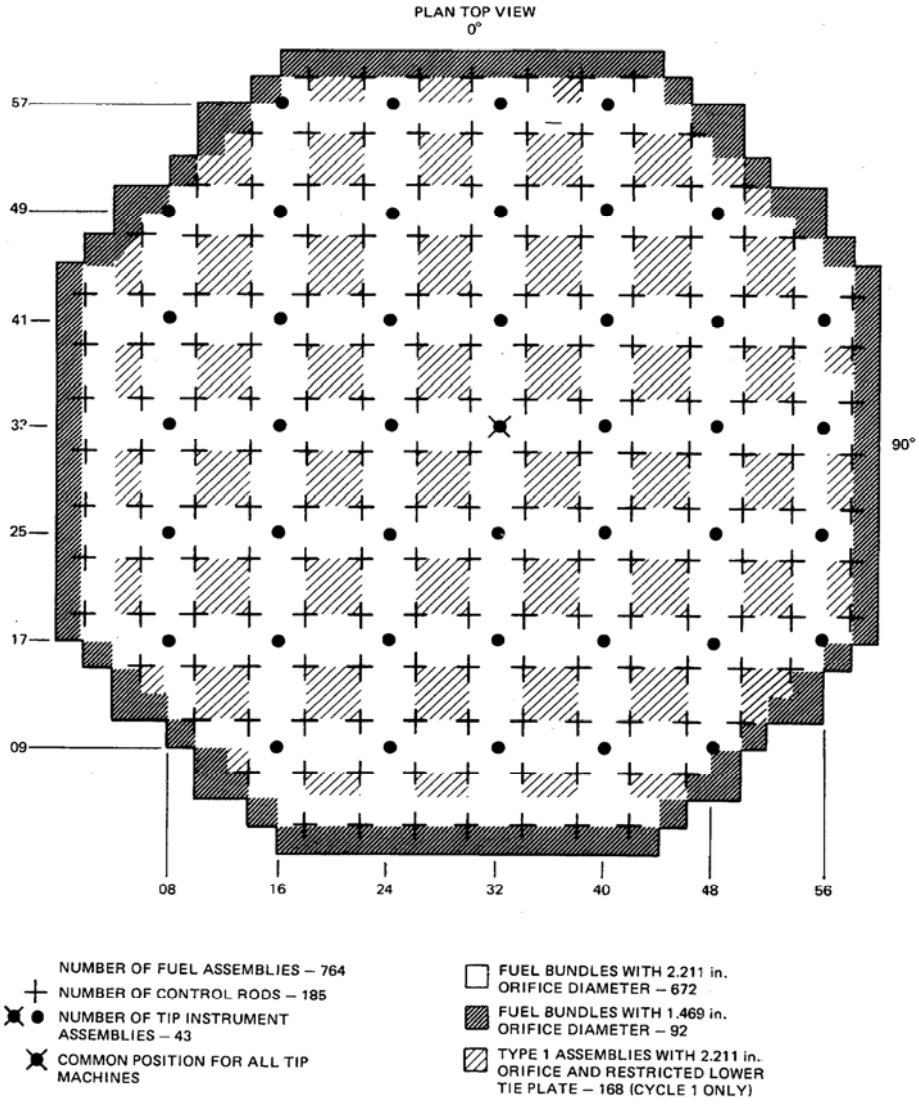

PWR Core Model: TMI-1

The information for the PWR core model is given in Figure 26 through Figure 28. The information about the distribution of fuel assemblies in 1/8 core sector of symmetry is given in Figure 27. Uniform axial distribution of fuel composition for each assembly is specified following the assembly compositions given in Figure 27. Figure 28 shows the TMI-1 assembly design with 8 Gd pins while Figure 9 presents the other TMI-1 design with 4 Gd pins used in the TMI-1 core. The participants are advised to divide the active fuel length into 16 equal-distant nodes with a thickness of 22.32 cm each. Top and bottom axial reflectors with a thickness of 21.84 cm are added with reflector composition as specified in Figure 13. The control rod positions for the HZP case are provided in [7]. Only fresh fuel assemblies are considered. The critical boron concentration for this core is about 1900 ppm.

Figure 26: TMI-1 reactor core cross-sectional view and characteristics

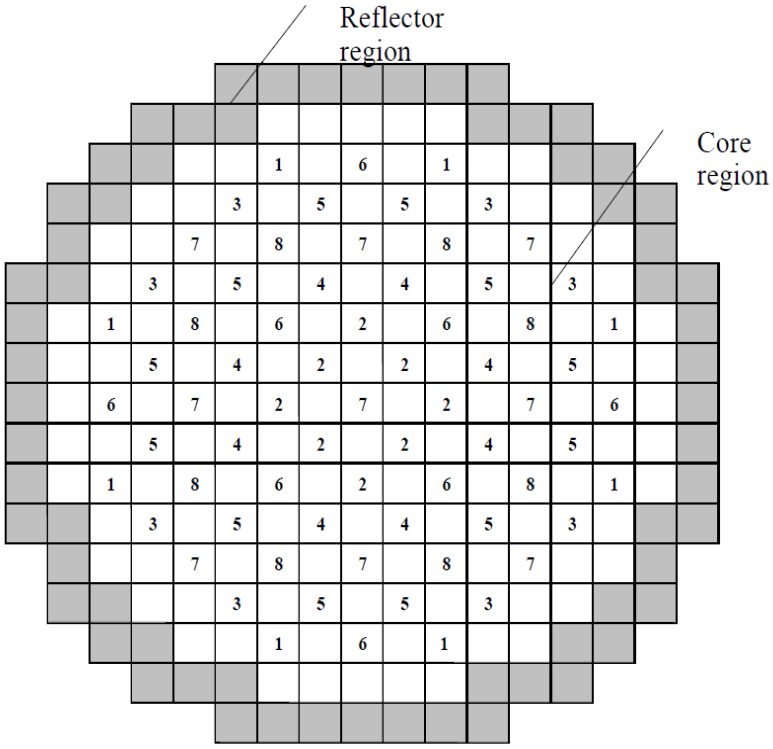

Parameter	Value		Bank	No. rods	Purpose
Total number of fuel assemblies	177		1	8	Safety
Total number of reflector assemblies	64		2	8	Safety
Fuel assembly pitch, mm	218.110		3	8	Safety
Gap between fuel assemblies, mm	1.702		4	8	Safety
Active core length, mm	3571.20		5	12	Regulating
Total core length, mm	4007.42		6	8	Regulating
			7	9	Regulating
			8	8	APSR

Figure 27: TMI-1 – definition of fuel assembly types

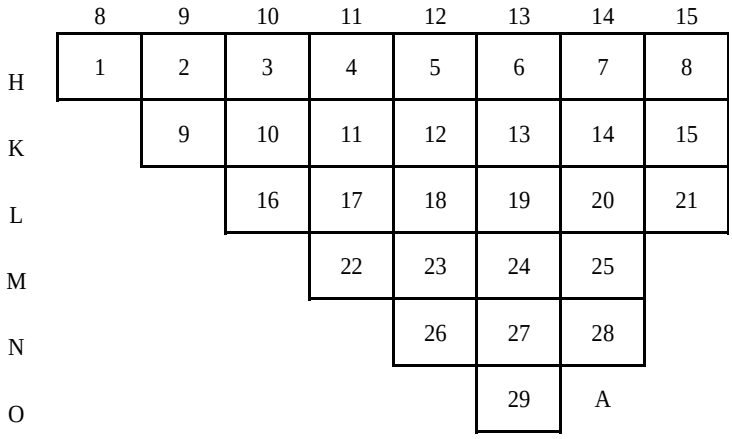

Assembly	Characteristics		
1	4.00 w/o	No BP	No Gd pins
2	4.95 w/o	3.5 % BP	4 Gd pins
3	5.00 w/o	No BP	4 Gd pins
4	4.95 w/o	3.5 % BP	4 Gd pins
5	4.40 w/o	No BP	No Gd pins
6	5.00 w/o	3.5 % BP	4 Gd pins
7	4.85 w/o	No BP	4 Gd pins
8	4.85 w/o	No BP	4 Gd pins
9	4.95 w/o	No BP	4 Gd pins
10	4.95 w/o	3.5 % BP	4 Gd pins
11	4.85 w/o	No BP	4 Gd pins
12	4.95 w/o	3.5 % BP	4 Gd pins
13	5.00 w/o	No BP	4 Gd pins
14	5.00 w/o	No BP	8 Gd pins
15	4.95 w/o	No BP	8 Gd pins
16	4.95 w/o	No BP	4 Gd pins
17	4.95 w/o	3.5 % BP	4 Gd pins
18	4.95 w/o	No BP	4 Gd pins
19	5.00 w/o	3.5 % BP	4 Gd pins
20	4.40 w/o	No BP	No Gd pins
21	4.85 w/o	No BP	4 Gd pins
22	4.40 w/o	No BP	No Gd pins
23	4.95 w/o	3.5 % BP	No Gd pins
24	4.95 w/o	No BP	4 Gd pins
25	5.00 w/o	No BP	8 Gd pins
26	5.00 w/o	No BP	4 Gd pins
27	5.00 w/o	No BP	No Gd pins
28	4.95 w/o	3.5 % BP	4 Gd pins
29	5.00 w/o	No BP	4 Gd pins

Figure 28: TMI-1 assembly design with 8 Gd pins

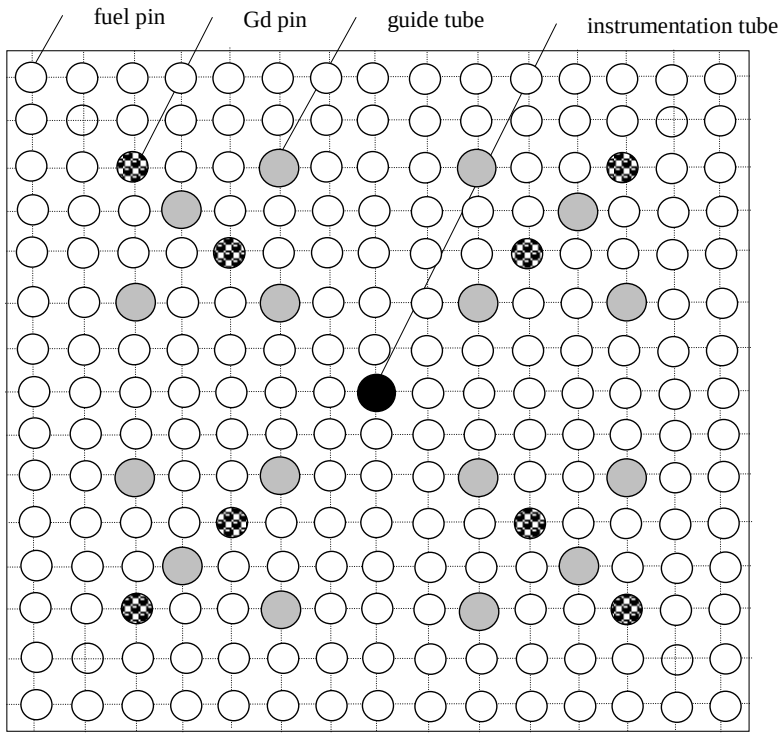

Some assemblies in addition to the integral Gd BPs also have discrete BPs located in the guide tubes. The BP material is Al_2O_3-B_4C (see Table 21) and the material of the guide tube is Zircaloy-2.

Table 21: TMI-1 composition of BP material

3.5 wt. % (w/o) B_4C of Al_2O_3-B_4C	**Nuclide ID**	**Wt. %**
	Al	51.0871
	O	45.4117
	C	0.76076
	^{10}B	0.50211
	^{11}B	2.2372

VVER-1 000 Core Model: Kozloduy-6

The information for the VVER core model is given in Figure 29 through Figure 31. The participants are advised to divide the active fuel length in 10 equal-distant nodes with a thickness of 35.5 cm each. Top and bottom axial reflectors with a thickness of 23.6 cm are added with reflector composition as specified in Figure 14. The control rod positions for HZP case are provided in [8]. Uniform axial distribution of fuel composition for each assembly is specified following the assembly compositions given in Figure 14. Only fresh fuel assemblies are considered. The critical boron concentration for this core is about 6.4 g/kg.

Figure 29: Kozloduy-6 reactor core cross-sectional view and characteristics

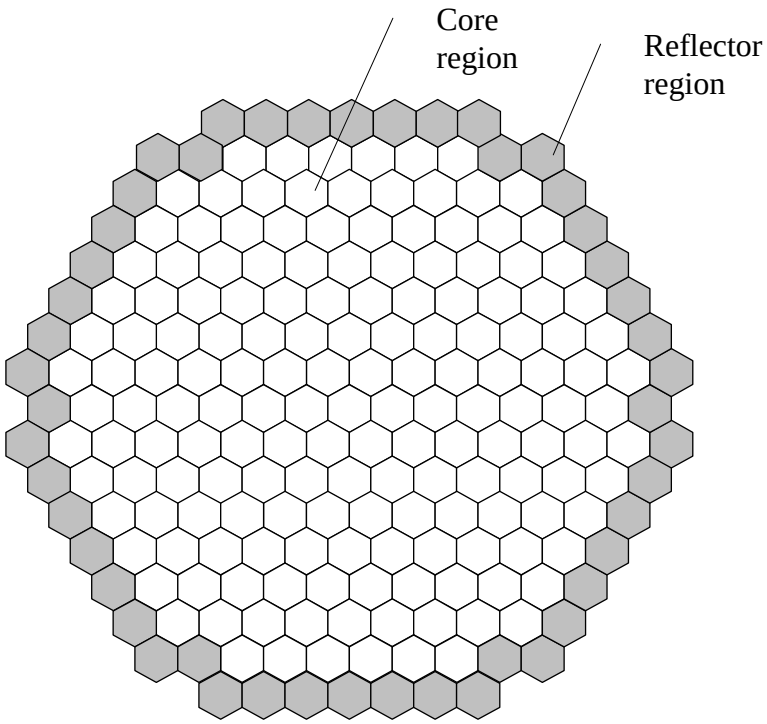

Parameter	Value
Total number of fuel assemblies	163
Total number of reflector assemblies	48
FA wrench size, mm	234
FA lattice pitch, mm	236
Fuel rod total length, mm	3 837
Fuel rod active length (cold state), mm	3 530
Fuel rod active length (hot state), mm	3 550

Figure 30: Kozloduy-6 – control rod arrangement

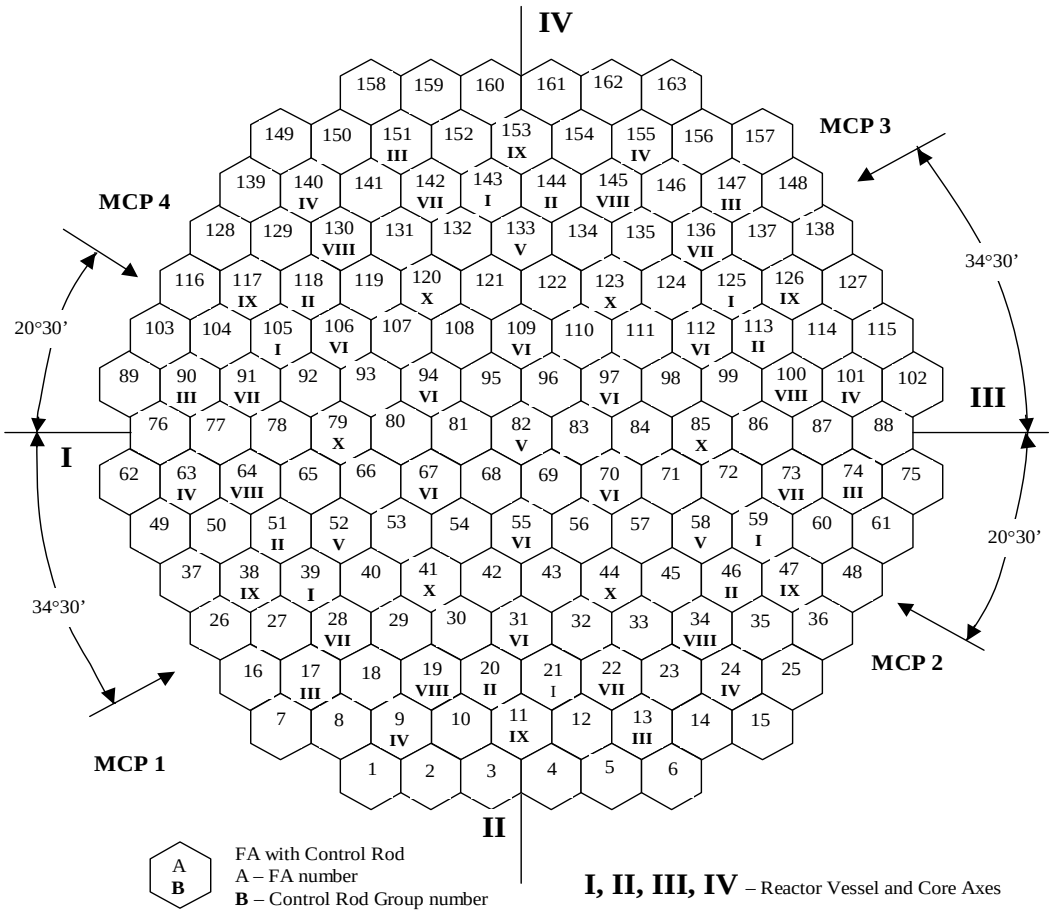

Bank	No. of rods	Purpose
I	6	Safety
II	6	Safety
III	6	Safety
IV	6	Safety
V	4	Part-length
VI	9	Safety
VII	6	Safety
VIII	6	Safety
IX	6	Safety
X	6	Regulating

Figure 31: Kozloduy-6 – core loading

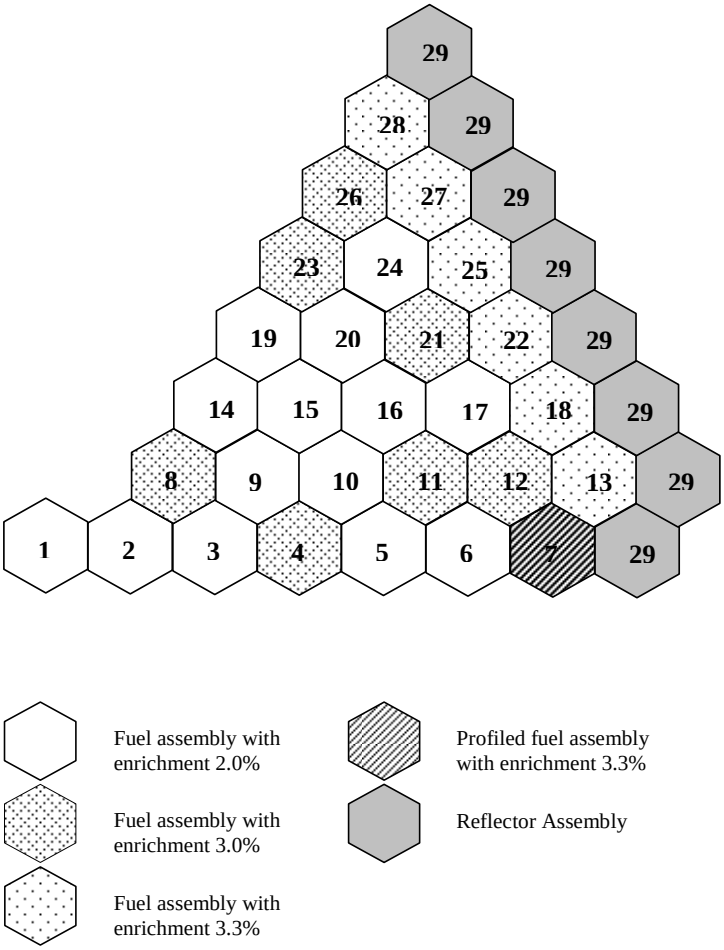

Assembly Type	Enrichment, w/o
1	2.0
2	2.0
3	2.0
4	3.0
5	2.0
6	2.0
7	3.3
8	3.0
9	2.0
10	2.0
11	3.0
12	3.0
13	3.3
14	2.0
15	2.0
16	2.0
17	2.0
18	3.3
19	2.0
20	2.0
21	3.0
22	3.3
23	3.0
24	2.0
25	3.3
26	3.0
27	3.3
28	3.3
29	Radial Reflector

GEN-III Core Models: UOX core and MOX core [14]

The information for the GEN-III core model was provided by Alain Santamarina and Claire Vaglio-Gaudard from CEA. Unit cell information and operating conditions are given in Figure 11 and Table 18. The GEN-III benchmark for Exercise I-3 corresponds to core calculation [with a stainless steel (SS) heavy reflector] and the study of nuclear data uncertainty propagation for two fresh core loadings:

- UOX core as shown in Figure 32;
- Mixed UOX/MOX core as shown in Figure 33.

The addition of these cases makes it possible to quantify the uncertainty due to reflector (stainless steel) nuclear data on the radial power peak and control rod efficiency, which is a key issue for the PWR GEN-III safety. The design of the assemblies and the material compositions have already been given in Chapter 3, except for the core reflector. The radial reflector is modelled by homogeneous assemblies in SS at the core boundary; beyond this SS reflector, borated water is represented. Concerning the core axial description, the axial reflector at the bottom and the top of the active fuel length is modelled by clads (same diameter, same lattice pitch as fuel assemblies described in Chapter 3) bathed with borated water. Clads are filled with a zircaloy tube (Zr represents 22% and He 78% of the volume) for the lower axial reflector, and with a diluted SS material to model springs (the SS composition will have to be multiplied by 0.2 in order to fill the clad inner part) for the upper axial reflector. The axial reflectors are 20 cm thick. The SS heavy radial reflector is represented on the total core length. The outer boundary conditions are defined as zero albedo.

Table 22: UOX/MOX core design

Parameter	Value
Fuel assembly pitch, mm	216.1
Reflector assembly pitch, mm	216.1
Reflector material (homogeneous)	Steel 304 or borated water
Total core length, mm	4 600
Active length, mm	4 200

Table 23: Zircaloy/He composition for the upper axial reflector

Isotope	10^{24} at/cm^3
FE56	2.933E-05
O16	6.655E-05
ZR90	4.787E-03
ZR91	1.032E-03
ZR92	1.561E-03
ZR94	1.548E-03
ZR96	2.442E-04

Table 24: Stainless steel composition for the reflector

Isotope	10^{24} at/cm^3
FE54	3.247E-03
FE56	5.098E-02
FE57	1.177E-03
FE58	1.567E-04
CR50	6.763E-04
CR52	1.303E-02
CR53	1.478E-03
CR54	3.678E-04
NI58	6.622E-03
NI60	2.551E-03
NI61	1.109E-04
NI62	3.534E-04
NI64	9.005E-05
MN55	1.732E-03
C	3.171E-04
SI28	1.562E-03
SI29	7.910E-05
SI30	5.251E-05
MO95	1.253E-03

Figure 32: GEN-III UOX core

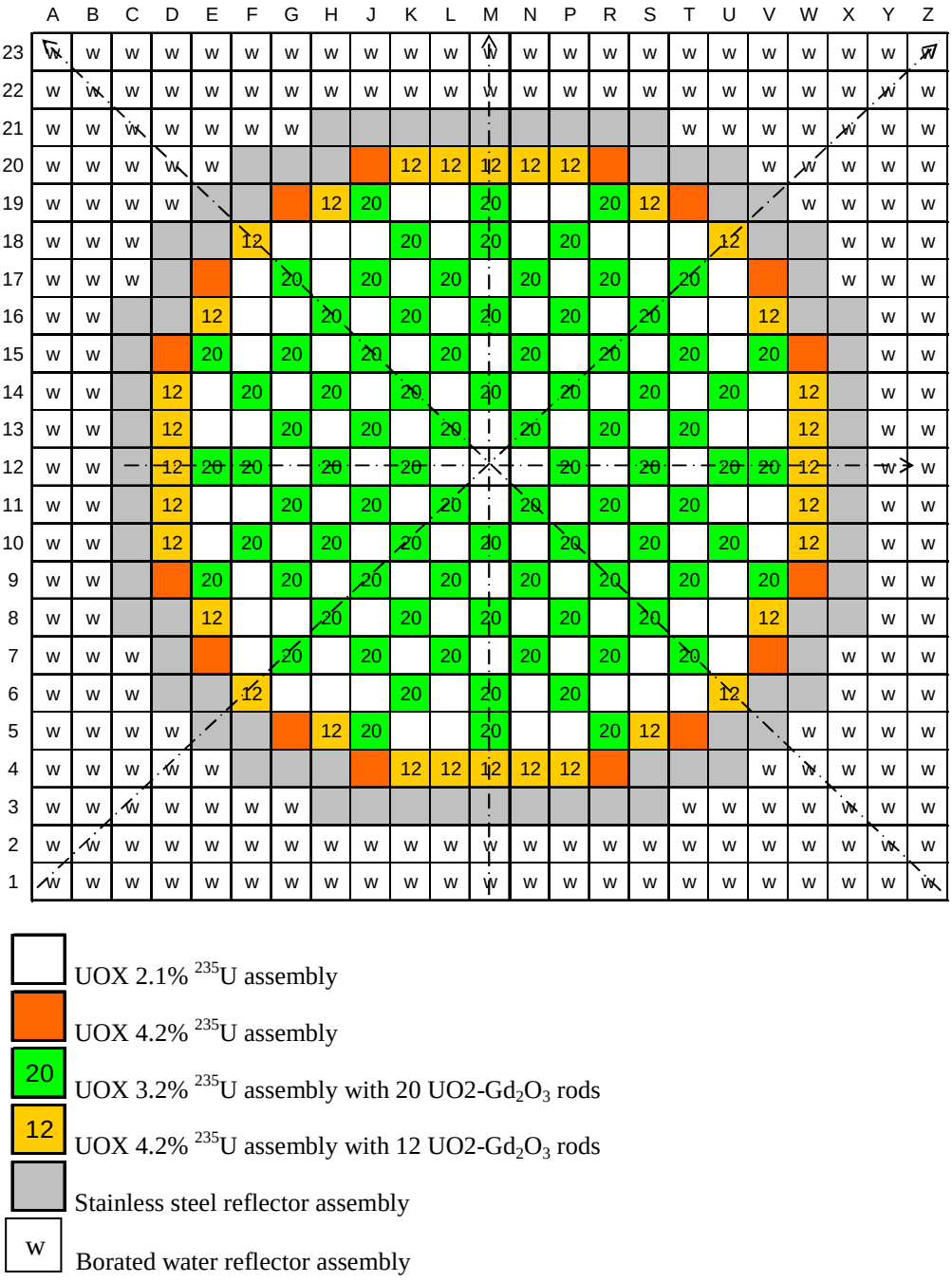

UOX 2.1% ^{235}U assembly

UOX 4.2% ^{235}U assembly

20 UOX 3.2% ^{235}U assembly with 20 UO2-Gd_2O_3 rods

12 UOX 4.2% ^{235}U assembly with 12 UO2-Gd_2O_3 rods

Stainless steel reflector assembly

w Borated water reflector assembly

Figure 33: GEN-III MOX core

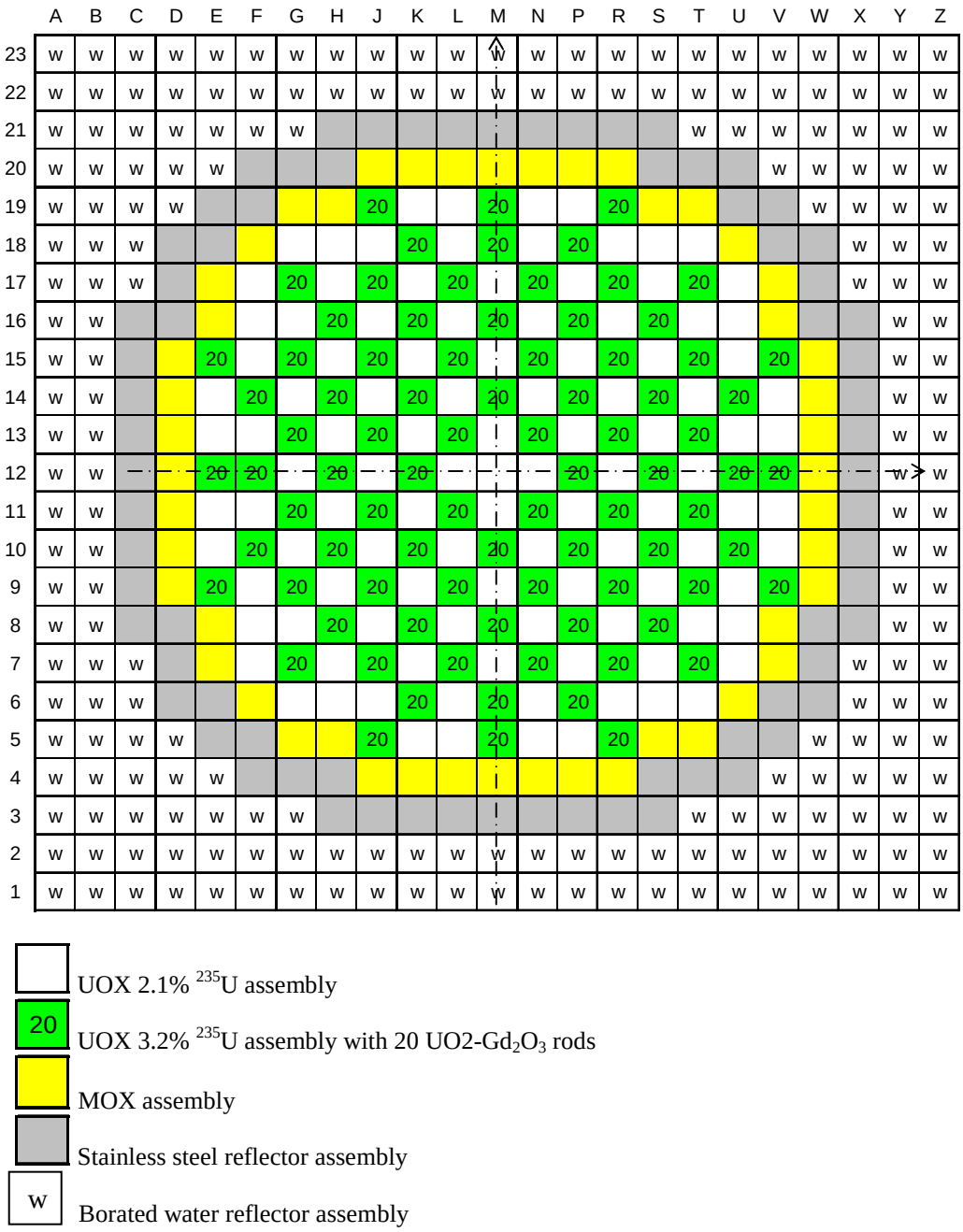

These problems are to be analysed at Hot Zero Power (HZP) conditions as well as Hot Full Power (HFP). Information for these operating conditions is available in Table 18.

For each problem the participants should calculate the core multiplication factors (k_{eff}), assembly power (radial) distribution, axial core averaged power distribution, axial offset, relative pin power distribution and assembly reaction rates for selected fuel assemblies and axial layers (nodes),

control rod worth, and core average (point) kinetic parameters as well as associated uncertainties due to core simulation within Exercise I-3.

2. Documented experimental benchmark plant cold critical data and critical lattice data.

   a) BWR experimental plant cold critical data were reported in [57] [58]. The first reference will be provided in electronic format to the interested participants. This EPRI report provides reactor design and operating data for Cycle 1 and Cycle 2 of Quad Cities Unit 1 BWR. The attractive features of these data are that 7x7 BWR assembly designs similar to those utilised in the Cycle 1 of PB-2 are used for Cycle 1 of Quad Cities Unit 1. The benchmark cold critical data were taken during start-ups following outages, which were long enough to assume Xe-free conditions and they include core average exposure, reactor water temperature, rod pattern, and rising period. For the purposes of the OECD LWR UAM benchmark the cold critical state at the beginning of Cycle 1 (Exposure = 0.0 MWd/t) is used. The participants should calculate k_{eff} and associated uncertainties for this state.

   b) PWR benchmark critical lattice data were reported in [59] [60]. At the beginning of 1970, a series of experiments with heterogeneous lattices of low-enriched UO_2 fuel rods was performed at B&W Research Center. For these experiments, the central region of the core closely resembled a 3x3 array of PWR fuel assemblies with fuel rods arranged in a 15x15 lattice (similar to TMI-1 core). Loading 2 is selected for the purposes of the OECD LWR UAM benchmark. The necessary data for modelling can be obtained from [59] [NEA/NSC/DOC (95)03/IV – LEU-COMP-THERM-008]. The participants should calculate k_{eff} of the core and relative rod-by-rod power densities (fission rate distributions) of the central assembly (using pin power reconstruction methods available in their core simulator codes) as well as the associated uncertainties in these parameters.

   c) VVER-1 000 benchmark critical lattice data were reported in [59]. Ten experiments were performed in 1998 at the experimental zero-power reactor LR-0 (Nuclear Research Institute Řež plc, Czech Republic). The core was assembled from 6 VVER-1 000 fuel assemblies and the experiments were carried out at atmospheric pressure and "room" temperature. Case 3 is selected for the purposes of the OECD LWR UAM benchmark. The necessary data for modelling can be obtained from [59] [NEA/NSC/DOC (95)03/IV – LEU-COMP-THERM-086]. The participants should calculate k_{eff} of the core and the associated uncertainties.

3. Optional SNEAK 7A&7B benchmark test problems [15].

   The main objective of this work is to study the influence of cross-section uncertainties on the evaluation of the accuracy of the β_{eff} computations in the SNEAK 7A and 7B reactors. The β_{eff} measured values are given for both SNEAK 7A and 7B assemblies and for two applied techniques: for a deterministic one with the ^{252}Cf pseudo-reactivity traverse and for noise. The neutron generation lifetime can be reconstructed from the transfer functions. But for our needs to demonstrate the methodology of uncertainty propagation the test models were simplified.

   The detailed models are presented in Figure 34.

Figure 34: Vertical cut of benchmark models for SNEAK 7A and SNEAK 7B assemblies [66]

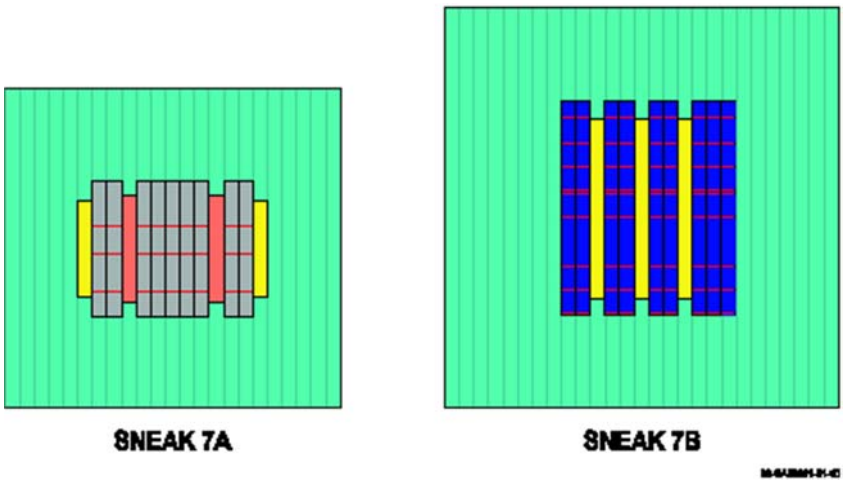

There are T (shim) and S (safety) rods with heights different from the core size. The 3D models with tubes and cans were simplified by homogenising fuel elements radially and axially, and heights of T, S and TP rods were revised to be equal to the heights of their cores. The R-Z models are kept as benchmark models for coarse approximate studying of main critical parameters and integral functions. The R-Z model for SNEAK 7A contains three physical zones: inner core, outer core with the homogenised shim and safety rods, and the blanket. The R-Z model for SNEAK 7B contains two physical zones: core with the homogenised shim and safety rods and the blanket. Both models are symmetric around the cylinder axis and across the horizontal mid plane. R-Z models are presented in Figures 35 and 36. The material data are described in Tables 26-28. The material contents of the models differ only in the rods homogenised together with core materials but blankets are the same for both R-Z and 3D models.

Figure 35: SNEAK 7A R-Z Model [66]

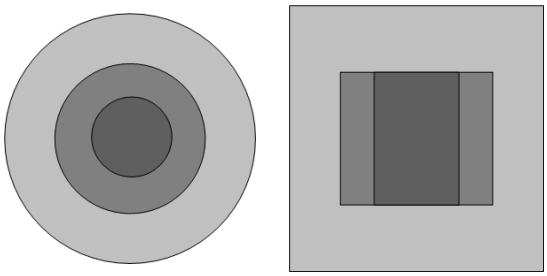

Mid-plan section Axial section

Table 25: The materials for SNEAK 7A R-Z model, 10^{24} cm^{-3} [49]

Isotope	SNEAK 7A		
	Inner Core	Outer core	Blanket
Al	8.00000E-06	1.19060E-03	0.00000E+00
C	2.60987E-02	2.55387E-02	1.35000E-05
Cr	2.24230E-03	2.23900E-03	1.10800E-03
Fe	7.97130E-03	7.98240E-03	3.95490E-03
H	0.00000E+00	0.00000E+00	0.00000E+00
Mg	0.00000E+00	0.00000E+00	0.00000E+00
Mn	1.10900E-04	1.17800E-04	8.75000E-05
Mo	1.65000E-05	1.45000E-05	1.00000E-05
Nb	8.90000E-06	7.70000E-06	8.50000E-06
Ni	1.16640E-03	1.18180E-03	9.84500E-04
O	2.18462E-02	2.11909E-02	0.00000E+00
^{239}Pu	2.63740E-03	2.34340E-03	0.00000E+00
^{240}Pu	2.36900E-04	2.10500E-04	0.00000E+00
^{241}Pu	2.15000E-05	1.91000E-05	0.00000E+00
^{242}Pu	1.10000E-06	1.00000E-06	0.00000E+00
Si	9.33000E-05	9.32000E-05	4.53000E-05
^{235}U	5.86000E-05	2.95800E-04	1.62400E-04
^{238}U	7.96040E-03	8.04560E-03	3.99401E-02

Figure 36: SNEAK 7B R-Z Model [66]

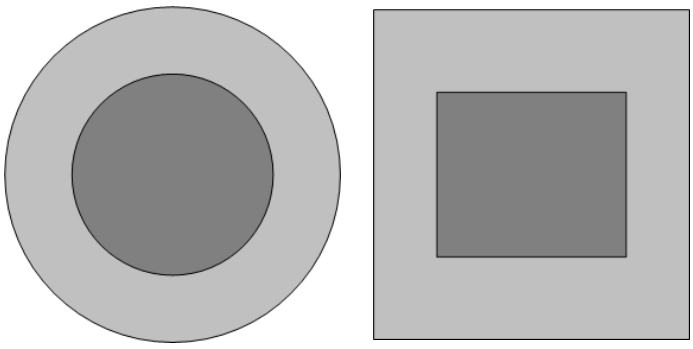

Mid-plan section Axial section

Table 26: The materials for SNEAK 7B R-Z model, 10^{24} cm^{-3} [49]

Isotope	SNEAK 7B	
	core	blanket
Al	1.21120E-03	0.00000E+00
C	6.31000E-05	1.35000E-05
Cr	2.75600E-03	1.10800E-03
Fe	9.80210E-03	3.95490E-03
H	7.10000E-06	0.00000E+00
Mg	9.50000E-06	0.00000E+00
Mn	6.46000E-05	8.75000E-05
Mo	1.84000E-05	1.00000E-05
Nb	8.40000E-06	8.50000E-06
Ni	1.45940E-03	9.84500E-04
O	3.31936E-02	0.00000E+00
^{239}Pu	1.83120E-03	0.00000E+00
^{240}Pu	1.64500E-04	0.00000E+00
^{241}Pu	1.49000E-05	0.00000E+00
^{242}Pu	7.00000E-07	0.00000E+00
Si	1.17400E-04	4.53000E-05
^{235}U	2.66300E-04	1.62400E-04
^{238}U	1.45794E-02	3.99401E-02

The 3D models were simplified in order to represent only homogeneous tubes instead of stretched plates modelling. The configurations are presented in Figures 37 and 38 below.

Figure 37: SNEAK 7A 3D heterogeneous model [66]

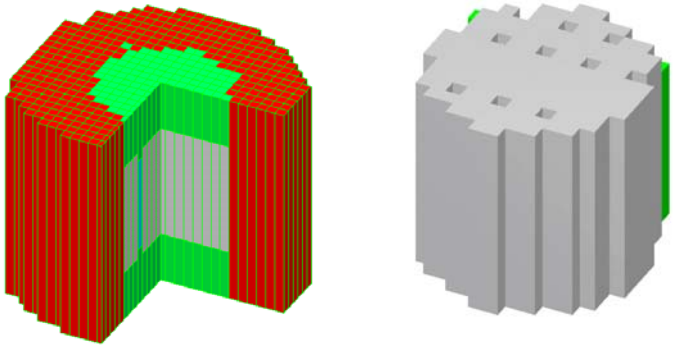

Entire Assembly **Core**

Table 27: Atomic densities for SNEAK 7A rods, 10^{24} cm^{-3} [49]

	SNEAK 7A		
	Core	T_P rods	Shim/safety rods
Al	8.00000E-06	6.90000E-06	1.10350E-02
C	2.60987E-02	2.18819E-02	2.18280E-02
Cr	2.24230E-03	2.99070E-03	2.02550E-03
Fe	7.97130E-03	1.07955E-02	7.38070E-03
H	0.00000E+00	0.00000E+00	0.00000E+00
Mg	0.00000E+00	0.00000E+00	0.00000E+00
Mn	1.10900E-04	1.81900E-04	1.60000E-04
Mo	1.65000E-05	5.60000E-06	0.00000E+00
Nb	8.90000E-06	3.00000E-07	0.00000E+00
Ni	1.16640E-03	1.50660E-03	1.22580E-03
O	2.18462E-02	1.80535E-02	1.65945E-02
^{239}Pu	2.63740E-03	2.17950E-03	0.00000E+00
^{240}Pu	2.36900E-04	1.95800E-04	0.00000E+00
^{241}Pu	2.15000E-05	1.78000E-05	0.00000E+00
^{242}Pu	1.10000E-06	9.00000E-07	0.00000E+00
Si	9.33000E-05	1.24800E-04	8.40000E-05
^{235}U	5.86000E-05	4.84000E-05	2.27220E-03
^{238}U	7.96040E-03	6.57830E-03	9.06730E-03

Figure 38: SNEAK 7B 3D heterogeneous model [66]

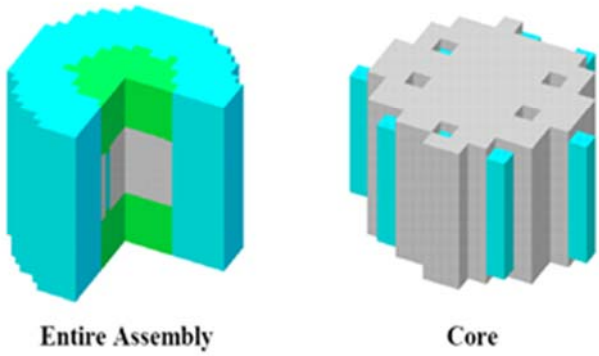

Table 28: Atomic densities for SNEAK 7B 3D homogenised model, 10^{24} cm^{-3} [49]

	SNEAK 7B	
	Core	Shim/safety rods
Al	1.20000E-05	1.65823E-02
C	6.59000E-05	2.64000E-05
Cr	2.80300E-03	2.15350E-03
Fe	9.95760E-03	7.80860E-03
H	7.60000E-06	0.00000E+00
Mg	5.30000E-06	6.31000E-05
Mn	1.22400E-04	1.58500E-04
Mo	1.98000E-05	0.00000E+00
Nb	9.00000E-06	0.00000E+00
Ni	1.46020E-03	1.44960E-03
O	3.38377E-02	2.49366E-02
^{239}Pu	1.97410E-03	0.00000E+00
^{240}Pu	1.77300E-04	0.00000E+00
^{241}Pu	1.61000E-05	0.00000E+00
^{242}Pu	8.00000E-07	0.00000E+00
Si	1.19700E-04	8.88000E-05
^{235}U	1.06300E-04	2.31720E-03
^{238}U	1.45684E-02	1.47206E-02

For each problem the participants should calculate the core multiplication factors (k_{eff}), assembly power (radial) distribution, axial core averaged power distribution, axial offset, relative pin power distribution and assembly reaction rates for selected fuel assemblies and axial layers (nodes), control rod worth, and core average (point) kinetic parameters as well as associated uncertainties due to core simulation within Exercise I-3.

In summary, this exercise is focused on stand-alone neutronics core calculations and associated prediction uncertainties. It does not analyse uncertainties related to cycle and depletion calculations. No feedback modelling is assumed, thus it will address the propagation of uncertainties associated with few-group cross-section generation but not cross-section modelling, i.e. methodologies used for cross-section parameterisation as a function of history and instantaneous variables.

Exercise I-3 propagates the input uncertainty obtained from Exercise I-2 (few-group cross-section covariance matrix), and in addition, introduces new input uncertainties (geometry variations, numerical simplifications, and modelling approximations) to obtain prediction uncertainties in stand-alone core neutronics parameters.

The output uncertainty of Exercise I-3 is propagated in Exercises II-1, II-2, II-3, and III-1 and III-3.

Chapter 5: Requested output

5.1 Introduction

The analysis of results of Phase I will be presented in a benchmark analysis report, which will be available in both a hard copy and an electronic form.

Participants should provide the output information with the given requirements:

- Results should be submitted in an electronic format according to templates, which will be provided to participants by the benchmark team.
- All data should be in SI units.

5.2 Results for Exercise I-1

The following results will be compared for Exercise I-1:

Set 1: Two-dimensional fuel pin-cell test problems representatives of PB-2 BWR, TMI-1 PWR, Kozloduy-6 VVER-1 000 and GEN-III

- Participants are requested to calculate k_{inf} and associated uncertainties (in absolute k% instead of relative k/k %). In addition, participants are requested to identify and list the top five nuclide reactions that contribute the most to the uncertainties in k_{inf}.
- One-group microscopic cross-section (in lieu of reaction rates as suggested) and associated uncertainties homogenised of fuel region only (gap and cladding are excluded).
- One-group effective uncertainties of the top five neutron-nuclide reactions (selected based on the size of their contributions to the uncertainty in k_{inf}.) should be calculated. In addition, participants are requested to include the corresponding variance and un-weighted (α=1) one-group effective cross-section uncertainties as well.

  The primary focus of this output is the "size" of the relative covariance matrix. This effective uncertainty is not to be confused with the uncertainty in k_{inf}. The uncertainty in k_{inf} is used to identify the largest contributors to the changes in k_{inf}. For each reactor type, the relationships between "effective size of the covariance matrix" and the "effective variance" will be further examined.

Set 2: Fuel pin-cell test problems from the KRITZ-2 critical experiments

- Participants are requested to calculate k_{inf} and associated uncertainties (in absolute k% instead of relative k/k %). In addition, participants are requested to identify and list the top five nuclide reactions that contribute the most to the uncertainties in k_{inf}.
- One-group microscopic cross-section (In lieu of reaction rates as suggested) and associated uncertainties homogenised of fuel region only (gap and cladding are excluded).

Participants are encouraged to submit the output as shown in Figure 39. Similar templates are provided to the participants as Excel files for the other two exercises of Phase I. The request for output of Exercise I-1b is provided in Appendix VIII.

Figure 39: Output sample of Exercise 1

Output Sample

Experiment Name	*KRITZ-2.1*	
Operating Condition	*Cold*	
Nuclear Data Library Used		
Covariance Data Library Used		
Computer Code Used		
Criticality Calculation Method		
Uncertainty Calculation Method		
k_{inf} (forward)	**k_{inf} (adjoint)**	**uncertainties** (%Δk/k)
Top 5 contributors the uncertainty in k_{inf}		**uncertainties** (%Δk/k)
Reaction	**Rate** ($cm^{-3}s^{-1}$)	**uncertainty** (% standard deviation)
Total Absorption Rate		
Absorption Rate in ^{235}U		
Absorption Rate in ^{238}U		
Total Fission Rate		
Fission Rate in ^{235}U		
Fission Rate in ^{238}U		

Name of Participant(s)						**E-mail Address**		
Organization								
Country								
Reactor Name						*PB-2*		
Operating Condition						*Hot Full Power*		
Reactor type						*BWR*		
Nuclear Data Library Used								
Covariance Data Library Used								
Computer Code Used								
Criticality Calculation Method								
Uncertainty Calculation Method								
One-group effective uncertainty								
Matrices						variance	α=1	$\alpha=\sigma_{eff}/\sigma_{total}$
nuclide	Reactions	mt	nuclide	Reactions	mt	(off-diagonal values = 0)	(un-weighted matrix)	(weighted- matrix)

5.3 Results for Exercise I-2

The following results will be compared for Exercise I-2:

Set 1: 2-D assembly models including GEN-III with reflective boundary conditions

- Assembly k_{inf} and associated uncertainties:
  - for HZP of unrodded case;
  - for HZP of rodded case;
  - for HFP of unrodded case;
  - for HFP of rodded case.
- Pin-power-distribution and associated uncertainties:
  - center pin of rodded cases;
  - center pin of unrodded cases;
  - corner pin of rodded cases;
  - corner pin of unrodded case.
- Homogenised two group cross-sections and associated uncertainties (using 0.625 eV as cut-off point);

Set 2: 1-D assembly/reflector model

- The output uncertainties of the reflector DFs at the core/reflector interface.

Set 3: 2-D assembly color sets (mini-cores)

- Mini-core multiplication factors (k_{eff}) and associated uncertainties;
- Mini-core relative pin powers and associated uncertainties.

Set 4: Core test problems from the KRITZ-2 LEU critical experiments

- k_{eff} and associated uncertainties at "room" temperature;
- k_{eff} and associated uncertainties at "elevated" temperature;
- Relative rod powers for the rods and associated uncertainties.

5.4 Results for Exercise I-3

The following results will be compared for Exercise I-3:

Set 1: 3-D core models at HZP conditions (output sample – template for submitting results for the three different reactor types for the first three parameters listed below is provided at the end of this section)

- k_{eff} and associated uncertainties;
- core axial power distribution and associated uncertainties;
- radial assembly power distribution and associated uncertainties;
- axial offset;

- relative pin power distribution and assembly reaction rates for selected fuel assemblies and axial layers (nodes),
- control rod worth,
- Core average (point) kinetic parameters.

Set 2: BWR experimental plant cold critical data for BOC of Cycle 1

- k_{eff} and associated uncertainties;

Set 3: PWR benchmark critical lattice data

- k_{eff} and associated uncertainties;
- Relative rod-by-rod power densities (fission rate distributions) of the central assembly.

Set 4: VVER-1 000 benchmark critical lattice data

- k_{eff} and associated uncertainties.

A suggestion was made as to include the mean and standard deviation against the mean when submitting results for the power distributions and the associated uncertainties – see Figure 40.

Figure 40: Sample output for core power distribution associate uncertainties

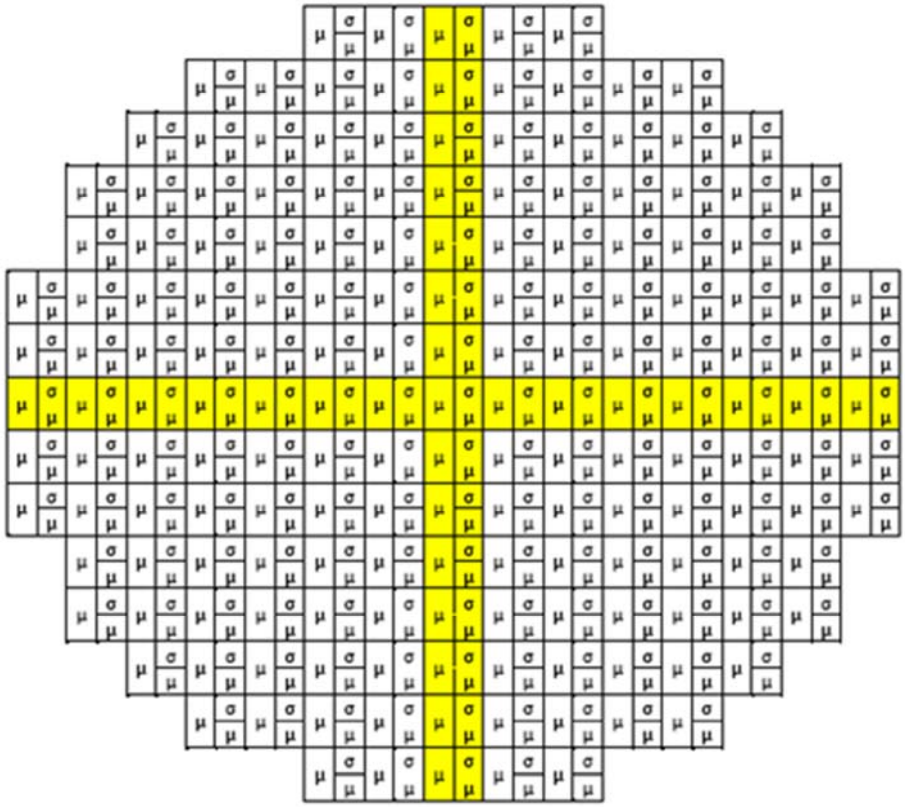

Output samples

- PB-2 BWR results

A Peach bottom - 2 BWR results from code “xxxxxxxx”, exercise I-3

B Steady-state results

B.1 k_{eff} = 1.00000

B.2 Radial power distribution (full core) – start each line in column one, leave a blank space in between each number, and use a total of six spaces per number:

0.9999 0.9999 0.9999 0.9999 0.9999

0.9999 0.9999 0.9999 0.99990.9999 0.9999 0.9999 0.9999 0.9999

0.9999 0.9999 0.9999 0.9999 0.9999 0.9999 0.9999 0.9999 0.9999 0.9999 0.9999

0.9999 0.9999 0.9999 0.9999 0.9999 0.9999 0.9999 0.9999 0.9999 0.9999 0.9999 0.9999 0.9999

0.9999 0.9999 0.9999 0.9999 0.9999 0.9999 0.9999 0.9999 0.9999 0.9999 0.9999 0.9999 0.9999

0.9999 0.9999 0.9999 0.9999 0.9999 0.9999 0.9999 0.9999 0.9999 0.9999 0.9999 0.9999 0.9999 0.9999 0.9999

0.9999 0.9999 0.9999 0.9999 0.9999 0.9999 0.9999 0.9999 0.9999 0.9999 0.9999 0.9999 0.9999 0.9999 0.9999

0.9999 0.9999 0.9999 0.9999 0.9999 0.9999 0.9999 0.9999 0.9999 0.9999 0.9999 0.9999 0.9999 0.9999 0.9999

0.9999 0.9999 0.9999 0.9999 0.9999 0.9999 0.9999 0.9999 0.9999 0.9999 0.9999 0.9999 0.9999 0.9999 0.9999

0.9999 0.9999 0.9999 0.9999 0.9999 0.9999 0.9999 0.9999 0.9999 0.9999 0.9999 0.9999 0.9999 0.9999 0.9999

0.9999 0.9999 0.9999 0.9999 0.9999 0.9999 0.9999 0.9999 0.9999 0.9999 0.9999 0.9999 0.9999

0.9999 0.9999 0.9999 0.9999 0.9999 0.9999 0.9999 0.9999 0.9999 0.9999 0.9999 0.9999 0.9999

0.9999 0.9999 0.9999 0.9999 0.9999 0.9999 0.9999 0.9999 0.9999 0.9999 0.9999

0.9999 0.9999 0.9999 0.9999 0.9999 0.9999 0.9999 0.9999 0.9999

0.9999 0.9999 0.9999 0.9999 0.9999

B.3 Axial power distribution – place all data starting in column one, leave a blank in between each number, and use a total of six spaces per number:

0.9999 0.9999 0.9999 0.9999 0.9999 0.9999 0.9999 0.9999 0.9999 0.9999 0.9999 0.9999

0.9999 0.9999 0.9999 0.9999 0.9999 0.9999 0.9999 0.9999 0.9999 0.9999 0.9999 0.9999

Forms for radial and axial power distributions are given in Figures 41 and 42.

Figure 41: Form for radial power distribution for PB-2 BWR results

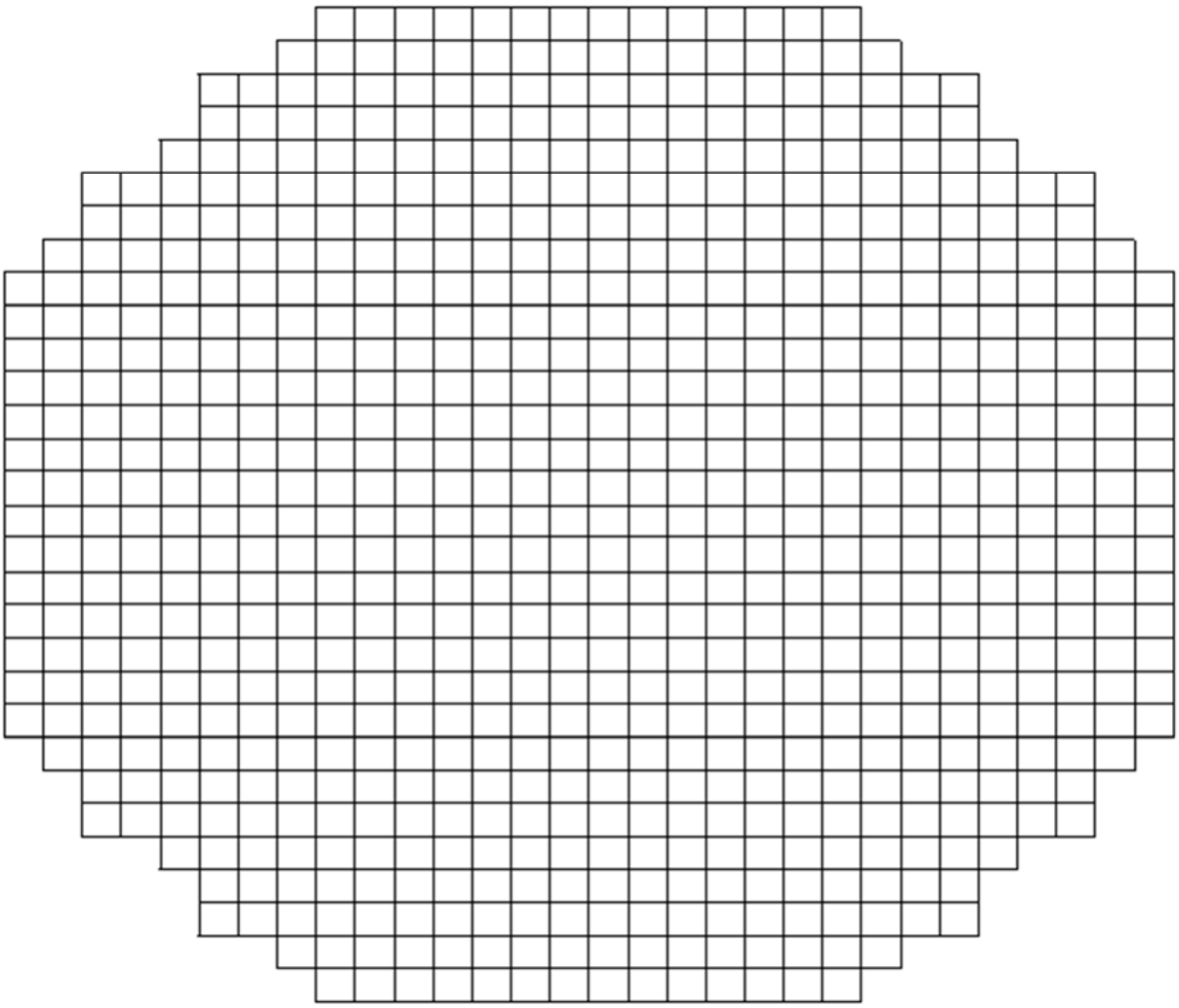

Figure 42: Form for axial power distribution for PB-2 BWR results

Bottom

1	2	3	4	5	6	7	8	9	10	11	12
13	14	15	16	17	18	19	20	21	22	23	24

Top

- TMI-1 PWR results

A TMI-1 PWR results from code "xxxxxxxx", exercise I-3

B Steady-state results

B.1 k_{eff} = 1.00000

B.2 Radial power distribution (full core) – start each line in column one, leave a blank space in between each number, and use a total of six spaces per number:

0.9999 0.9999 0.9999 0.9999 0.9999
0.9999 0.9999 0.9999 0.99990.9999 0.9999 0.9999 0.9999 0.9999
0.9999 0.9999 0.9999 0.9999 0.9999 0.9999 0.9999 0.9999 0.9999 0.9999 0.9999
0.9999 0.9999 0.9999 0.9999 0.9999 0.9999 0.9999 0.9999 0.9999 0.9999 0.9999 0.9999 0.9999
0.9999 0.9999 0.9999 0.9999 0.9999 0.9999 0.9999 0.9999 0.9999 0.9999 0.9999 0.9999 0.9999
0.9999 0.9999 0.9999 0.9999 0.9999 0.9999 0.9999 0.9999 0.9999 0.9999 0.9999 0.9999 0.9999 0.9999 0.9999
0.9999 0.9999 0.9999 0.9999 0.9999 0.9999 0.9999 0.9999 0.9999 0.9999 0.9999 0.9999 0.9999 0.9999 0.9999
0.9999 0.9999 0.9999 0.9999 0.9999 0.9999 0.9999 0.9999 0.9999 0.9999 0.9999 0.9999 0.9999 0.9999 0.9999
0.9999 0.9999 0.9999 0.9999 0.9999 0.9999 0.9999 0.9999 0.9999 0.9999 0.9999 0.9999 0.9999 0.9999 0.9999
0.9999 0.9999 0.9999 0.9999 0.9999 0.9999 0.9999 0.9999 0.9999 0.9999 0.9999 0.9999 0.9999 0.9999 0.9999
0.9999 0.9999 0.9999 0.9999 0.9999 0.9999 0.9999 0.9999 0.9999 0.9999 0.9999 0.9999 0.9999
0.9999 0.9999 0.9999 0.9999 0.9999 0.9999 0.9999 0.9999 0.9999 0.9999 0.9999 0.9999 0.9999
0.9999 0.9999 0.9999 0.9999 0.9999 0.9999 0.9999 0.9999 0.9999 0.9999 0.9999
0.9999 0.9999 0.9999 0.9999 0.9999 0.9999 0.9999 0.9999 0.9999
0.9999 0.9999 0.9999 0.9999 0.9999

B.3 Axial power distribution – place all data starting in column one, leave a blank in between each number, and use a total of six spaces per number:

0.9999 0.9999 0.9999 0.9999 0.9999 0.9999 0.9999 0.9999 0.9999 0.9999 0.9999 0.9999
0.9999 0.9999 0.9999 0.9999 0.9999 0.9999 0.9999 0.9999 0.9999 0.9999 0.9999 0.9999

Forms for radial and axial power distributions are given in Figures 43 and 44.

Figure 43: Form for radial power distribution for TMI-1 PWR results

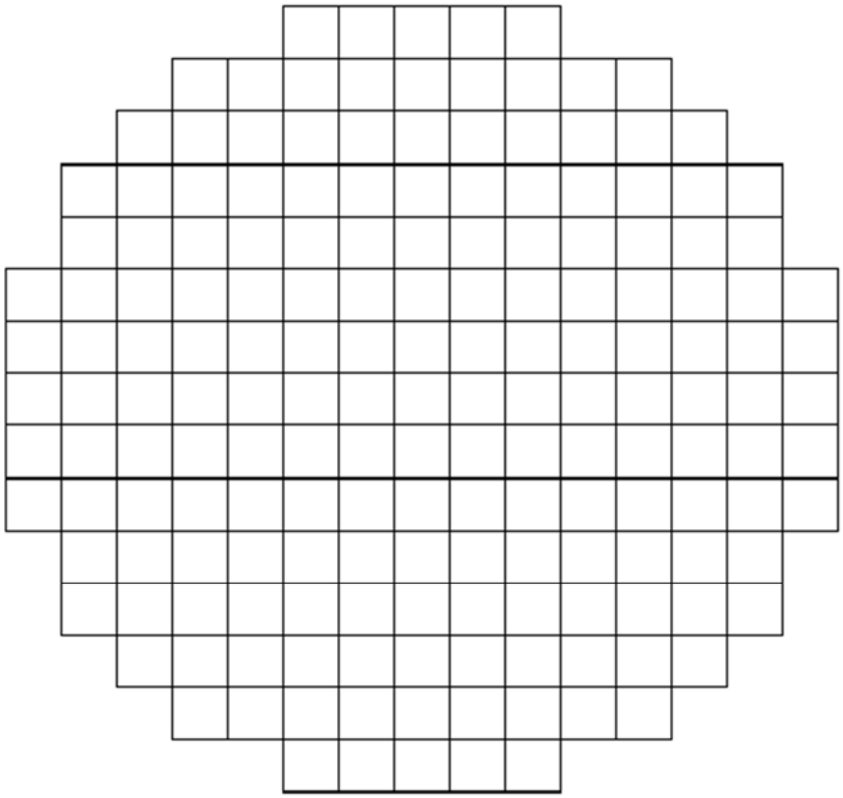

Figure 44: Form for axial power distribution for TMI-1 PWR results

Bottom

13	14	15	16	17	18	19	20	21	22	23	24

Top

- Kozloduy-6 VVER results

A Kozloduy-6 VVER results from code "xxxxxxxx", exercise I-3

B Steady-state results

B.1 k_{eff} = 1.00000

B.2 Radial power distribution (full core) – start each line in column one, leave a blank space in between each number, and use a total of six spaces per number:

0.9999 0.9999 0.9999 0.9999 0.9999 0.9999

0.9999 0.9999 0.9999 0.99990.9999 0.9999 0.9999 0.9999 0.9999

0.9999 0.9999 0.9999 0.9999 0.9999 0.9999 0.9999 0.9999 0.9999 0.9999

0.9999 0.9999 0.9999 0.9999 0.9999 0.9999 0.9999 0.9999 0.9999 0.9999 0.9999

0.9999 0.9999 0.9999 0.9999 0.9999 0.9999 0.9999 0.9999 0.9999 0.9999 0.9999 0.9999

0.9999 0.9999 0.9999 0.9999 0.9999 0.9999 0.9999 0.9999 0.9999 0.9999 0.9999 0.9999 0.9999

0.9999 0.9999 0.9999 0.9999 0.9999 0.9999 0.9999 0.9999 0.9999 0.9999 0.9999 0.9999 0.9999 0.9999

0.9999 0.9999 0.9999 0.9999 0.9999 0.9999 0.9999 0.9999 0.9999 0.9999 0.9999 0.9999 0.9999

0.9999 0.9999 0.9999 0.9999 0.9999 0.9999 0.9999 0.9999 0.9999 0.9999 0.9999 0.9999 0.9999 0.9999

0.9999 0.9999 0.9999 0.9999 0.9999 0.9999 0.9999 0.9999 0.9999 0.9999 0.9999 0.9999 0.9999

0.9999 0.9999 0.9999 0.9999 0.9999 0.9999 0.9999 0.9999 0.9999 0.9999 0.9999 0.9999

0.9999 0.9999 0.9999 0.9999 0.9999 0.9999 0.9999 0.9999 0.9999 0.9999 0.9999

0.9999 0.9999 0.9999 0.9999 0.9999 0.9999 0.9999 0.9999 0.9999 0.9999

0.9999 0.9999 0.9999 0.9999 0.9999 0.9999 0.9999 0.9999 0.9999

0.9999 0.9999 0.9999 0.9999 0.9999 0.9999

B.3 Axial power distribution – place all data starting in column one, leave a blank in between each number, and use a total of six spaces per number:

0.9999 0.9999 0.9999 0.9999 0.9999 0.9999 0.9999 0.9999 0.9999 0.9999

Forms for radial and axial power distributions are given in Figures 45 and 46.

Figure 45: Form for radial power distribution for Kozloduy-6 results

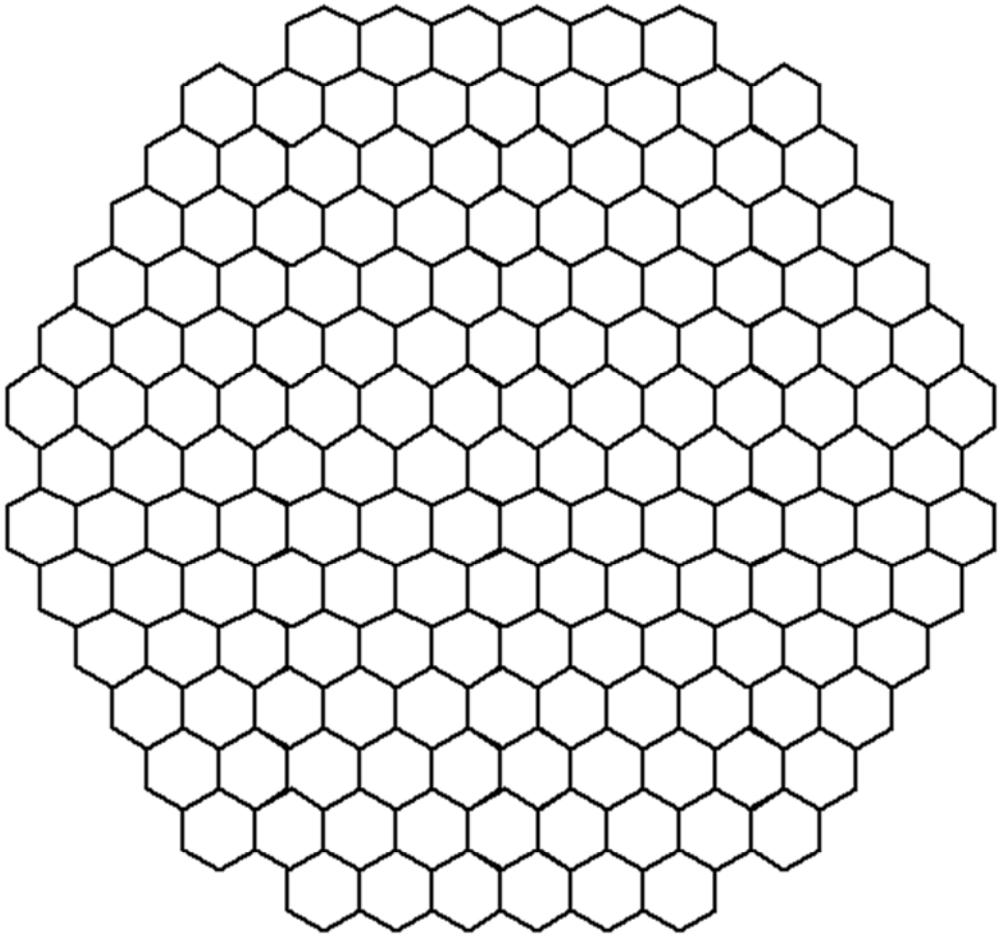

Figure 46: Form for axial power distribution for Kozloduy-6 results

Bottom Top

1	2	3	4	5	6	7	8	9	10

The samples for GEN-III UOX and MOX cores are similar to the above samples taking into account radial and axial core layouts. These two cores are analysed at both HZP and HFP conditions and results should be provided using the same templates for both conditions. The requested output and templates for SNEAK 7A and SNEAK 7B calculations are described in Appendix VII.

Chapter 6: Conclusions

The objective of the OECD LWR UAM activity is to establish an internationally accepted benchmark framework to compare, assess and further develop different uncertainty analysis methods associated with the design, operation and safety of LWRs. As a result, the LWR UAM benchmark will help to address current nuclear power generation industry and regulation needs and issues related to practical implementation of risk-informed regulation. The realistic evaluation of consequences must be made with best-estimate coupled codes, but to be meaningful, such results should be supplemented by an uncertainty analysis. The use of coupled codes allows us to avoid unnecessary penalties due to incoherent approximations in the traditional decoupled calculations, and to obtain more accurate evaluation of margins regarding licensing limit. This becomes important for licensing power upgrades, improved fuel assembly and control rod designs, higher burn-up and others issues related to operating LWRs as well as to the new Generation 3+ designs being licensed now (ESBWR, AP-1 000, EPR-1 600, etc.). Establishing an internationally accepted LWR UAM benchmark framework offers the possibility to accelerate the licensing process when using best estimate methods.

The proposed technical approach is to establish a benchmark for uncertainty analysis in best-estimate modelling and coupled multi-physics and multi-scale LWR analysis, using as bases a series of well-defined problems with complete sets of input specifications and reference experimental data. The objective is to determine the uncertainty in LWR system calculations at all stages of coupled reactor physics/thermal hydraulics calculations. The full chain of uncertainty propagation from basic data, engineering uncertainties, across different scales (multi-scale), and physics phenomena (multi-physics) will be tested on a number of benchmark exercises for which experimental data are available and for which the power plant details have been released.

This report presents benchmark specifications for Phase I (Neutronics Phase) of the OECD LWR UAM benchmark in a format similar to the previous OECD/NRC benchmark specifications. Phase I consists of the following exercises:

- Exercise 1 (I-1): “Cell Physics” focused on the derivation of the multi-group microscopic cross-section libraries and their uncertainties.
- Exercise 2 (I-2): “Lattice Physics” focused on the derivation of the few-group macroscopic cross-section libraries and their uncertainties.
- Exercise 3 (I-3): “Core Physics” focused on the core steady-state stand-alone neutronics calculations and their uncertainties.

These exercises follow those established in the industry and regulation routine calculation scheme for LWR design and safety analysis. This phase is focused on understanding uncertainties in the prediction of key reactor core parameters associated with LWR stand-alone neutronics core simulation. Such uncertainties occur due to input data uncertainties, modelling errors, and numerical approximations. The chosen approach in Phase I is to select/propagate the most important contributors for each exercise which can be treated in a practical manner. The cross-section uncertainty information is considered as the most important source of input uncertainty for Phase I. The cross-section related uncertainties are propagated through the 3 Exercises of Phase I. In Exercise I-1 these are the variance and covariance data associated with continuous energy cross-sections in evaluated nuclear data files. In Exercise I-2 these are the variance and covariance data associated with multi-group cross-sections used as input in the lattice physics codes. In Exercise I-3 these are the variance and covariance data associated with few-group cross-sections used as input in the core simulators.

Depending on the availability of different methods in the computer code of choice for a given exercise, the related methodological uncertainties can play a smaller or larger role. The participants are responsible for performing convergence studies with their computer codes in order to remove the uncertainties

associated with numerical approximations (numerical method uncertainties) and reduce the uncertainties associated with the methods (physics uncertainties) used in their codes. The method related contribution of uncertainty can be derived from earlier benchmarks conducted within NEA/OECD or from the verification (mathematics) and validation (physics) studies performed with the computer code of choice.

In the current LWR standard calculation scheme (utilised in industry and regulation) different modelling approximations are usually used at different stages of the calculation. These approximations are the second important source of input uncertainty. In order to assess the uncertainties due to utilisation of the above-mentioned approximations, one has to decompose and evaluate the errors of these approximations. Evaluation of the uncertainties introduced with such modelling approximations is important because in some situations these approximations work well and in others they do not. This is accomplished by designing appropriate test problems for a given exercise.

Geometry, material properties and manufacturing uncertainties are also an important source of calculation uncertainty. Information for these uncertainties for the different test models as well as on their propagation will be provided in the final report on Phase I by the benchmark team.

Understanding the uncertainties in key output reactor core parameters associated with steady-state core simulation is important with regard to introducing appropriate design margins and deciding where efforts should be directed to reduce uncertainties. The obtained output uncertainties from Phase I of the OECD LWR UAM benchmark will be utilised as input uncertainties in the remaining two phases – Phase II (Core Phase) and Phase III (System Phase).

References

1. "Neutronics/Thermal-hydraulics Coupling in LWR Technology", Vol. 3, CRISSUE-S-WP3: Achievements and Recommendations Report, ISBN 92-64-02085-3, NEA No. 5434, OECD, 2004.
2. "Uncertainty Analysis in Modelling UAM-2006 Workshop", Summary Record, NEA/NSC/DOC (2006)15.
3. "Expert Group on Uncertainty Analysis in Modelling", Mandate and Programme of Work, NEA/NSC/DOC (2006)17.
4. "Uncertainty Analysis in Modeling First Workshop (UAM-1)", Summary Record, NEA/NSC/DOC (2007)17.
5. Technology Relevance of the "Uncertainty Analysis In Modelling" Project for Nuclear Reactor Safety, NEA/NSC/DOC (2007)15.
6. J. Solis, K. Ivanov, B. Sarikaya, A. Olson, and K. Hunt, "BWR TT Benchmark. Volume I: Final Specifications", NEA/NSC/DOC (2001)1.
7. K. Ivanov, T. Beam, A. Baratta, A. Irani, and N. Trikouros, "PWR MSLB Benchmark. Volume 1: Final Specifications", NEA/NSC/DOC (99)8, April 1999.
8. B. Ivanov, K. Ivanov, P. Groudev, M. Pavlova, and V. Hadjiev, "VVER-1000 Coolant Transient Benchmark (V1 000-CT). Phase 1 – Final Specification". NEA/NSC/DOC (2002)6.
9. B. Neykov, F. Aydogan, L. Hochreiter, K. Ivanov (PSU), H. Utsuno, F. Kasahara (JNES), E. Sartori (OECD/NEA), M. Martin (CEA), "OECD/NEA/US-NRC/NUPEC BWR Full-size Fine-mesh Bundle Test (BFBT) Benchmark", Volume I: Specifications, © OECD 2006, NEA No. 6212, NEA/NSC/DOC(2005)5.
10. A. Rubin, A. Schoedel, M. Avramova *et al.* "OECD/NRC Benchmark Based on NUPEC PWR Subchannel and Bundle Tests; Vol. I: Experimental Database and Final Problem Specifications", NEA/NSC/DOC(2010)1 (November 2010).
11. "Core Design and Operating Data for Cycles 1 and 2 of Peach Bottom 2", EPRI NP-563, June 1978.
12. "Transient and Stability Tests at Peach Bottom Atomic Power Station Unit 2 at End of Cycle 2", EPRI NP-564, June 1978.
13. A. M. Olson, "Methods for Performing BWR System Transient Analysis", Philadelphia Electric Company, Topical Report PECo-FMS-0004-A (1988).
14. Claire Vaglio and Alain Santamarina "Assembly and Core Specification of Generation 3 PWR", October 2010, CEA, France.
15. E. Ivanov, V. Mastrangelo, A. Duranti, and I. Kodeli, "Specification of Kinetic Parameters Benchmark SNEAK", January 2011, France.
16. Dermott E. Cullen, "A Temperature Dependent ENDF/B-VI, Release 8 Cross Section Library", UCRL-TR-202284, INT 2004.
17. M.B. Chadwick, P. Obložinský, M. Herman *et al.* "ENDF/B-VII.0: Next Generation Evaluated Nuclear Data Library for Nuclear Science and Technology, Nuclear Data Sheets 107 (2006), Pages 2931-3060.
18. P. Obložinský, "New ENDF/B-VII Library", Proceeding of PHYSOR-2006 Conference (2006).
19. A.J. Koning, O. Bersillon, R.A. Forrest, R. Jacqmin, M.A. Kellett, A. Nouri *et al.* "Status of the JEFF Nuclear Data Library", Proceedings of the International Conference on Nuclear Data for Science and Technology, Santa Fe, 2004, pp. 177–182.
20. A.Santamarina *et al.* "The JEFF-3.1.1 Nuclear Data Library", JEFF Report 22, OECD/NEA, No. 6807 (2009).
21. K. Shibata, T. Kawano *et al.* "Japanese Evaluated Nuclear Data Library Version 3 Revision-3: JENDL-3.3", J. Nucl. Sci. Technol. 39, 1125 (2002).

22. A.J. Koning and D. Rochman, TENDL-2008: Consistent TALYS-base Evaluated Nuclear Data Library including covariance data, www.talys.eu/tendl-2008, *OECD/NEA JEF/DOC-1262*, November 2008.

23. M. Herman *et al.* "EMPIRE – New Reaction Model Code (Version: 2.19 Lodi)", 2005.

24. M. Herman, P. Obložinský, R. Capote, M. Sin, A. Trkov, A. Ventura, V. Zerkin, "Recent Developments of the Nuclear Reaction Model Code EMPIRE", Proc. Int. Conf. Nucl. Data for Sci. Tech., Santa Fe, New Mexico, 26 September – 1 October, 2004, AIP 769 (2005) 1184.

25. S.F. Mughabghab, "Atlas of Neutron Resonances", Resonance Parameters and Thermal Cross Sections, Elsevier 2006.

26. N. M. Larson, "Updated Users' Guide for SAMMY: Multilevel R-matrix Fits to Neutron Data Using Bayes' Equations", ORNL/TM-9179/7, Oak Ridge National Laboratory, Oak Ridge, TN, USA (2006). Also available as ENDF-364/R1.

27. L. C. Leal, H. Derrien, N. M. Larson and A. Alpan, Covariance and Sensitivity Data Generation at ORNL", Radiation Protection Dosimetry, Vol. 115, No. 1–4, pp. 133–135 (2005).

28. M. L. Williams, B. L. Broadhead, M. E. Dunn, B. T. Rearden, "Approximate Techniques For Representing Nuclear Data Uncertainties," Eighth International Topical Meeting on Nuclear Applications and Utilization of Accelerators (AccApp'07)," Pocatello, ID (30 July -2 August 2007).

29. D. Knott, B. H. Forssen, and M. Edenius "CASMO-4. A Fuel Assembly Burn-up Program Methodology", STUDSVIK/SOA-95/2, 1995.

30. "HELIOS Methods", StudsvikScandpower, 2000.

31. N.Hfaiedh, A.Santamarina, Determination of the Optimized SHEM Mesh for Neutron Transport Calculation, Proc. Int. Conf. of Math. and Comp, React. Phys.and Nucl. Appl. M&C 2005, Avignon, France, 12-15 September 2005.

32. M. DeHart, "TRITON: A Two-Dimensional Depletion Sequence for Characterization of Spent Nuclear Fuel", NUREG-0200, ORNL/NUREG/CSD-2/R7 (2004).

33. D. F. Hollenbach and P. B. Fox, "CENTRM Validation", ORNL/TM-2004/66, May 2005.

34. R.E. MacFarlane and D.W. Muir: The NJOY Nuclear Data Processing System, Version 1. LA12740-M (October 1994) and R.E. MacFarlane: "README0" (December 31 1999).

35. NJOY99, < http://www.oecd-nea.org/tools/abstract/detail/PSR-0480/> Data Processing System of Evaluated Nuclear Data Files ENDF Format, in particular the modules ERRORR computes multi-group covariance matrices from ENDF uncertainties and COVR performs covariance plotting and output formatting operations.

36. G. Chiba, "ERRORJ – A Code to Process Neutron-nuclide Reaction Cross Section Covariance, Version 2.3", (JAEA-Data/Code 2007-007, January 2007) ERRORJ, Multi-group covariance matrices generation from ENDF-6 format for the JENDL 3.3 data, http://www.oecd-nea.org/tools/abstract/detail/NEA-1676/.

37. D. Wiarda and M.E. Dunn: PUFF-IV: A Code for Processing ENDF Uncertainty Data into Multi-group Covariance Matrices,' Informal report (2006), and M. E. Dunn and B. L. Broadhead, PUFF-III: A Multi-group Covariance Processing Code for the AMPX Cross Section Processing System, PHYSOR-2000, and USA.

38. N. M. Larson, "Updated Users' Guide for SAMMY: Multilevel R-Matrix Fits to Neutron Data Using Bayes' Equations", ORNL/TM-9179/R7 (September 2006, corrected February 2007).

39. M. C. Moxon, T. C. Ware, C. J. Dean *et al.* REFIT-2007 A Least-Square Fitting Program for Resonance Analysis of Neutron Transmission, Capture, Fission and Scattering Data Users. Guide for REFIT-2007-08 UKNSF (2007) P216, August 2007.

40. M. L. Williams, B.L. Broadhead, C.V. Parks, "Eigenvalue Sensitivity Theory for Resonance Shielded Cross Sections", *Nucl. Sci. and Engr. 138*, pp. 177-191 (2001).

41. B. Rearden *et al.* "Applications of the TSUNAMI Sensitivity and Uncertainty Analysis Methodology", Proceeding of ICNC2003 Conference, October 20–24, 2003, Japan.

42. G. Aliberti *et al*. Nuclear data sensitivity, uncertainty and target accuracy assessment for future nuclear systems, Annuals of Nuclear Energy 33 (2006) 700–733.
43. B. L. Broadhead, "SCALE 5.1 Cross-Section Covariance Libraries", ORNL/TM-2005/39, Version 5.1, Vol. I, Book 3, Sect. M19, November 2006.
44. SCALE: A Modular Code System for Performing Standardized Computer Analyses for Licensing Evaluations, ORNL/TM-2005/39, Version 5.1, Vols. I-III, November 2006.
45. M. L. Williams, D. Wiarda, G. Arbanas, B. L. Broadhead, "SCALE-6.0 Nuclear Data Covariance Library", January 2009, ORNL/TM-2005/39, Version 6, Vol. III, Sect. M19.
46. I. Kodeli, "Manual for ANGELO2 and LAMBDA codes", NEA-1264/05 package (2003).
47. I. Kodeli and E. Sartori, "ZZ-VITAMIN/COVA, Covariance Data Library", NEA1264/03, 1990.
48. "Benchmark on the KRITZ-2 LEU and MOX Critical Experiments – Final Report", NEA/NSC/DOC (2005)24, ISBN 92-64-02298-8.
49. International Reactor Physics Experiments Database Project (IRPhE), "International Handbook of Evaluated Reactor Physics Benchmark Experiments", NEA/NSC/DOC (2006)1, March 2009 Edition, OECD/NEA.
50. I. Kodeli, "Multidimensional Deterministic Nuclear Data Sensitivity and Uncertainty Code System: Method and Application", *Nuclear Science and Engineering*: 138, 45-66 (2001).
51. H. Abdel-Khalik and P. Turinsky, "Evaluation of Core Attribute Uncertainties due to Input Data Uncertainties", TANSAO 92, pp. 546-547, 2005.
52. M. Jessee, H. Abdel-Khalik and P. Turinsky, "Evaluation of BWR Core Attribute Uncertainties due to Multi-group Cross-Section Uncertainties", Proc. of M&C 2007, Monterey, California, USA (2007).
53. T. Horiuchi *et al.* "Error Decomposition of Approximations for BWR Core Calculations", Proc. of PHYSOR-2002, Seoul, Korea, 2002.
54. R. Macian, M. Zimmermann, R. Chawla, "Uncertainty Analysis Applied to Fuel Depletion Calculations", Proc. of PHYSOR-2004, Chicago, USA (2004).
55. D. Colemann, *et al*. "As-Built Design and Material Characteristics of the TMI-2 Core", NSAC, EPRI, 1986.
56. "Delayed Neutron Data for Major Actinides", Volume 6, NEA/WPEC-6, 2002.
57. EPRI NP-240 (1976), "Core Design and Operating Data for Cycles 1 and 2of Quad Cities 1".
58. A. Karve *et al.* "Uncertainty Estimates in Cold Critical Eigenvalue Predictions", Proc of ANFM-2003 Conference, Hilton Head Island, South Carolina, USA (2003).
59. International Handbook of Evaluated Criticality Benchmark Experiments, "International Handbook of Evaluated Reactor Physics Benchmark Experiments", NEA/NSC/DOC (95)03, September 2007 Edition.
60. S. Baker, "TransLAT Lattice Physics Code Benchmark to B&W Gadolinia Criticals", Proc. of PHYSOR-2004, Chicago, USA (2004).
61. K. Shibata *et al.*"JENDL-4.0: A New Library for Nuclear Science and Engineering," *Journal of Nuclear Science and Technology*, Vol. 48, No. 1, p. 1–30 (2011).
62. I. Kodeli, Sensitivity and uncertainty in effective delayed neutron fraction, presented at the UAM-5 Meeting, Stockholm, April 2011.
63. A. Zukeran, H. Hanaki, S. Sawada, T. Suzuki, Uncertainty Evaluation of Effective Delayed Neutron Fraction beff of Typical Proto-type Fast Reactor, J. Nucl. Sci. and Technology, Vol. 36, No.1, p. 61-80 (Jan. 1999).
64. R. K. Meule Kamp, S. C. van der Marck, Calculating the Effective Delayed Neutron Fraction with Monte Carlo, Nucl. Sci. and Eng., 152, 142-148 (2006).
65. L. Snoj, A. Kavčič, G. Žerovnik, M. Ravnik, Calculation of kinetic parameters for mixed TRIGA cores with Monte Carlo, Annals of Nuclear Energy (2009).

66. E. Ivanov, S. Pignet, Calculational modelling for the development of βeff experimental based benchmarks Proc M&C 2011, Rio de Janeiro, Brazil, May 8-12, 2011, on CD-ROM, Latin American Section (LAS)/American Nuclear Society (ANS), ISBN 978-85-63688-00-2.

67. L. N. Usachev, "Equation for the value of neutrons in a kinetic reactor in perturbation theory", Reactor contruction and reactor theory, (Publishing House of the USSR Academy of Sciences, Moscow), 1955, 251 (in Russian).

Appendix I: List of nuclides with covariance information in 44GROUPV5COV set

Nuclide	Data source	Nuclide	Data source
^{27}Al	ENDF/B-V	^{55}Mn	ENDF/B-V
^{241}Am	ENDF/B-V	^{14}N	ENDF/B-V
^{197}Au	ENDF/B-V	^{23}Na	ENDF/B-V
^{10}B	ENDF/B-V	Ni	ENDF/B-V
C	ENDF/B-V	^{237}Np	ENDF/B-V
C-graphite	ENDF/B-V	^{16}O	ENDF/B-V
^{252}Cf	χ only	Pb	ENDF/B-V
^{59}Co	ENDF/B-V	^{239}Pu	ENDF/B-V
Cr	ENDF/B-V	^{240}Pu	ENDF/B-V
^{19}F	ENDF/B-V	^{241}Pu	ENDF/B-V
Fe	ENDF/B-V	^{242}Pu	ENDF/B-V
^{1}H	ENDF/B-V	Si	ENDF/B-V
H-ZrH	ENDF/B-V	^{232}Th	ENDF/B-V
H-poly	ENDF/B-V	^{233}U	χ only
^{115}In	ENDF/B-V	^{235}U	ENDF/B-V
^{6}Li	ENDF/B-V	^{238}U	ENDF/B-V
^{7}Li	ENDF/B-V		

Appendix II: List of nuclides with covariance information in 44GROUPV6COV set

Nuclide	Data source	Nuclide	Data source
^{27}Al	ENDF/B-VI	^{7}Li	ENDF/B-VI
^{241}Am	ENDF/B-VI	^{55}Mn	ENDF/B-VI
^{197}Au	ENDF/B-VI	^{23}Na	ENDF/B-VI
^{10}B	ENDF/B-V	^{93}Nb	ENDF/B-VI
^{11}B	JENDL 3.3	^{58}Ni	ENDF/B-VI
^{209}Bi	ENDF/B-VI	^{60}Ni	ENDF/B-VI
C	ENDF/B-VI	^{61}Ni	ENDF/B-VI
C-graphite	ENDF/B-VI	^{62}Ni	ENDF/B-VI
^{252}Cf	χ only	^{64}Ni	ENDF/B-VI
^{59}Co	ENDF/B-VI	^{16}O	JENDL 3.3
^{50}Cr	ENDF/B-VI	^{206}Pb	ENDF/B-VI
^{52}Cr	ENDF/B-VI	^{207}Pb	ENDF/B-VI
^{53}Cr	ENDF/B-VI	^{208}Pb	ENDF/B-VI
^{54}Cr	ENDF/B-VI	^{239}Pu	ENDF/B-V
^{63}Cu	ENDF/B-VI	^{240}Pu	JENDL 3.3
^{65}Cu	ENDF/B-VI	^{241}Pu	JENDL 3.3
^{19}F	ENDF/B-VI	^{242}Pu	ENDF/B-VI
^{54}Fe	ENDF/B-VI	^{185}Re	ENDF/B-VI
^{56}Fe	ENDF/B-VI	^{187}Re	ENDF/B-VI
^{57}Fe	ENDF/B-VI	^{45}Sc	ENDF/B-VI
^{58}Fe	ENDF/B-VI	Si	ENDF/B-VI
^{1}H	JENDL 3.3	^{28}Si	ENDF/B-VI
H-ZrH	JENDL 3.3	^{29}Si	ENDF/B-VI
H-poly	JENDL 3.3	^{30}Si	ENDF/B-VI
Hfreegas	JENDL 3.3	^{232}Th	ENDF/B-VII Beta 2
^{2}H	CENDL 2	^{233}U	ENDF/B-VII Beta 2
Dfreegas	CENDL 2	^{235}U	JENDL 3.3
^{3}H	JEF 3.1	^{238}U	JENDL 3.3
^{3}He	CENDL 2	V	ENDF/B-VI
In	ENDF/B-VI	^{89}Y	ENDF/B-VI

Appendix III: List of nuclides with covariance information in 44GROUPV5REC set

Nuclide	Data source	Nuclide	Data source	Nuclide	Data source
^{107}Ag	Mughabghab	^{133}Cs	Mughabghab	^{83}Kr	Mughabghab
^{109}Ag	Mughabghab	^{134}Cs	Mughabghab	^{84}Kr	Mughabghab
^{111}Ag	Mughabghab	^{135}Cs	Mughabghab	^{85}Kr	Mughabghab
^{27}Al	ENDF/B-V	^{137}Cs	Mughabghab	^{86}Kr	Mughabghab
^{241}Am	ENDF/B-VI	Cu	ENDF/B-VI	^{139}La	Mughabghab
^{242}Am	Mughabghab	^{160}Dy	Mughabghab	^{140}La	Mughabghab
^{242m}Am	Mughabghab	^{161}Dy	Mughabghab	^{6}Li	ENDF/B-V
^{243}Am	Mughabghab	^{162}Dy	Mughabghab	^{7}Li	ENDF/B-V
^{75}As	Mughabghab	^{163}Dy	Mughabghab	^{175}Lu	Mughabghab
^{197}Au	ENDF/B-V	^{164}Dy	Mughabghab	^{176}Lu	Mughabghab
^{10}B	ENDF/B-V	^{166}Er	Mughabghab	Mg	Mughabghab
^{11}B	JENDL 3.3	^{167}Er	Mughabghab	^{55}Mn	ENDF/B-VI
^{134}Ba	Mughabghab	^{253}Es	Mughabghab	Mo	Mughabghab
^{135}Ba	Mughabghab	^{151}Eu	Mughabghab	^{94}Mo	Mughabghab
^{136}Ba	Mughabghab	^{152}Eu	Mughabghab	^{95}Mo	Mughabghab
^{137}Ba	Mughabghab	^{153}Eu	Mughabghab	^{96}Mo	Mughabghab
^{138}Ba	Mughabghab	^{154}Eu	Mughabghab	^{97}Mo	Mughabghab
^{140}Ba	Mughabghab	^{155}Eu	Mughabghab	^{14}N	ENDF/B-V
^{9}Be	Mughabghab	^{19}F	ENDF/B-V	^{15}N	Mughabghab
Be-bound	Mughabghab	Fe	ENDF/B-V	^{23}Na	ENDF/B-V
^{209}Bi	ENDF/B-VI	Ga	Mughabghab	^{93}Nb	ENDF/B-V
^{249}Bk	Mughabghab	^{152}Gd	ENDF/B-VII Beta 2	^{94}Nb	Mughabghab
^{79}Br	Mughabghab	^{154}Gd	ENDF/B-VII Beta 2	^{95}Nb	Mughabghab
^{81}Br	Mughabghab	^{155}Gd	ENDF/B-VII Beta 2	^{142}Nd	Mughabghab
C	ENDF/B-V	^{156}Gd	ENDF/B-VII Beta 2	^{143}Nd	Mughabghab
C-graphite	ENDF/B-V	^{157}Gd	ENDF/B-VII Beta 2	^{144}Nd	Mughabghab
Ca	Mughabghab	^{158}Gd	ENDF/B-VII Beta 2	^{145}Nd	Mughabghab
Cd	Mughabghab	^{160}Gd	ENDF/B-VII Beta 2	^{146}Nd	Mughabghab
^{106}Cd	Mughabghab	^{72}Ge	Mughabghab	^{147}Nd	Mughabghab
^{108}Cd	Mughabghab	^{73}Ge	Mughabghab	^{148}Nd	Mughabghab
^{110}Cd	Mughabghab	^{74}Ge	Mughabghab	^{150}Nd	Mughabghab
^{111}Cd	Mughabghab	^{76}Ge	Mughabghab	Ni	ENDF/B-V
^{112}Cd	Mughabghab	^{1}H	ENDF/B-V	^{237}Np	ENDF/B-V
^{113}Cd	Mughabghab	H-ZrH	ENDF/B-V	^{16}O	ENDF/B-V
^{114}Cd	Mughabghab	H-poly	ENDF/B-V	^{17}O	Mughabghab
^{116}Cd	Mughabghab	^{2}H	CENDL 2	^{31}P	Mughabghab
^{140}Ce	Mughabghab	^{3}H	JEF 3.1	^{231}Pa	Mughabghab
^{141}Ce	Mughabghab	^{3}He	CENDL 2	^{233}Pa	Mughabghab
^{142}Ce	Mughabghab	^{4}He	Mughabghab	Pb	ENDF/B-V
^{143}Ce	Mughabghab	Hf	Mughabghab	^{102}Pd	Mughabghab
^{144}Ce	Mughabghab	^{174}Hf	Mughabghab	^{104}Pd	Mughabghab
^{249}Cf	Mughabghab	^{176}Hf	Mughabghab	^{105}Pd	Mughabghab
^{250}Cf	Mughabghab	^{177}Hf	Mughabghab	^{106}Pd	Mughabghab
^{251}Cf	Mughabghab	^{178}Hf	Mughabghab	^{107}Pd	Mughabghab
^{252}Cf	Mughabghab	^{179}Hf	Mughabghab	^{108}Pd	Mughabghab
^{253}Cf	Mughabghab	^{180}Hf	Mughabghab	^{110}Pd	Mughabghab
Cl	Mughabghab	^{165}Ho	Mughabghab	^{147}Pm	Mughabghab
^{242}Cm	Mughabghab	^{127}I	Mughabghab	^{148}Pm	Mughabghab
^{243}Cm	Mughabghab	^{129}I	Mughabghab	^{148m}Pm	Mughabghab
^{244}Cm	Mughabghab	^{130}I	Mughabghab	^{149}Pm	Mughabghab
^{245}Cm	Mughabghab	^{131}I	Mughabghab	^{141}Pr	Mughabghab
^{246}Cm	Mughabghab	^{115}In	ENDF/B-V	^{142}Pr	Mughabghab
^{247}Cm	Mughabghab	K	Mughabghab	^{143}Pr	Mughabghab
^{248}Cm	Mughabghab	^{78}Kr	Mughabghab	^{238}Pu	Mughabghab
^{59}Co	ENDF/B-V	^{80}Kr	Mughabghab	^{239}Pu	ENDF/B-V
Cr	ENDF/B-V	^{82}Kr	Mughabghab	^{240}Pu	JENDL 3.3

^{241}Pu	ENDF/B-V	^{149}Sm	Mughabghab	^{128}Te	Mughabghab
^{242}Pu	ENDF/B-V	^{150}Sm	Mughabghab	^{130}Te	Mughabghab
^{243}Pu	Mughabghab	^{151}Sm	Mughabghab	^{230}Th	Mughabghab
^{244}Pu	Mughabghab	^{152}Sm	Mughabghab	^{232}Th	ENDF/B-V
^{85}Rb	Mughabghab	^{153}Sm	Mughabghab	Ti	Mughabghab
^{87}Rb	Mughabghab	^{154}Sm	Mughabghab	^{232}U	Mughabghab
^{185}Re	ENDF/B-VI	^{112}Sn	Mughabghab	^{233}U	ENDF/B-VII Beta 2
^{187}Re	ENDF/B-VI	^{114}Sn	Mughabghab	^{234}U	Mughabghab
^{103}Rh	Mughabghab	^{115}Sn	Mughabghab	^{235}U	ENDF/B-V
^{105}Rh	Mughabghab	^{116}Sn	Mughabghab	^{236}U	Mughabghab
^{96}Ru	Mughabghab	^{117}Sn	Mughabghab	^{237}U	Mughabghab
^{99}Ru	Mughabghab	^{118}Sn	Mughabghab	^{238}U	ENDF/B-V
^{100}Ru	Mughabghab	^{119}Sn	Mughabghab	V	ENDF/B-V
^{101}Ru	Mughabghab	^{120}Sn	Mughabghab	W	Mughabghab
^{102}Ru	Mughabghab	^{122}Sn	Mughabghab	^{182}W	Mughabghab
^{104}Ru	Mughabghab	^{124}Sn	Mughabghab	^{183}W	Mughabghab
^{105}Ru	Mughabghab	^{84}Sr	Mughabghab	^{184}W	Mughabghab
^{106}Ru	Mughabghab	^{86}Sr	Mughabghab	^{186}W	Mughabghab
S	Mughabghab	^{87}Sr	Mughabghab	^{124}Xe	Mughabghab
^{32}S	Mughabghab	^{88}Sr	Mughabghab	^{126}Xe	Mughabghab
^{121}Sb	Mughabghab	^{89}Sr	Mughabghab	^{128}Xe	Mughabghab
^{123}Sb	Mughabghab	^{90}Sr	Mughabghab	^{129}Xe	Mughabghab
^{124}Sb	Mughabghab	^{181}Ta	Mughabghab	^{130}Xe	Mughabghab
^{45}Sc	ENDF/B-VI	^{182}Ta	Mughabghab	^{131}Xe	Mughabghab
^{74}Se	Mughabghab	^{159}Tb	Mughabghab	^{132}Xe	Mughabghab
^{76}Se	Mughabghab	^{160}Tb	Mughabghab	^{133}Xe	Mughabghab
^{77}Se	Mughabghab	^{99}Tc	Mughabghab	^{134}Xe	Mughabghab
^{78}Se	Mughabghab	^{120}Te	Mughabghab	^{135}Xe	Mughabghab
^{80}Se	Mughabghab	^{122}Te	Mughabghab	^{136}Xe	Mughabghab
^{82}Se	Mughabghab	^{123}Te	Mughabghab	^{89}Y	ENDF/B-VI
Si	ENDF/B-V	^{124}Te	Mughabghab	^{90}Y	Mughabghab
^{144}Sm	Mughabghab	^{125}Te	Mughabghab	^{91}Y	Mughabghab
^{147}Sm	Mughabghab	^{126}Te	Mughabghab	Zr	Mughabghab
^{148}Sm	Mughabghab	^{127m}Te	Mughabghab	^{90}Zr	Mughabghab

Appendix IV: List of nuclides with covariance information in 44GROUPV6REC set

Nuclide	Data source	Nuclide	Data source	Nuclide	Data source
^{107}Ag	Mughabghab	^{52}Cr	ENDF/B-VI	^{129}I	Mughabghab
^{109}Ag	Mughabghab	^{53}Cr	ENDF/B-VI	^{130}I	Mughabghab
^{111}Ag	Mughabghab	^{54}Cr	ENDF/B-VI	^{131}I	Mughabghab
^{27}Al	ENDF/B-VI	^{133}Cs	Mughabghab	In	ENDF/B-VI
^{241}Am	ENDF/B-VI	^{134}Cs	Mughabghab	^{113}In	Mughabghab
^{242}Am	Mughabghab	^{135}Cs	Mughabghab	^{191}Ir	Mughabghab
^{242m}Am	Mughabghab	^{137}Cs	Mughabghab	^{193}Ir	Mughabghab
^{243}Am	Mughabghab	^{63}Cu	ENDF/B-VI	K	Mughabghab
^{75}As	Mughabghab	^{65}Cu	ENDF/B-VI	^{78}Kr	Mughabghab
^{197}Au	ENDF/B-VI	^{160}Dy	Mughabghab	^{80}Kr	Mughabghab
^{10}B	ENDF/B-V	^{161}Dy	Mughabghab	^{82}Kr	Mughabghab
^{11}B	JENDL 3.3	^{162}Dy	Mughabghab	^{83}Kr	Mughabghab
^{134}Ba	Mughabghab	^{163}Dy	Mughabghab	^{84}Kr	Mughabghab
^{135}Ba	Mughabghab	^{164}Dy	Mughabghab	^{85}Kr	Mughabghab
^{136}Ba	Mughabghab	^{166}Er	Mughabghab	^{86}Kr	Mughabghab
^{137}Ba	Mughabghab	^{167}Er	Mughabghab	^{139}La	Mughabghab
^{138}Ba	Mughabghab	^{253}Es	Mughabghab	^{140}La	Mughabghab
^{140}Ba	Mughabghab	^{151}Eu	Mughabghab	^{6}Li	Mughabghab
^{9}Be	Mughabghab	^{152}Eu	Mughabghab	^{7}Li	ENDF/B-Vi
Be-bound	Mughabghab	^{153}Eu	Mughabghab	^{175}Lu	Mughabghab
^{209}Bi	ENDF/B-VI	^{154}Eu	Mughabghab	^{176}Lu	Mughabghab
^{249}Bk	Mughabghab	^{155}Eu	Mughabghab	Mg	Mughabghab
^{79}Br	Mughabghab	^{19}F	ENDF/B-VI	^{55}Mn	ENDF/B-VI
^{81}Br	Mughabghab	^{54}Fe	ENDF/B-VI	Mo	Mughabghab
C	ENDF/B-VI	^{56}Fe	ENDF/B-VI	^{94}Mo	Mughabghab
C-graphite	ENDF/B-VI	^{57}Fe	ENDF/B-VI	^{95}Mo	Mughabghab
Ca	Mughabghab	^{58}Fe	ENDF/B-VI	^{96}Mo	Mughabghab
Cd	Mughabghab	Ga	Mughabghab	^{97}Mo	Mughabghab
^{106}Cd	Mughabghab	^{152}Gd	ENDF/B-VII Beta 2	^{14}N	Mughabghab
^{108}Cd	Mughabghab	^{154}Gd	ENDF/B-VII Beta 2	^{15}N	Mughabghab
^{110}Cd	Mughabghab	^{155}Gd	ENDF/B-VII Beta 2	^{23}Na	ENDF/B-VI
^{111}Cd	Mughabghab	^{156}Gd	ENDF/B-VII Beta 2	^{93}Nb	ENDF/B-VI
^{112}Cd	Mughabghab	^{157}Gd	ENDF/B-VII Beta 2	^{94}Nb	Mughabghab
^{113}Cd	Mughabghab	^{158}Gd	ENDF/B-VII Beta 2	^{95}Nb	Mughabghab
^{114}Cd	Mughabghab	^{160}Gd	ENDF/B-VII Beta 2	^{142}Nd	Mughabghab
^{116}Cd	Mughabghab	^{72}Ge	Mughabghab	^{143}Nd	Mughabghab
^{140}Ce	Mughabghab	^{73}Ge	Mughabghab	^{144}Nd	Mughabghab
^{141}Ce	Mughabghab	^{74}Ge	Mughabghab	^{145}Nd	Mughabghab
^{142}Ce	Mughabghab	^{76}Ge	Mughabghab	^{146}Nd	Mughabghab
^{143}Ce	Mughabghab	^{1}H	JENDL 3.3	^{147}Nd	Mughabghab
^{144}Ce	Mughabghab	H-ZrH	JENDL 3.3	^{148}Nd	Mughabghab
^{249}Cf	Mughabghab	H-poly	JENDL 3.3	^{150}Nd	Mughabghab
^{250}Cf	Mughabghab	H-freegas	JENDL 3.3	^{58}Ni	ENDF/B-VI
^{251}Cf	Mughabghab	^{2}H	CENDL 2	^{60}Ni	ENDF/B-VI
^{252}Cf	Mughabghab	^{3}H	JEF 3.1	^{61}Ni	ENDF/B-VI
^{253}Cf	Mughabghab	^{3}He	CENDL 2	^{62}Ni	ENDF/B-VI
Cl	Mughabghab	^{4}He	Mughabghab	^{64}Ni	ENDF/B-VI
^{242}Cm	Mughabghab	Hf	Mughabghab	^{237}Np	Mughabghab
^{243}Cm	Mughabghab	^{174}Hf	Mughabghab	^{238}Np	Mughabghab
^{244}Cm	Mughabghab	^{176}Hf	Mughabghab	^{239}Np	Mughabghab
^{245}Cm	Mughabghab	^{177}Hf	Mughabghab	^{16}O	JENFL 3.3
^{246}Cm	Mughabghab	^{178}Hf	Mughabghab	^{17}O	Mughabghab
^{247}Cm	Mughabghab	^{179}Hf	Mughabghab	^{31}P	Mughabghab
^{248}Cm	Mughabghab	^{180}Hf	Mughabghab	^{231}Pa	Mughabghab
^{59}Co	ENDF/B-VI	^{165}Ho	Mughabghab	^{233}Pa	Mughabghab
^{50}Cr	ENDF/B-VI	^{127}I	Mughabghab	^{206}Pb	ENDF/B-VI

^{207}Pb	ENDF/B-VI
^{208}Pb	ENDF/B-VI
^{102}Pd	Mughabghab
^{104}Pd	Mughabghab
^{105}Pd	Mughabghab
^{106}Pd	Mughabghab
^{107}Pd	Mughabghab
^{108}Pd	Mughabghab
^{110}Pd	Mughabghab
^{147}Pm	Mughabghab
^{148}Pm	Mughabghab
^{148m}Pm	Mughabghab
^{149}Pm	Mughabghab
^{141}Pr	Mughabghab
^{142}Pr	Mughabghab
^{143}Pr	Mughabghab
^{238}Pu	Mughabghab
^{239}Pu	ENDF/B-V
^{240}Pu	JENDL 3.3
^{241}Pu	JENDL 3.3
^{242}Pu	ENDF/B-VI
^{243}Pu	Mughabghab
^{244}Pu	Mughabghab
^{85}Rb	Mughabghab
^{87}Rb	Mughabghab
^{185}Re	ENDF/B-VI
^{187}Re	ENDF/B-VI
^{103}Rh	Mughabghab
^{105}Rh	Mughabghab
^{96}Ru	Mughabghab
^{99}Ru	Mughabghab
^{100}Ru	Mughabghab
^{101}Ru	Mughabghab
^{102}Ru	Mughabghab
^{104}Ru	Mughabghab
^{105}Ru	Mughabghab
^{106}Ru	Mughabghab
S	Mughabghab
^{32}S	Mughabghab
^{121}Sb	Mughabghab
^{123}Sb	Mughabghab
^{124}Sb	Mughabghab
^{45}Sc	ENDF/B-VI
^{74}Se	Mughabghab
^{76}Se	Mughabghab
^{77}Se	Mughabghab
^{78}Se	Mughabghab
^{80}Se	Mughabghab
^{82}Se	Mughabghab
Si	ENDF/B-VI
^{28}Si	ENDF/B-VI
^{29}Si	ENDF/B-VI
^{30}Si	ENDF/B-VI
^{144}Sm	Mughabghab
^{147}Sm	Mughabghab
^{148}Sm	Mughabghab
^{149}Sm	Mughabghab
^{150}Sm	Mughabghab
^{151}Sm	Mughabghab
^{152}Sm	Mughabghab
^{153}Sm	Mughabghab
^{154}Sm	Mughabghab
^{112}Sn	Mughabghab
^{114}Sn	Mughabghab
^{115}Sn	Mughabghab
^{116}Sn	Mughabghab
^{117}Sn	Mughabghab
^{118}Sn	Mughabghab
^{119}Sn	Mughabghab
^{120}Sn	Mughabghab
^{122}Sn	Mughabghab
^{124}Sn	Mughabghab
^{84}Sr	Mughabghab
^{86}Sr	Mughabghab
^{87}Sr	Mughabghab
^{88}Sr	Mughabghab
^{89}Sr	Mughabghab
^{90}Sr	Mughabghab
^{181}Ta	Mughabghab
^{182}Ta	Mughabghab
^{159}Tb	Mughabghab
^{160}Tb	Mughabghab
^{99}Tc	Mughabghab
^{120}Te	Mughabghab
^{122}Te	Mughabghab
^{123}Te	Mughabghab
^{124}Te	Mughabghab
^{125}Te	Mughabghab
^{126}Te	Mughabghab
^{127m}Te	Mughabghab
^{128}Te	Mughabghab
^{130}Te	Mughabghab
^{230}Th	Mughabghab
^{232}Th	ENDF/B-VII Beta 2
Ti	Mughabghab
^{232}U	Mughabghab
^{233}U	ENDF/B-VII Beta 2
^{234}U	Mughabghab
^{235}U	JENDL 3.3
^{236}U	Mughabghab
^{237}U	Mughabghab
^{238}U	JENDL 3.3
V	ENDF/B-VI
W	Mughabghab
^{182}W	Mughabghab
^{183}W	Mughabghab
^{184}W	Mughabghab
^{186}W	Mughabghab
^{124}Xe	Mughabghab
^{126}Xe	Mughabghab
^{128}Xe	Mughabghab
^{129}Xe	Mughabghab
^{130}Xe	Mughabghab
^{131}Xe	Mughabghab
^{132}Xe	Mughabghab
^{133}Xe	Mughabghab
^{134}Xe	Mughabghab
^{135}Xe	Mughabghab
^{136}Xe	Mughabghab
^{89}Y	ENDF/B-VI
^{90}Y	Mughabghab
^{91}Y	Mughabghab
Zr	Mughabghab
^{90}Zr	Mughabghab

Appendix V: The 44-group structure

The 44-group structure is collapsed from a 238 fine-group structure. The broad-group boundaries subset was chosen for emphasising the key spectral aspects of a typical LWR fuel package. In particular, the broad-group structure was designed to accommodate the following features: two windows in the oxygen cross-section spectrum; a window in the cross-section of iron; the Maxwellian peak in the thermal range; and the 0.3-eV resonance in ^{239}Pu. The resulting boundaries represent 22 fast and 22 thermal energy groups. The group structure upper energy boundaries are as follows:

Group	Upper E (eV) boundary
1	2.0000E+07
2	8.1873E+06
3	6.4340E+06
4	4.8000E+06
5	3.0000E+06
6	2.4790E+06
7	2.3540E+06
8	1.8500E+06
9	1.4000E+06
10	9.0000E+05
11	4.0000E+05
12	1.0000E+05
13	2.5000E+04
14	1.7000E+04
15	3.0000E+03
16	5.5000E+02
17	1.0000E+02
18	3.0000E+01
19	1.0000E+01
20	8.1000E+00
21	6.0000E+00
22	4.7500E+00
23	3.0000E+00
24	1.7700E+00
25	1.0000E+00
26	6.2500E−01
27	4.0000E−01
28	3.7500E−01
29	3.5000E−01
30	3.2500E−01
31	2.7500E−01
32	2.5000E−01
33	2.2500E−01
34	2.0000E−01
35	1.5000E−01
36	1.0000E−01
37	7.0000E−02
38	5.0000E−02
39	4.0000E−02
40	3.0000E−02
41	2.5300E−02
42	1.0000E−02
43	7.5000E−03
44	3.0000E−03
	1.0000E−05

Appendix VI: ANGELO and LAMBDA description

Input descriptions for ANGELO-2.3 code	
Ivo Kodeli and Enrico Sartori	
NEA Data Bank Version 2.3 (February 2010)	
The purpose of this programme is the expansion or collapsing of relative neutron cross-section covariance matrices into a new energy group structure.	
Read input parameters and options	
record 1	
Read TITLE (60 characters)	
	TITLE is general title of the library
record 2	
Read IGO,IGM,NCAS,IBOX,NSW1,IPRT,MODE,IDEBUG (free format)	
IGO	No. of groups in input matrix
IGM	No. of groups in output matrix
NCAS	No. of matrices to be processed =0 process all MTs found on COVERX file (for IBOX=1 only)
IBOX	=0 input library in BOXER format
	=1 input library in COVERX format
	=2 others (specified by NSW2 parameter)
NSW1	=0 lethargy boundaries in the input (IGO+1)
	=1 group boundaries in the input (IGO+1)
	=2 VITAMIN-J 175 group structure (built in)
IPRT	=0 minimum print option (recommended)
	#0 maximum print option (NOT TESTED)
MODE	mode of storage on output library
	=0 relative covariance/binary
	=1 standard deviations and relative covariance/binary
	=2 standard deviations and fractional correlations/binary
	=3 relative covariance in NJOY ERRORR format (recommended)
NLIB	=0 create a new library
	#0 append to the old library (if MODE=3 only)
IDEBUG	=0 do not print information useful for debug
	#0 print information useful for debug
record 3 :	
Read MATD,ZA,(MT(i),i=1,NCAS) (free format)	
MATD	material to be processed (use ENDF/B-6 standard)
ZA	1000*Z+A for principal scatterer
MT	reactions desired (all X-correlations will be evaluated as
	well if found, otherwise they will be set to 0).
Notes: - Only one MATD/ZA can be read at a time. - Either MATD or ZA should be provided (NOT BOTH), depending on what is used in the input library - For IBOX=1 only: if NCAS=0 values of NCAS & MT are read from CVX file	
records 4 and 5: Read input and output energy/lethargy grid	
If(NSW1=1 and IBOX=2)Read(X(I),I=1,IGOP1)input energy group structure in decreasing order (free format)	

If(NSWl=1)Read(XF(I),I=1,IGMP1) output energy group structure in decreasing order (free format)	
If(NSW1=0 and IBOX=2)	
Read (XOL(I),I=1,IGOP1) input lethargy group structure in increasing order (free format)	
Read (XNL(I),I=1,IGMP1) output lethargy group structure (free form.)	
Omit the next records if (IBOX=0 or IBOX=1):	
--->	Loop over all input matrices (NCAS) Read covariance information
next two records	
Read TITOLO Matrix Description (characters 80) Read MATD,ZA,MT(i),MT1(i) (free format) (same as above) Read BB,NSW2 (E12.6,I3) BB Threshold for zero setting (>0) If abs(value)<BB then value set to 0 (not used in this version) NSW2 Covariance information and format options	
next records	
if NSW2 =0	SYMMETRIC relative covariance matrix
	(only non-zero elements of the matrix should be provided) read n,m,COV(n,m) format(4(2I4,E10.2)) COV is the relative covariance matrix (end with 0 0 0) COV(m,n) will be set equal to COV(n,m)
if BSW2 =1	SYMMETRIC relative covariance matrix read (STD1(i),i=1,IGO) format(6F12.5) STD1 is relative standard deviation of reaction in % read n,m,CORR(n,m) format(6(2I3,F6.3)) CORR is the correlation matrix (end with 0 0 0) (only non-zero elements of the matrix should be provided) CORR(m,n) will be set equal to CORR(n,m)
if RSW2 =2	NON-SYMMETRIC relative covariance matrix read (STD1(i),i=1,IGO) format(6F12.5) read (STD2(i),i=1,IGO) format(6F12.5) STD1 is relative standard deviation of reaction 1 in % STD2 is relative standard deviation of reaction 2 in % read n,m,CORR(n,m) format(6(213,F6.3)) CORR is the correlation matrix (end with 0 0 0) (only non-zero elements of the matrix should be provided)
if NSW2 =3	SYMMETRIC relative covariance matrix read ((COV(n,m),n=1,IGO),m=1,IGO) free format full matrix must be provided
if NSW2 =4	NON-SYMMETRIC relative covariance matrix read (STD1(i),i=1,IGO) free format read (STD2(i),i=1,IGO) free format STD1 is relative standard deviation of reaction 1 in % STD2 is relative standard deviation of reaction 2 in % read ((COV(n,m),n=1,IGO),m=1,IGO) format (6E13.6) full matrix must be provided
if NSW2 =5	NON-SYMMETRIC relative covariance matrix read(STD1(i),i=1,IGO) free format read(STD2(i),i=1,IGO) free format STD1 is relative standard deviation of reaction 1 in %

	STD2 is relative standard deviation of reaction 2 in % read((CORR(n,m),n=1,IGO),m=1,IGO) free format full matrix must be provided
<-----continue loop NCAS times	
end of input description	

ANGELO 2.3 Output tape description		
Output library is on logical unit 10 file called **LIB.NEW**		
for MODE=0 to =2: output is written in binary form with the format:		
1st part: file identification		
record 1		
TITLE (80 characters)		
	TITLE Library description (80 characters)	
record 2		
IGM,(XF(i),i=1,IGM+1),(XNL(i),i=1,IGM+1)		
	IGM	No. of output groups
	XF	The energy group boundaries vector
	XNL	The lethargy group boundaries vector
	2nd part:	
--->	Loop over all output matrices, as specified in input (NCAS)	
next record		
N, MODE, IGM, TITOLO		
	N	Covariance matrix sequence number
	MODE	Mode of storage (see input parameter RODE)
	IGM	No. of output groups
	TITOLO Description of the matrix (80 characters)	
next record		
if	MODE	=0 new interpolated relative covariance matrix (IGM*IGM values)
	=1	1st relative standard deviation (fractions)
		2nd relative standard deviation (fractions)
		relative covariance matrix (IGM*(IGM+2) values)
	=2	1st relative standard deviation (fractions)
		2nd relative standard deviation (fractions)
		relative correlation matrix (IGM*(IGM+2) values)
<-----continue loop NCAS times		
for MODE=3:		
covariance matrices are written in the standard NJOY ERRORR format		
(recommended).		

Input descriptions for LAMBDA-2.3 code	
Ivo Kodeli NEA Data Bank Version 2.3 (February 2010)	
The purpose of this programme is to check the mathematical properties of the multi-group covariance matrices. The correlation matrices are tested to determine if any element exceeds unity. The number of positive, negative, and zero eigenvalues is calculated and the matrix is classified on this basis. For LAMBDA the same input as for ANGELO 2.3 can be used.	
Read input parameters and options	
record 1	
Read TITLE (60 characters)	
	TITLE is general title of the library
record 2	
Read IGO,IGM,NCAS,IBOX (free format)	
IGO	No. of groups in input matrix
IGM	Not used (enter 0)
NCAS	No. of matrices to be processed =0 test all data found in COVERX file (for IBOX=1 only)
IBOX	=0 input library in BOXER format =1 input library in COVERX format
record 3	
Read MATD,ZA,(MT(i),i=1,NCAS) (free format)	
MATD	material to be processed (use ENDF/B-6 standard)
ZA	1000*Z+A for principal scatterer
MT	reactions desired (all X-correlations will be evaluated as well if found, otherwise they will be set to 0). Not used if (NCAS=0 and IBOX=1)
Notes: - only one MATD can be read at a time. - either MATD or ZA should be provided but NOT BOTH, depending on what is used in the input library.	

COVR MODULE OF NJOY99 CODE

Subroutine COVR

```
*****************************************************************
*                                                               *
* plot covariance data from errorr or make a condensed library. *
*                                                               *
* in the plot option, covr plots a matrix of correlation        *
* coefficients and an associated pair of standard deviation     *
* vectors, i.e. a covariance matrix. the correlation            *
* matrix is plotted as a shaded contour plot and the vectors    *
* are plotted as semi-log plots, one rotated by 90 degrees.     *
* the log energy grids for the vector plots are identical       *
* to the grids for the matrix plot.  this version plots         *
* through viewr.                                                *
*                                                               *
* in the library option, covr produces a condensed bcd          *
* covariance library in the boxer format.  this format is       *
* efficient for matrices of simple blocks.                      *
*                                                               *
*---input specifications (free format)--------------------------*
*                                                               *
*  card 1                                                       *
*     nin            input tape unit                           *
*     nout           output tape unit                          *
*                    (default=0=none)                          *
*     nplot          viewr output unit                         *
*                    (default=0=none)                          *
*                                                              *
*   ---cards 2, 2a, and 3a for nout.ne.0 only (plot option)    *
*                                                              *
*  card 2                                                      *
*     icolor          select color or monochrome style         *
*                       0=monochrome (uses cross hatching)     *
*                       1=color background and contours        *
*                       (default=0)                            *
*  card 2a                                                     *
*     epmin          lowest energy of interest (default=0.)    *
*  card 3a                                                     *
*     irelco         type of covariances present on nin        *
*                    0/1=absolute/relative covariances         *
*                    (default=1)                               *
*     ncase          no. cases to be run (maximum=40)          *
*                    (default=1)                               *
*     noleg          plot legend option                        *
*                    -1/0/1=legend for first subcase only/     *
*                    legend for all plots/no legends           *
*                    (default=0)                               *
*     nstart         sequential figure number                  *
*                    0/n=not needed/first figure is figure n.  *
*                    (default=1)                               *
*     ndiv           no. of subdivisions of each of the        *
*                    gray shades (default=1)                   *
*                                                              *
*   ---cards 2b, 3b, and 3c for nout gt 0 (library option) only--*
*                                                              *
*  card 2b                                                     *
*     matype         output library matrix option              *
*                    3/4=covariances/correlations              *
*                    (default=3)                               *
*     ncase          no. cases to be run (maximum=40)          *
*                    (default=1)                               *
*  card 3b                                                     *
*     hlibid         up to 6 characters for identification     *
*  card 3c                                                     *
*     hdescr         up to 21 characters of descriptive        *
*                    information                               *
*                                                              *
*   ---cards 4 for both options---                             *
*                                                              *
```

```
*  card 4                                                              *
*     mat            desired mat number                               *
*     mt             desired mt number                                *
*     mat1           desired mat1 number                              *
*     mt1            desired mt1 number                               *
*                    (default for mt, mat1 and mt1 are 0,0,0          *
*                    meaning process all mts for this mat             *
*                    with mat1=mat)                                   *
*                    (neg. values for mt, mat1, and mt1 mean          *
*                    process all mts for this mat, except for         *
*                    the mt-numbers -mt, -mat1, and -mt1.  in         *
*                    general, -n will strip both mt=1 and mt=n.       *
*                    -4 will strip mt=1, mt=3, and mt=4, and          *
*                    -62, for example, will strip mt=1, mt=62,        *
*                    mt=63, ... up to and incl. mt=90.)               *
*          repeat card 4 ncase times                                  *
*                                                                     *
* note---if more than one material appears on the input tape,         *
* the mat numbers must be in ascending order.                         *
*                                                                     *
***********************************************************************
```

UTILITY MODULES OF ERRORJ-3.2 CODE SYSTEM

```
**********************************************************************
*                                                                    *
*                            EDITCVX                                 *
*                                                                    *
*   The editing program of COVERX format files (covariance file      *
*   with group structure) by the interactive mode.                   *
*   This is a family of the ERRORJ system.                           *
*                                                                    *
**********************************************************************
*   Manager:    M. Ishikawa  (JNC)                                   *
*   Maker:      K. Kosako  (SAEI)                                    *
**********************************************************************
*   Function:                                                        *
*     1) the four rule operations of arithmetic to data (cross       *
*        sections and covariance matrices)                           *
*     2) replacement or deletion of requested data                   *
*     3) addition of new data                                        *
*     4) union of two coverx format files into one                   *
*     5) division of a coverx format file into files by nuclides     *
**********************************************************************

**********************************************************************
*                                                                    *
*                            VIEWCVX                                 *
*                                                                    *
*   The viewer program of COVERX format file (covariance file with   *
*   group structure) by the interactive mode.                        *
*   This is a family of the ERRORJ system.                           *
*                                                                    *
**********************************************************************
*   Manager:    M. Ishikawa  (JNC)                                   *
*   Maker:      K. Kosako  (SAEI)                                    *
**********************************************************************
*   Function:                                                        *
*     1) list of nuclides and reaction types                         *
*     2) cross sections by each reaction (and relative error or      *
*        standard deviation)                                         *
*     3) matrix with group structure of absolute or relative         *
*        covariance                                                  *
*     4) correlation matrix                                          *
*     5) general information for coverx format file (number of       *
*        groups and nuclides, comment, storage data format, etc.)    *
**********************************************************************

**********************************************************************
*                                                                    *
*                            NJOYCOVX                                *
*                                                                    *
*      This program produces the COVERX format file of covariance    *
*  data from the output covariance file of ERRORR module in the      *
*  njoy94 code.                                                      *
*      It is used the COVERX format with date of nov. 1,1996.        *
*                                                                    *
**********************************************************************
*  history                                                           *
*    12/03/96 ..... create the NJOYCOVX program by K. Kosako (SAEI). *
*    10/05/97 ..... automatic execution version following to the     *
*                   ERRORJ code by K. Kosako (SAEI).                 *
**********************************************************************
```

Appendix VII: Perturbation theory and kinetic parameters uncertainty propagation[11]

Perturbation theory algorithm for sensitivity coefficients calculations [15]

For sensitivity analysis, sensitivity coefficients are the key quantities that have to be evaluated. The sensitivity coefficients are determined in a way that when multiplied by the variation of the corresponding input parameter, i.e. cross-section, they will quantify the impact on the targeted values whose sensitivity is referred to, e.g. the multiplication factor. Sensitivity coefficients can be used for different objectives like uncertainty estimates, design optimisation, determination of target accuracy requirements, adjustment of input parameters, and evaluations of the representativeness of an experiment with respect to a reference design configuration. Any deterministic algorithm for uncertainty propagations is based on the sensitivity coefficients application.

Conventional perturbation theory and sensitivities of k_{eff}

The conventional perturbation theory has been developed initially to calculate the reactivity coefficients, which are the variation of the reactivity of the reactor due to a specified variation of a parameter.

Uncertainty propagation, another perturbation theory application, is based on the sensitivity coefficients S_{keff} of the multiplication factor k_{eff} at the parameter $P_{i,}$ which are expressed as follows:

$$S_{keff} = \frac{\Delta k_{eff} / k_{eff}}{\Delta P_i / P_i} \qquad \text{(A.1)}$$

The sensitivity coefficients are calculated as a small variation of reactivity with the following formula which is correct if bi-orthogonal conditions are satisfied.

$$\Delta\rho = \frac{\delta k}{k^2} = -\frac{\int \Phi^* \cdot \left(\delta A_{nrg} - \frac{\delta F_{nrg}}{k} \right) \cdot \Phi \cdot dr}{\int \Phi^* \cdot F \cdot \Phi \cdot dr} \qquad \text{(A.2)}$$

where Φ and Φ^* are direct and adjoint solutions of the transport equation, A and F are the absorption and fission operators subsequently.

The first order sensitivity coefficient of the multiplication factor is the ratio of the relative increase of k to the infinitesimal relative increase of the parameter p. In this case the parameter p is the cross-section of the nuclide n for the reaction r in the energy group g, which will be addressed as σ_{nrg}.

The sensitivity coefficient of k to a specific σ_{nrg} cross-section can be derived by replacing the operator variation δA and δF by restricting the operators to the term involving the specific cross section δA_{nrg} and δF_{nrg}, because the cross-section is a parameter involved linearly in the matrix operators, so the sensitivity coefficient will be:

$$S(k,\sigma_{nrg}) = \frac{\frac{\delta k}{k}}{\frac{\delta \sigma_{nrg}}{\sigma_{nrg}}} = -k \frac{\int \Phi^* \cdot \left(\delta A_{nrg} - \frac{\delta F_{nrg}}{k} \right) \cdot \Phi \cdot dr}{\int \Phi^* \cdot F \cdot \Phi \cdot dr} \qquad \text{(A.3)}$$

[11] Text prepared by Evgeny Ivanov, IRSN.

The overall variation of the multiplication factor, or as shown in the following paragraph of any integral parameter R, due to variation of cross sections σ is then:

$$\frac{\delta k}{k} = \sum_j S_j \frac{\delta \sigma_j}{\sigma_j} \qquad \text{(A.4)}$$

According to this formula, knowing the sensitivity coefficients and the variation in the cross-section of interest it is possible to calculate their influence on the integral parameter.

Our further analysis requires the evaluation of the reaction rate balance on the perturbation of cross-sections. This could be done using the Generalised Perturbation Theory (GPT), which is an extension of the Conventional Perturbation Theory. An integral parameter can be defined in general as:

$$R = R\left(\Phi^*, \Phi\right) = \frac{\left\langle \Phi^*, a\Phi \right\rangle}{\left\langle \Phi^*, b\Phi \right\rangle} \qquad \text{(A.5)}$$

where *a* and *b* can be either a constant, a cross-section or an operator and the brackets mean the phase space integration. The parameter R can be linear if it depends on the flux only, or bilinear if it depends on both the direct and the adjoint flux. The direct and the adjoint flux are solutions of the respective direct and adjoint equation reported in the previous paragraph.

The GPT uses the generalised importance function, direct Ψ and adjoint Ψ^*, which are introduced defining the following functional (considering a homogeneous, external source free, problem):

$$G = R - \left\langle \Psi^*, \left(A - \frac{1}{k} F \right) \Phi \right\rangle - \left\langle \Psi, \left(A^* - \frac{1}{k} F^* \right) \Phi^* \right\rangle \qquad \text{(A.6)}$$

The sensitivity of the integral parameter R to the cross-sections can be expressed by the following equation, derived from $\partial G / \partial \sigma$:

$$S\left(R,\sigma\right) = \frac{\sigma}{R}\frac{dR}{d\sigma} = \frac{\sigma}{R}\left\{ \frac{\partial R}{\partial \sigma} - \left\langle \Psi^*, \left(\frac{\partial A}{\partial \sigma} - \frac{1}{k}\frac{\partial F}{\partial \sigma} \right) \Phi \right\rangle - \left\langle \Psi, \left(\frac{\partial A^*}{\partial \sigma} - \frac{1}{k}\frac{\partial F^*}{\partial \sigma} \right) \Phi^* \right\rangle \right\} \qquad \text{(A.7)}$$

It is composed by two terms representing the direct and the indirect effect:

$$S_{DIR}\left(R,\sigma\right) = \frac{\sigma}{R}\frac{\partial R}{\partial \sigma} \qquad \text{(A.8)}$$

$$S_{IND}\left(R,\sigma\right) = \frac{\sigma}{R}\left\{ -\left\langle \Psi^*, \left(\frac{\partial A}{\partial \sigma} - \frac{1}{k}\frac{\partial F}{\partial \sigma} \right) \Phi \right\rangle - \left\langle \Psi, \left(\frac{\partial A^*}{\partial \sigma} - \frac{1}{k}\frac{\partial F^*}{\partial \sigma} \right) \Phi^* \right\rangle \right\} \qquad \text{(A.8)}$$

The direct effect corresponds to the variation of the integral parameter *R* with the cross-sections by which *R* is explicitly dependent. The indirect effect instead corresponds to the variation of the parameter *R* with other cross-sections by which *R* is implicitly dependent through the direct and the adjoint flux.

The formulae given above are used for calculations with ERANOS 2.2 of the reaction rates (ratio of fissions of plutonium and uranium) sensitivity.

Kinetic parameters uncertainty propagation [15]

The interest in kinetic parameters uncertainty analysis appears because of their outstanding role in safety assessment support and safety studies. Indeed, the effective delayed neutron fraction, for example, is

a natural unit of reactivity, so its accuracy is exactly the ultimate limit of reactivity and uncertainty both for control rods worth and for reactivity feedbacks to be validated against experimental data.

The delayed neutron effective fraction is one of the most important parameters to be used in the interpretation of the benchmark calculations. First, β_{eff} will be used for interpretation of reactivity measurements and calculations because all reactivity measurements have been expressed in units of β_{eff}.

Definitely delayed neutron effective fraction will be also used in transient calculations. But concerning the accuracy of β_{eff} itself any conclusions could be only done together with the neutron generation lifetime calculations. The neutron generation lifetime calculations and the applied algorithm are also given hereinafter.

Being defined at the very beginning of reactor technology [67] both β_{eff} and Λ_{eff} have not yet been a subject of the deterministic sensitivity/uncertainty analysis, contrary to the reactivity and criticality parameters. It was because the perturbation formalism had been developed for integral parameters analysis.

Hereinafter we explain the approach that is based on the reduction of the kinetic parameters study problem to the zero dimension reactivity study. It allows us to apply the ordinary perturbation theory for the sensitivity analysis.

For example the neutron generation lifetime could be derived from the asymptotic representation of the transient process. In this case Λ_{eff} is only a linear response to the appearance of the *1/v* absorber. The idea of using a *1/v* absorber is not a new one; the method of *1/v* poisoning was used widely for experimental studies of kinetic parameters (with ^{10}B as *1/v* absorber). But hereinafter we propose to apply similar ideas for the sensitivity-uncertainty analysis.

The neutron generation lifetime is defined typically with the formalism of perturbation theory. As it has been derived in [67] the lifetime of neutrons in respect of their role in chain reaction maintaining could be represented as the following formula:

$$\Lambda_{eff} = \frac{\int_V \int_E \int_{4\pi} \int_{E'} \sqrt{m_n/2E} \cdot \Phi(\vec{r}, E', \Omega) \cdot \Psi(\vec{r}, E, \Omega) \cdot d\vec{r} \cdot d\Omega \cdot dE' \cdot dE}{\int_V \int_{4\pi} \int_{E'} \int_E \nu \cdot \chi(E' \to E) \cdot \Sigma_f(\vec{r}, E') \cdot \Phi(\vec{r}, E', \Omega) \cdot \Psi(\vec{r}, E, \Omega) \cdot d\vec{r} \cdot d\Omega \cdot dE' \cdot dE} \tag{A.9}$$

where notations are the same as given before.

But at the same time the neutron generation lifetime relates to the asymptotic behaviour of the neutron field in a supercritical reactor. This fact has been used for the Λ_{eff} experimental measurements. The idea was to use a *1/v* absorber and the boron as the most close to *1/v* poison has been applied in the past.

Let us consider the simplified kinetic model without delayed neutrons given below:

$$\frac{dQ}{dt} \approx \frac{\rho}{\Lambda} Q \to \alpha_P \cdot Q \tag{A.10}$$

where Q is capacity, ρ is reactivity α_p is the prompt neutron decay constant defined as reactivity to neutron generation lifetime ratio.

$$\alpha_P \approx \frac{\rho}{\Lambda}. \tag{A.11}$$

Instead of the transient Boltzmann equation we can use the asymptotic one such as the following:

$$\vec{\Omega}\cdot grad(\Phi_{as}(\vec{r},E,\vec{\Omega}))+(\Sigma_a(\vec{r},E,\vec{\Omega})+\frac{\alpha_{as}}{v})\cdot\Phi_{as}(\vec{r},E,\vec{\Omega})$$
$$-\int_{E',\Omega'}\Sigma_S(\vec{r},E'\to E,\vec{\Omega}'\to\vec{\Omega})\cdot\Phi_{as}(\vec{r},E',\vec{\Omega}')\cdot dE'd\vec{\Omega}' \qquad (A.12)$$
$$=\frac{1}{k_{eff}=1}\cdot\frac{1}{4\pi}\cdot\int_{E',\Omega'}\chi_p(E',E)\cdot\nu(E')\cdot\Sigma_f(\vec{r},E')\cdot\Phi_{as}(\vec{r},E',\vec{\Omega}')\cdot dE'd\vec{\Omega}'$$

where eigenvalue α_{as} is the critical concentration of the *1/v* pseudo-absorber.

Since the α_{as} corresponds to the $1/k_{eff}$=1.0 and α=0 corresponds to the existing $1/k_{eff}$ and in assumption small difference between asymptotic and semi-critical flux distribution we can associate them finally with the prompt neutron decay constant.

In this case the eigen-values of α and λ (k_{eff}) could be translated into another by the following approximated expression:

$$\alpha\approx\frac{\sigma_{1/v}}{k_{eff}}\cdot\frac{\partial k_{eff}}{\partial\sigma_{1/v}}\cdot\frac{1}{\sigma_{1/v}(E_T=0.0253\text{eV})\cdot(v(E_T=0.0253\text{eV})=2200\cdot{}^{m}\!/_{\text{sec}})} \qquad (A.13)$$

where it was assumed an *1/v* absorber with cross-section of 1 barn for the thermal point.

Finally we have the following formula for the neutron generation:

$$\Lambda_{eff}\approx(1-k(1/v)/\left(k(1/v)\cdot2200\cdot10^{-24}\right)\text{sec}, \qquad (A.14)$$

where k(1/v) is poisoned by *1/v* absorber multiplication factor and then the variation of lifetime can be built in the same way as variation of a reactivity:

$$\delta\Lambda_{as}\approx$$
$$1/\Lambda\sqrt{\sum S_k\cdot\text{cov}(XS)\cdot S_k+\sum S_k(1/v)\cdot\text{cov}(XS)\cdot S_k(1/v)}. \qquad (A.15)$$

The contributions of the different groups in neutron generation lifetime uncertainty could be represented by a response matrix such as the following:

$$U=COV_{XS}\cdot\left[S_k^0-S_k^{pert}\right]\cdot\left[S_k^0-S_k^{pert}\right], \qquad (A.16)$$

where COV_{XS} is the covariance matrix of cross-sections by groups, reactions and nuclides and $\left[S_k^0-S_k^{pert}\right]$ are the group-wise differences between sensitivity coefficients.

The values obtained for the SNEAK 7A and SNEAK 7B cases are presented in Figure A.1 through Figure A.8.

Figure A.1: The SNEAK 7A U matrices for group-wise ^{238}U and ^{239}Pu fission for Λ_{eff} analysis

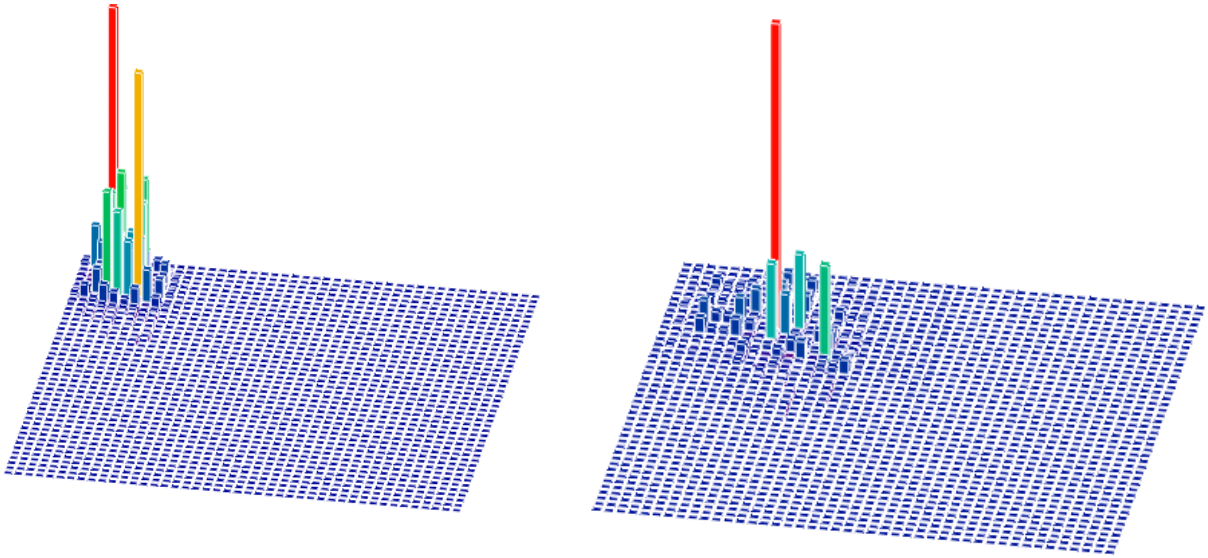

a b

Figure A.2: The SNEAK 7A U matrices for group-wise ^{238}U and ^{239}Pu capture for Λ_{eff} analysis

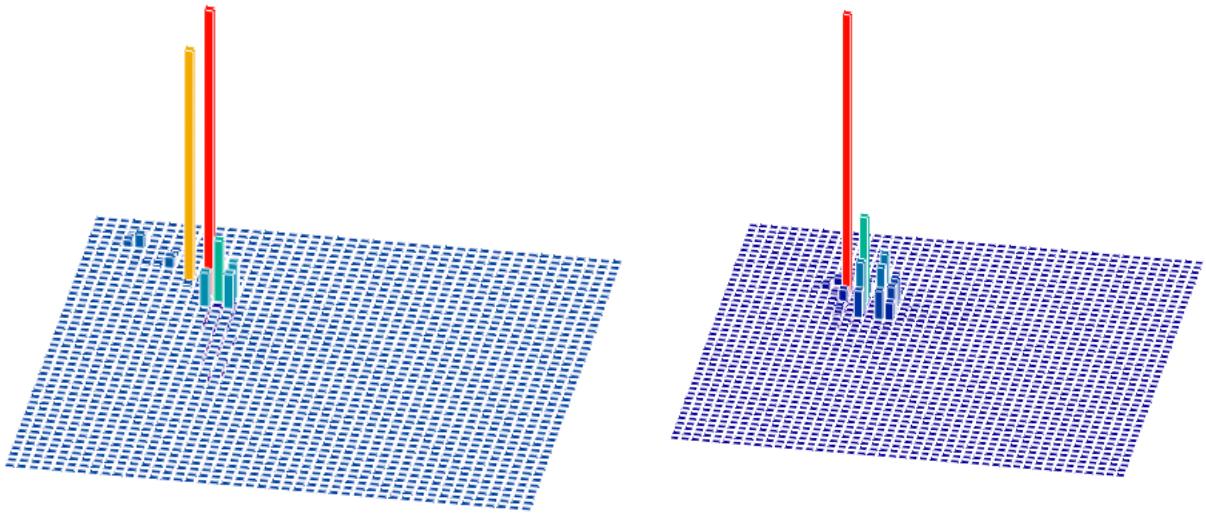

a b

Figure A.3: The SNEAK 7A U matrices for group-wise ^{238}U and ^{239}Pu fission spectra for β_{eff} analysis

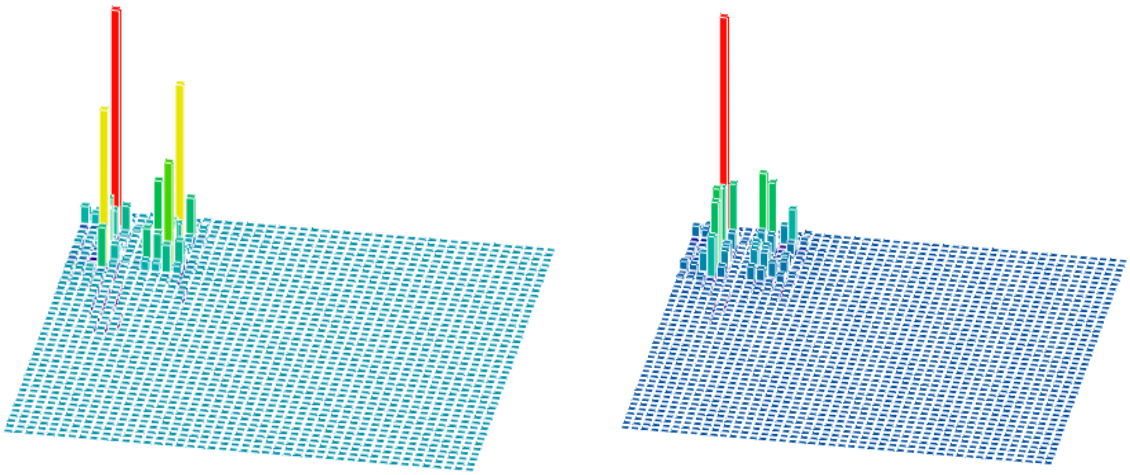

a b

Figure A.4: The SNEAK 7A U matrices for group-wise ^{238}U and ^{239}Pu nu-bar for Λ_{eff} analysis

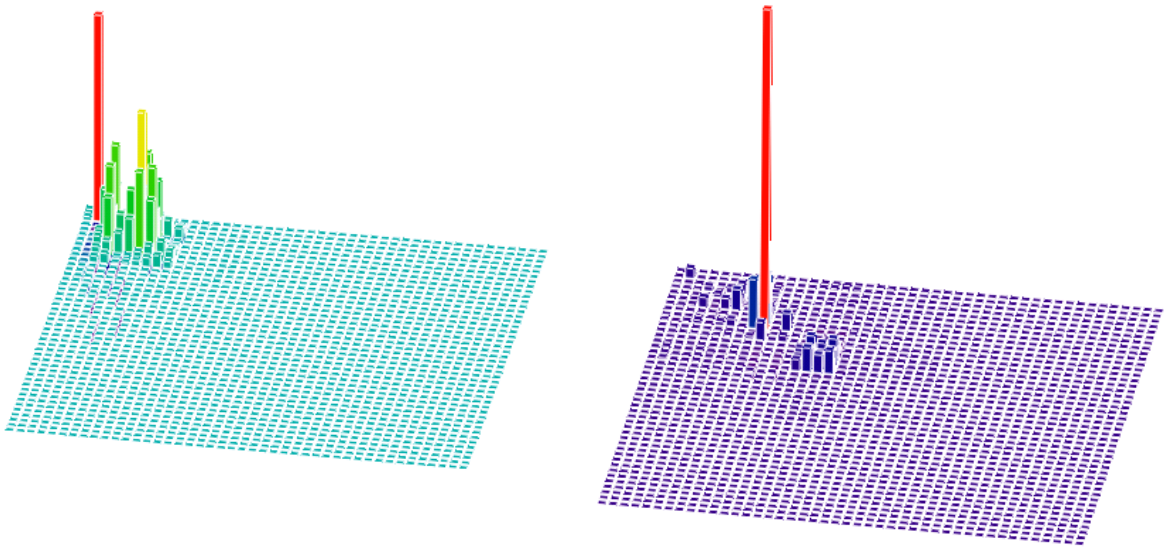

a b

The figures present only the major contributors to uncertainties that give the following uncertainties of calculated neutron generation lifetime (see Tables A.1 and A.2).

Table A.1: The main contributors to Λ_{eff} uncertainty for SNEAK 7A

Reaction	**^{239}Pu**	**^{238}U**
Capture	1.36%	0.15%
Fission	2.74%	2.67%
Inelastic	0.77%	0.02%

The final value calculated assuming the statistical independence of uncertainties gives the $\delta\Lambda/\Lambda$~4%. The same analysis done for SNEAK 7B gave the same order of magnitude for the final uncertainty.

Figure A.5: The SNEAK 7B U matrices for group-wise ^{238}U and ^{239}Pu fission for Λ_{eff} analysis

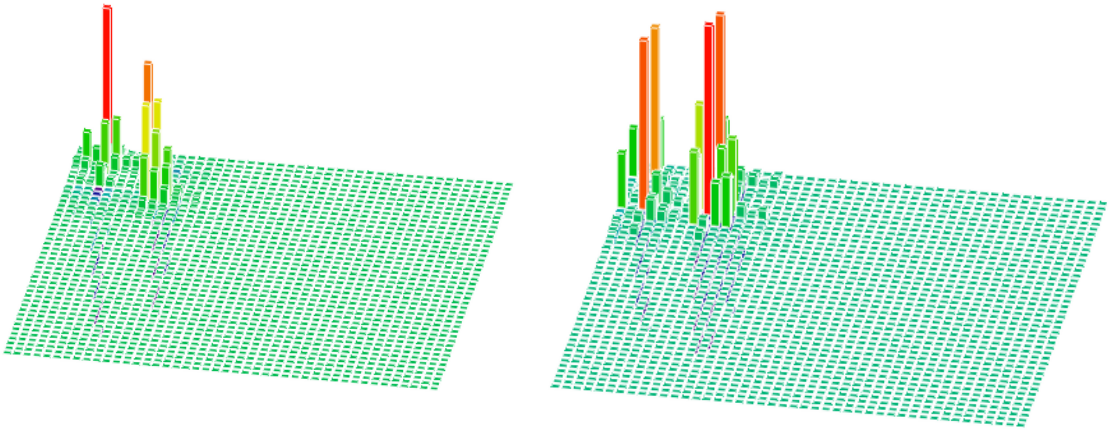

a b

Figure A.6: The SNEAK 7B U matrices for group-wise ^{238}U and ^{239}Pu capture for Λ_{eff} analysis

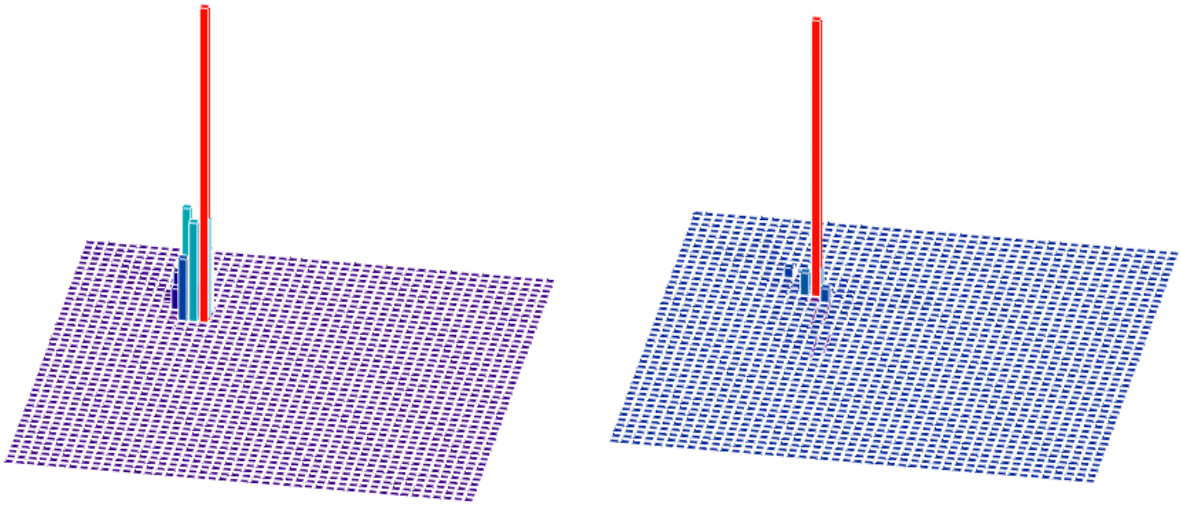

a b

Figure A.7: The SNEAK 7B U matrices for group-wise ^{238}U and ^{239}Pu nu-bar for Λ_{eff} analysis

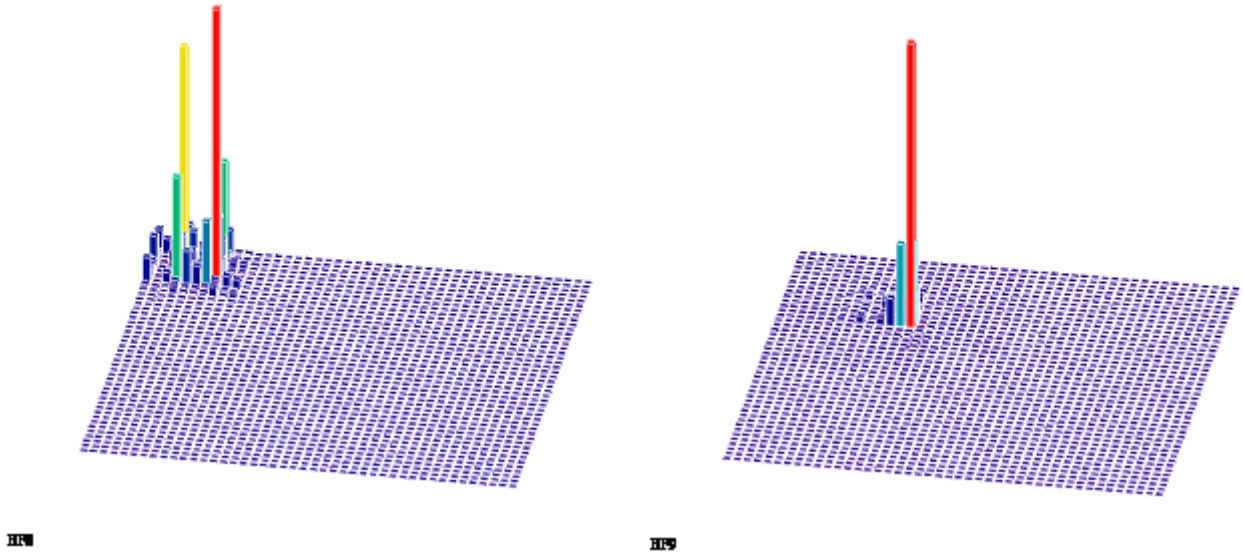

a b

Figure A.8: The SNEAK 7B U matrices for group-wise ^{238}U and ^{239}Pu fission spectra for Λ_{eff} analysis

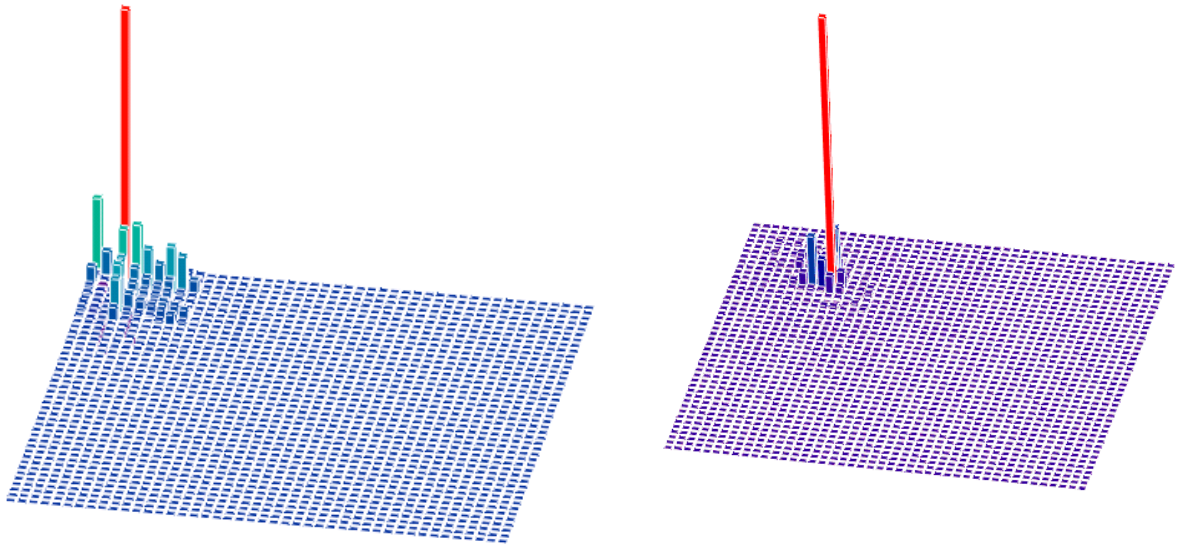

a b

Table A.2: The main contributors in Λ_{eff} uncertainty for SNEAK 7B

Reaction	**^{239}Pu**	**^{238}U**
Capture	2.03%	0.33%
Fission	0.96%	1.79%
Inelastic	0.57%	0.14%

The contributions by nuclides are given in Table A.3.

Table A.3: The main contributors in Λ_{eff} uncertainty for SNEAK 7A and 7B

nuclide	SNEAK 7A	SNEAK7 B
^{238}U	2,67%	1.90%
^{239}Pu	3,17%	2.59%
Σ	4,15%	3.21%

The final value for the Λ_{eff} uncertainty is given as $\delta\Lambda/\Lambda \sim 3.21 \div 4.15\%$ with respect to the case.

The uncertainty of the delayed neutron effective fraction has been proposed to be evaluated by the same technique. By definition, the effective delayed neutron fraction looks like the difference between two eigen-values as shown in the following equation:

$$\beta_{eff} \propto \lambda - \lambda_p = \frac{1}{k_{eff}} - \frac{1}{k_p}, \qquad \text{(A.17)}$$

where β_{eff} is the effective delayed neutron fraction, k_{eff} and k_p are complete and prompt multiplication factors.

So the difference between the sensitivity coefficients obtained with the χ total and χ prompt should provide the sensitivity of the effective delayed neutron fractions to the cross-section uncertainties.

The response to the variations of the given neutron data parameter σ_m could be represented through the sensitivity coefficients as follows:

$$\frac{\delta\beta_{eff}}{\beta_{eff}} = S_k(\sigma_m) \cdot \delta\sigma_m / \sigma_m - S_{k,p}(\sigma_m) \cdot \delta\sigma_m / \sigma_m, \qquad \text{(A.18)}$$

where $S_k(\sigma_m)$ is the sensitivity coefficient to the parameter for the complete transport operator, but $S_{k,p}(\sigma_m)$ is the sensitivity coefficient calculated for prompt neutrons only.

But in practice the difference is so small that numerical round-up errors would dominate over the effect to be studied. An alternative approach has been proposed which includes the delayed neutron fraction decomposition like it is done for an experimental study.

It is easy to select two kinds of components of delayed neutron fraction uncertainty. The first one is a contribution of spectra uncertainty and the second one is connected with the impact of uncertainty of nuclide fission balance.

The explanation of the idea is given below.

A delayed neutron effective fraction is defined as a response on changing of neutron spectra from total to prompt (see the equation below)

$$\beta_{eff} = \frac{\Delta k}{k} \approx \frac{\chi}{k} \cdot \frac{\partial k}{\partial \chi} \cdot \frac{\Delta\chi}{\chi} \equiv S_\chi \cdot \frac{\Delta\chi}{\chi}, \qquad \text{(A.19)}$$

where $\Delta\chi = \chi - \chi_p = \chi_d$ and S_χ is the group-wise sensitivity vector to fission neutron spectra.

The final value is actually the combination of different nuclides combinations:

$$\beta_{eff} \approx \sum_i S_{\chi;i} \cdot \frac{\chi_{d;i}}{\chi_i}, \qquad \text{(A.20)}$$

where the subscript i corresponds to the fissile nuclide and the other notations are the same as given above.

The fission spectra uncertainty is expressed in terms of covariance matrices and sensitivity coefficients.

$$\frac{\delta\beta_{eff}}{\beta_{eff}} \approx \left[\sum_i S_{\chi;i} \cdot Cov_{\chi,i} \cdot S_{\chi;i}\right]^{1/2}, \qquad \text{(A.21)}$$

where $Cov_{\chi,i}$ are the covariance matrices of fission spectra. But contributions of fissile nuclides are also uncertain. Thus, the formulae should be added by members, which take into account the neutron fission balance contribution. Finally, it is easy to show that the formula for uncertainty analysis is given by:

$$\delta\beta \sim (\Sigma\chi \mathrm{cov}(\chi)\, \Sigma\chi + \mathrm{fun}(\beta^9, \beta^8, \delta\phi^8/\phi^9))^{1/2}, \qquad \text{(A.22)}$$

where $S\chi$ is the sensitivity to spectra, cov(χ) spectra covariance matrix and fun(β^9,β^8, $\delta\phi^8/\phi^9$) is the contribution of the different nuclides fission balance obtained with Generalised Perturbation Theory which reduces the formula to the following one:

$$\delta\beta_{eff} \approx S_\chi \cdot \delta\chi + \sum_m \beta_{eff}^m \cdot \delta\left(f_m \Big/ \sum_n f_n\right), \qquad \text{(A.23)}$$

where $\delta\beta_{eff} \approx \sum_m \delta\left(f_m \Big/ \sum_n f_n\right)$, S_χ is the sensitivity to the fission spectra variations ($\delta\chi$), β_{eff}^m is the part of fission on the m-th nuclide and $f_m \Big/ \sum_n f_n$ is the partial m-th nuclide effective delayed neutron fraction.

The uncertainty is given by the covariance matrices, the examples of which are presented in Figure A.9.

Figure A.9: The χ-covariance for ^{239}Pu (a) and ^{238}U (b)

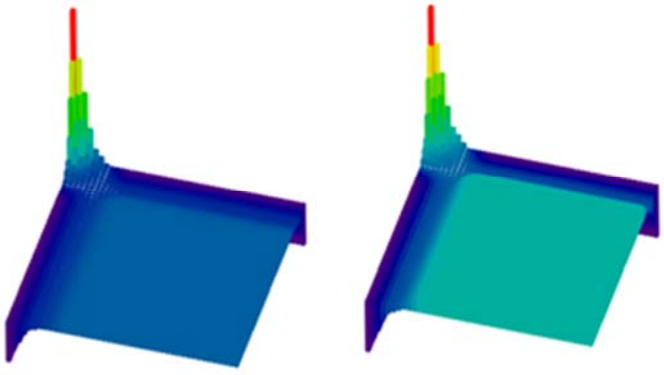

a b

The sensitivity coefficients to be combined with covariance matrices are presented in Figure A.10. It is easy to see that only the fast energy region is responsible for delayed neutron fraction uncertainty both in fast and in thermal reactors.

Figure A.10: The "unconstrained" sensitivity to χ for ^{239}Pu, ^{238}U in SNEAK 7A and for ^{235}U in a thermal reactor

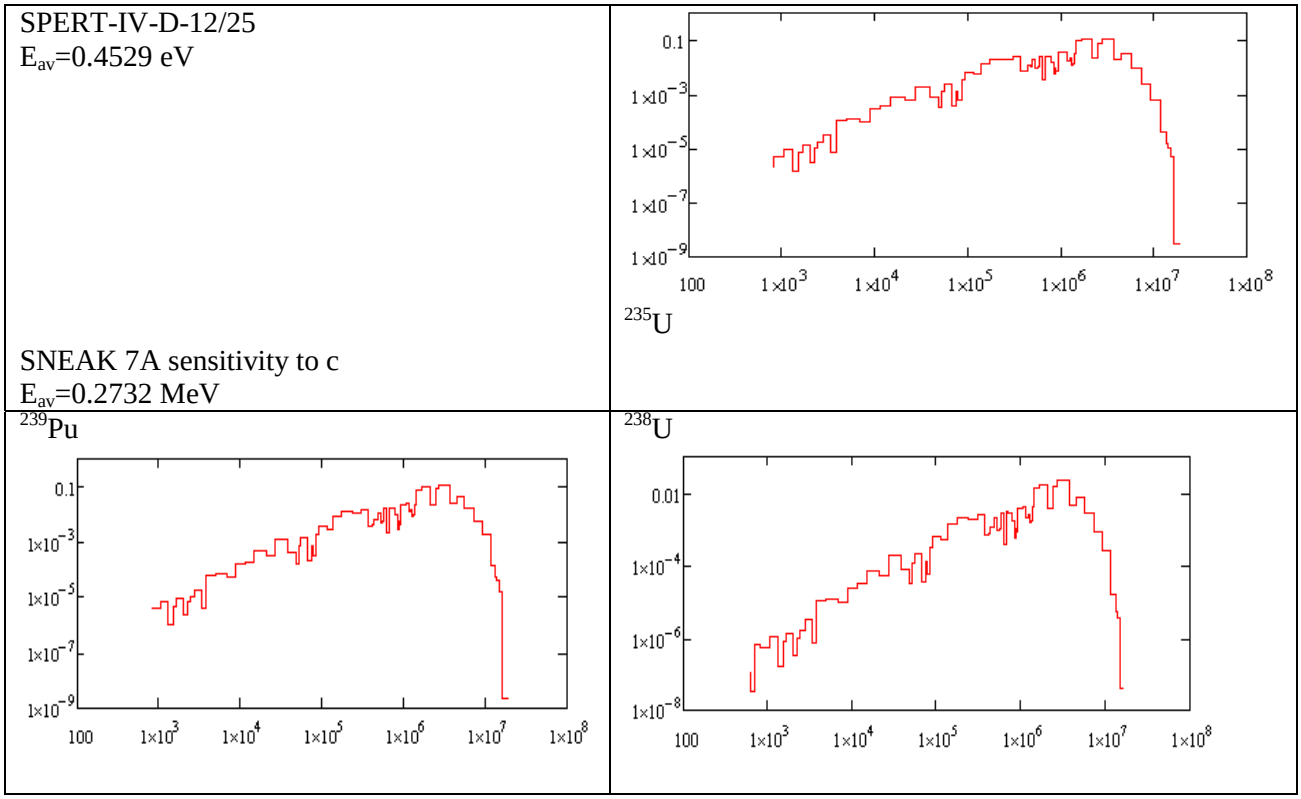

Equation (A.23) is reduced when the uncertainties of the neutron cross-sections are presented in the form of covariance matrices. Finally, the following equation gives the algorithms for the error propagation:

$$d(\beta_{eff}) \approx \sum_m S_\chi^m \cdot \mathrm{cov}(\chi_m) \cdot S_\chi^m + \sum_m \left[\beta_{eff}^m\right]^2 \cdot S(m, \frac{f_m}{f}) \cdot \mathrm{cov}(\Sigma) \cdot S(m, \frac{f_m}{f}) \quad , \qquad \text{(A.24)}$$

where the notations are the same as given above.

The first (direct) part of uncertainty is calculated easily as a dot product of sensitivities and co-variances (see in the table below).

The second part of formula was implemented only for the SNEAK 7A case because the GPT calculations were elaborated only for it. The following table demonstrates the major fission balance contributors in the effective delayed neutron fraction.

Table A.4: Effective delayed neutron fraction uncertainty by variations of fission spectra, %

Case	^{239}Pu	^{238}U	Σ
SNEAK 7A	3.93	1.11	2.0
SNEAK 7B	5.68	1.53	2.5

Table A.5: Effective delayed neutron fraction uncertainty by variations of fission balance, %

Reaction	^{238}U	^{239}Pu
Capture	0.45%	0.40%
Fission	1.90%	2.42%

Table A.6 contains the evaluated integral parameters of kinetic parameters calculations' uncertainties due to the available neutron data. The evaluations have been performed by the algorithms explained above on the basis of JENDL 4 [61] covariance data for major nuclides and reactions. The fission spectra uncertainties have been taken from the SCALE 5.1 44 groups' libraries but they were reprocessed in order to assure their consistency [44].

Table A.6: Benchmark data and expected due to cross-section errors

Parameters	SNEAK	SNEAK 7B
Λ, μs	0.180	0.159
Λ, expected uncertainty	4.15%	3.21%
β	0.00395	0.00429
β, expected uncertainty number	2.4%	2.5%(direct)

It should be noted that the first attempt of an error propagation technique has not been verified completely and there appeared some discrepancies between two alternative approaches in the effective delayed neutron fraction studies. The objective is to encourage further detailed analysis of the algorithms and of initial data.

Sensitivity and uncertainty in beta-effective-alternative approach [62][12]

According to the definition, the effective delayed neutron fraction (β_{eff}) is given by:

$$\beta_{eff} = \frac{P_{d,eff}}{P_{eff}} \qquad \text{(A.25)}$$

where:

$$P_{d,eff} = \int \Phi^{+}(\vec{r},E',\Omega')\chi_d(E')dE'd\Omega'\int \nu_d(E)\Sigma_f(\vec{r},E)\Phi(\vec{r},E,\Omega)dEd\Omega d\vec{r}$$

$$P_{eff} = \int \Phi^{+}(\vec{r},E',\Omega')\chi(E')dE'd\Omega'\int \nu(E)\Sigma_f(\vec{r},E)\Phi(\vec{r},E,\Omega)dEd\Omega d\vec{r}$$

and Φ and Φ^{+} are the direct and adjoint angular fluxes, Σ_f fission cross-section, χ_d, χ the fission spectra (delayed and total), ν_d, ν are delayed and total nu-bar.

In the SUSD3D code the sensitivity with respect to the prompt and delayed nu-bar are calculated as:

[12] Text prepared by I. Kodeli, IJS

$$S_{\nu_p}(E)=\frac{1}{R}\int d\vec{r}\int d\vec{\Omega}\left[\int d\vec{\Omega}'\int dE'\cdot\Phi(\vec{r},\vec{\Omega},E)\cdot\Phi^{*}(\vec{r},\vec{\Omega}',E')\chi_p(E')\nu_p(E)\sigma_f^i(E)N^i(\vec{r})\right]$$

$$S_{\nu_d}(E)=\frac{1}{R}\int d\vec{r}\int d\vec{\Omega}\left[\int d\vec{\Omega}'\int dE'\cdot\Phi(\vec{r},\vec{\Omega},E)\cdot\Phi^{*}(\vec{r},\vec{\Omega}',E')\chi_d(E')\nu_d(E)\sigma_f^i(E)N^i(\vec{r})\right]$$

Beta-effective values can be therefore obtained using the SUSD3D code as a ratio of the two sensitivity terms:

$$\beta_{eff}=\frac{\int S_{\nu_d}(E)dE}{\int\left(S_{\nu_p}(E)+S_{\nu_d}(E)\right)dE} \qquad \text{(A.26)}$$

Calculation of the sensitivity of beta-effective

The sensitivity and the uncertainties in beta-effective were studied by A. Zukeran *et al*. [63]. Here a different approach is presented, based on the following formulation of the beta-effective given in [64] [65].

$$\beta_{eff}=1-\frac{k_p}{k} \qquad \text{(A.27)}$$

From this expression the corresponding sensitivities can be readily obtained as a (properly weighted) difference between two standard terms:

$$\frac{\sigma}{\beta_{eff}}\frac{\partial\beta_{eff}}{\partial\sigma}=\frac{\sigma}{\beta_{eff}}\left(-\frac{\partial k_p}{k\partial\sigma}+\frac{k_p\partial k}{k^2\partial\sigma}\right)=\frac{k_p}{k-k_p}\left(-\frac{\sigma}{k_p}\frac{\partial k_p}{\partial\sigma}+\frac{\sigma}{k}\frac{\partial k}{\partial\sigma}\right)=\frac{k_p}{k-k_p}\left(S_k-S_{kp}\right)$$

Or alternatively:

$$\frac{\sigma}{\beta_{eff}}\frac{\partial\beta_{eff}}{\partial\sigma}=\frac{k_p}{k\beta_{eff}}\left(S_k-S_{kp}\right) \qquad \text{(A.28)}$$

Example of results for sneak-7a

A utility programme was prepared to calculate the above sensitivities (A.28) from the two terms S_k and S_{kp} which were obtained using the SUSD3D code in a standard way. An example of the results for the SNEAK-7A benchmark is given in Table A.7. It can be seen that the highest sensitivities of β_{eff} are with respect to the delayed and prompt nu-bar, fission and inelastic cross-sections.

The final folding with the covariance matrices to determine the corresponding uncertainties was also done using the SUSD3D code. Two sets of covariance matrices were used, SCALE-6 data processed by the ANGELO code, and the JENDL-4 [60] data processed by the NJOY/ERRORR code. Note that the SCALE-6 library does not include the covariance data relative to the delayed nu-bar, which is of particular interest for these studies. No covariance information was found on the other hand on the delayed fission spectra in any library, which is expected to have an important contribution to the final uncertainty in β_{eff}. According to the above covariance data the main sources of uncertainty in β_{eff} are the uncertainty in delayed nu-bar (^{238}U and ^{239}Pu), inelastic scattering on ^{238}U and fission cross-sections.

The total uncertainty in β_{eff} (not taking into account the uncertainty in the delayed fission spectra) is about 3%.

Table A.7: Sensitivity in beta-eff relative to the nuclear data

Material	Sensitivity (%/%)						
	elastic	inelastic	(n,2n)	(n,f)	(n,γ)	ν_{del}	ν_{pmt}*
U-235	-4.51E-4	-1.69E-3		-3.77E-2	8.54E-4	7.82E-2	-3.96E-2
U-238	-2.44E-2	-1.74E-1	-2.23E-3	-1.30E-1	1.66E-2	4.61E-1	-1.02E-1
Pu-239	-5.12E-3	-1.27E-2		-6.97E-1	1.92E-2	3.56E-1	-7.61E-1
Pu-240	-5.79E-4	-1.19E-3		-2.06E-2	1.92E-3	1.22E-2	-2.16E-2
Pu-241	-4.36E-5			-7.54E-3	1.66E-4	9.34E-3	-8.23E-3
Pu-242				-7.40E-5	7.35E-6		-7.73E-5

Table A.8: SNEAK-7A - Uncertainty (in %) in β_{eff} based on the covariance data from the JENDL-4 evaluation

Total uncertainty is 2.9 %

Material	Uncertainty (%)								
	elastic	inelast.	(n,2n)	(n,f)	(n,γ)	ν_{del}	ν_{pmt}*	χ_p	Total
U-235				0.004	0.003	0.207	0.008	0.056	0.23
U-238	0.073	1.889	0.035	0.076	0.123	1.552	0.062	0.092	2.45
Pu-239	0.017			0.374	0.080	1.398	0.129	0.497	1.55
Pu-240		0.009		0.014	0.008	0.060	0.004		0.08
Pu-241				0.009		0.047	0.004		0.05
Pu-242									$2 \cdot 10^{-4}$

Table A.9: SNEAK-7A - Uncertainty (in %) in β_{eff} based on the covariance data from the SCALE-6 library

Total uncertainty is 3.3 %

Material	Uncertainty (%)								
	elastic	**inelast.**	**(n,2n)**	**(n,f)**	**(n,γ)**	**ν_{del}**	**ν_{pmt}***	**χ_p**	**Total**
U-235		0.010		0.015	0.019	No covariance data	0.006	0.036	0.03
U-238	0.049	3.205	0.022	0.068	0.036		0.122	0.152	3.18
Pu-239	0.025	0.242		0.273	0.108		0.345	0.396	0.51
Pu-240		0.017		0.012	0.003		0.056		0.06
Pu-241				0.007			0.002		0.01
Pu-242									$3 \cdot 10^{-4}$

* obtained using the covariances for ν_{tot}

Participants are requested to submit their results as tables following the format of Tables A.7 through A.9.

Appendix VIII: PWR Burn-up pin-cell benchmark

The general frame of the OECD LWR UAM benchmark consists of three phases with different exercises for each phase. In the Phase I (Neutronics Phase), the Exercise 1 (I-1) "Cell Physics" is focused on the derivation of the multi-group microscopic cross-section libraries.

Since the OECD LWR UAM benchmark establishes a framework for propagating cross-section uncertainties in LWR design and safety calculations, the objective of the extension of this Exercise I (I-1) - I-1b (Cell Burn-up Physics) - is to address the uncertainties in the *depletion calculation* due to the basic nuclear data as well as the impact of processing of nuclear and covariance data.

In the calculations of this exercise, the participants have to utilise their cross-section libraries and associated uncertainties. The SCALE-6.0 covariance library is the recommended source of cross-section uncertainties in short-term to be used and propagated in the OECD LWR UAM benchmark. However, covariance data becoming from other source of uncertainties together with evaluated nuclear data files can be used without any inconvenience. They can utilise their own Sensitivity/Uncertainty (S/U) tools to propagate cross-section uncertainties to calculate quantities of interest in nuclear analysis or the ones available at NEA/OECD.

The purpose of calculation I-1b Exercise is to evaluate criticality values, reactions and collapsed cross-sections, and nuclide concentrations computed as well as their uncertainties for depletion in a simple pin-cell model. The proposed fuel test is a typical fuel rod from the TMI-1 PWR, 15x15 assembly design.

The specification of this test problem is given in Table A.10. Geometry and material specifications are shown in Table A.11.

Table A.10: Hot Full Power (HFP) conditions for fuel pin-cell test problem

Fuel temperature (K)	900.0
Cladding temperature (K)	600.0
Moderator (coolant) temperature (K)	562.0
Moderator (coolant) density (g/cm^3)	0.7484
Reactor power (MWt)	2772.0
Total number of fuel assemblies in the reactor core	177
Number of fuel rods per fuel assembly	208
Active core length (mm)	3571.20

Table A.11: Configuration of pin-cell test problem

Unit cell pitch (mm)	14.427
Fuel pellet diameter (mm)	9.391
Fuel pellet material	UO_2
Fuel density (g/cm^3)	10.283
Fuel enrichment (w/o)	4.85
Cladding outside diameter (mm)	10.928
Cladding thickness (mm)	0.673
Cladding material	Zircaloy-4
Cladding density (g/cm^3)	6.55
Gap material	He
Moderator material	H_2O

Composition of Zircaloy-4, using natural concentrations, is given by: O (0.125%), Cr (0.10%), Fe (0.21%), Zr (98.115%), Sn (1.45%). The ^{234}U atom density is equal to 0.05 wt%.

Figure A.11: The Configuration of unit-cell

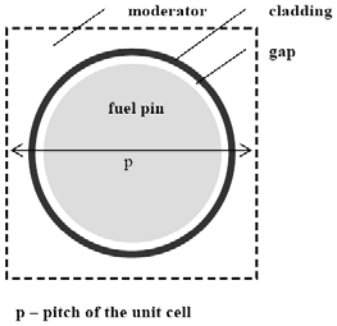

The linear fuel density (gU/cm) calculated according to values taken from Tables A.10 and A.11 is 6.2784 gU/cm. The average power density (W/gU) can be assumed to be equal to 33.58 W/gU. The fuel sample is burned for a unique complete cycle, the length of the burn time and subsequent cooling time is given in Table A.12. The specific power and the final cumulative burn-up is also given.

Table A.12: Simplified operating history data for benchmark problem pin-cell calculation and specific power

Operating cycle	1
Burn time (days)	1825.0
Final Burn-up (GWd/MTU)	61.28
Downtime (days)	1870.0
Specific power (kW/kgU)	25.00

Concerning boundary conditions, participants should apply the following type of boundary conditions in this case:

- For a "*cylindrical pin-cell*" model, reflective boundary conditions are utilised at the center-line boundary while white boundary conditions are applicable at the peripheries of the cell-model;
- For a "*square pin-cell*" model, reflective boundary conditions on all surfaces are applied.

This is shown in Table A.13 through Table A.15 for MCNP, TRITON and SERPENT codes, respectively. Tables A. 13, A.14 and A.15 provide three initial reference inputs. Participants are welcome to revise and modify these inputs. Note that the boron concentration is not considered in this exercise.

Table A.13: Initial MCNP input

```
PIN-CELL PWR ( UO2, 4.85 W/O U235)
c Cell structure
10 1 6.88299E-02   (-100 10 -20)         vol= 0.99928552  imp:n=1 $Fuel UO2
20 2 -1.000   (100 -110 10 -20)          vol= 0.192333    imp:n=1 $helium gap
30 3 -6.56     (110 -120 10 -20)         vol= 0.161535672 imp:n=1 $Zircaloy-4 Cladd
40 4 -0.7484  (30 -40 50 -60 120 10 -20) vol= 1.649657485 imp:n=1 $H2O
999 0 (-10:20:-30:40:-50:60)                               imp:n=0 $Void external universe

c Surfaces
*10  pz -0.72135
*20  pz 0.72135
*30  px -0.72135
*40  px 0.72135
*50  py -0.72135
*60  py 0.72135
100  cz 0.46955
110  cz 0.4791
120  cz 0.5464

c Isotopes
m1    8016.09c 6.66648E-01   $UO2
     92234.09c 1.69425E-04
     92235.09c 1.63641E-02
     92238.09c 3.16818E-01
m2    2004.06c  -1.000       $helium
m3   40000.06c -0.9823       $Zirc-4
     50000.06c -0.0145
     26000.06c -0.0021
     24000.06c -0.00100
     72000.06c -0.0001
m4    1001.06c -0.1119       $water
      8016.06c -0.8881
mt4   lwe7.10t
kcode 2000 1.0 100 1500
ksrc  0.0 0.0 0.0
prdmp 1500 1500 1500
print
```

Table A.14: TRITON/SCALE input

```
=t-depl parm=(nitawl,addnux=3)
Pin UAMPWR
'===============================================================================
44groupndf5
'===============================================================================
read composition
 uo2         10 den=10.283 1 900
                               92234 0.05
                               92235 4.85
                               92238 95.1   end
 zirc4       20 1 600   end
 h2o         30 den=0.7484 1 562 end
helium      40 1 900   end
end composition
'===============================================================================
read celldata
latticecell squarepitch hpitch=0.72135 30 fuelr=0.46955 10 gapr=0.4791 40 cladr=0.5464 20 end
end celldata
'===============================================================================
'===============================================================================
read depletion -10 end depletion
'===============================================================================
read burndata
   power=33.58179038 burn=30 down=0 nlib=1 end
end burndata
'===============================================================================
read model
Infinite-lattice pin model (one-fourth)
read parm
prtflux=no drawit=yes echo=yes
xnlib=4 run=yes collapse=yes prtmxsec=no prtbroad=yes
sn=4 inners=4 outers=200 epsilon=1e-4 epseigen=1e-3
end parm
read materials
10 1 ! test pin ! end
20 1 ! clad ! end
30 2 ! water ! end
40 0 ! gap ! end
end materials
read geom
global unit 1
cylinder 10 0.46955
cylinder 20 0.4791
cylinder 30 0.5464
cuboid 40  4p0.72135
media 10 1 10
media 40 1 20 -10
media 20 1 30 -20
media 30 1 40 -30
boundary 40 4 4
end geom
read bounds all=refl end bounds
end model
end
'===============================================================================
=shell
copy stdcmp_mix0010 %RTNDIR%\composicion_mix0010
end
```

Table A.15: SERPENT input

```
% --- Pin-cell burnup calculation ----------------------------

set title "Pin-cell burnup calculation"

% --- Pin definition:

pin 1
fuel   0.469550
void   0.479100
clad   0.546400
water

% --- Geometry:

surf 1  sqc 0.0 0.0 0.721350

cell 1  0  fill  1  -1
cell 2  0  outside   1

% --- Fuel (composition given in atomic densities):

mat fuel  -10.283  burn 1
92234.09c   -1.69425E-04
92235.09c   -1.63641E-02
92238.09c   -3.16818E-01
 8016.09c   -6.66648E-01

% --- Zircalloy cladding:

mat clad   -6.560
40000.06c  -0.9823
50000.06c  -0.0145
26000.06c  -0.0021
24000.06c  -0.0010
72000.06c  -0.0001

% --- Water (composition given in atomic densities):

mat water  -0.7484   moder lwtr 1001
 1001.06c   -0.1119
 8016.06c   -0.8881

% --- Thermal scattering data for light water:

therm lwtr lwj3.11t

% --- Cross section library file path:
% --- Cross section library file path:

set acelib "/xs/sss_jeff31u.xsdata"

% --- Periodic boundary condition:

set bc 3

% --- Group constant generation:

% universe = 0 (homogenization over all space)
% symmetry = 12
% 2-group structure (group boundary at 0.625 eV)

set gcu  0
set sym  12
set nfg  2  0.625E-6

% --- Neutron population and criticality cycles:

set pop 2000 500 20

% --- Geometry and mesh plots:

plot 3 500 500
mesh 3 500 500

% --- Decay and fission yield libraries:

set declib "/xs/sss_jeff31.dec"
set nfylib "/xs/sss_jeff31.nfy"
```

```
% --- Reduce energy grid size:

set egrid 5E-5 1E-9 15.0

% --- Cut-offs:

set fpcut   1E-6
set stabcut 1E-12

% --- Options for burnup calculation:

set bumode  2  % CRAM method
set pcc     1  % Predictor-corrector calculation on
set xscalc  2  % Cross sections from spectrum
set printm  0  % No material compositions

% --- Depletion steps:
% --- Depletion steps:

% Cycle 1

set powdens 25.00E-3
dep butot

0.10000
0.50000
1.00000
1.50000
2.00000
2.50000
3.00000
3.50000
4.00000
4.50000
5.00000
5.50000
6.00000
6.50000
7.00000
7.50000
8.00000
8.50000
9.00000
9.50000
10.00000
10.50000
11.00000
11.50000
12.00000
12.50000
13.00000
13.50000
14.00000
14.50000
15.00000
20.00000
25.00000
30.00000
35.00000
40.00000
45.00000
50.00000
55.00000
60.00000
61.28000

% --- Decay after fuel is removed from the reactor
dep decstep
365 % 1. year
365 % 2. year
365 % 3. year
365 % 4. year
365 % 5. year
365 % 6. year
365 % 7. year
365 % 8. year
365 % 9. year
365 % 10. year
3650 % 20. year
3650 % 30. year
3650 % 40. year
3650 % 50. year
```

```
3650 % 60. year
3650 % 70. year
3650 % 80. year
3650 % 90. year
3650 % 100. year
36500 % 200. year
36500 % 300. year

% --- Isotope list for inventory calculation:

set inventory
922330
922340
922350
922360
922380
932370
942380
942390
942400
942410
942420
952410
952430
962440
962460
420950
430990
441010
441060
451030
471090
551330
551340
551370
571390
581400
581420
581440
601420
601430
601450
621470
621480
621490
621500
621510
621520
621540
631510
631530
631540
631550
641540
641550
641560
641580

% -----------------------------------------------------------
```

Requested output
Participants are required to calculate the following results and associated uncertainties at these time-steps:

1	0 GWd/MTU
2	10 GWd/MTU
3	20 GWd/MTU
4	30 GWd/MTU
5	40 GWd/MTU
6	50 GWd/MTU
7	60 GWd/MTU
8	shutdown
9	1 year cooling time
10	3 years cooling time
11	5 years cooling time
12	10 years cooling time
13	50 years cooling time
14	100 years cooling time

Set 1: Criticality values

k_{inf}

In addition, participants are required to identify five nuclide reactions that contribute the most to the uncertainty in k_{inf}.

If it is possible, contribution of χ, ν and others (angular distributions, etc.) should be also reported.

Set 2: Reaction rates and collapsed cross-sections

Reaction rates and uncertainties for major isotopes:

- capture reaction rates for ^{235,238}U and ^{239,240,241}Pu
- fission reaction rates for ^{235,238}U and $^{239, 240,241}$Pu

In addition, a set of two-group macroscopic cross-sections and associated uncertainties for the homogenised pin-cell are required: absorption, fission, nu-fission cross-sections and diffusion coefficient.

Note: The thermal energy cut-off is $E_{thermal}$=0.625eV

Set 3: Number densities

Table A.16 gives a list of isotopes for which concentrations and associated uncertainties are requested.

Table A.16: Benchmark nuclides

Actinides (15)	Fission products (36)	
92 233	42 095	62 147
92 234	43 099	62 148
92 235	44 101	62 149
92 236	44 106	62 150
92 238	45 103	62 151
93 237	47 109	62 152
94 238	55 133	62 154
94 239	55 134	63 151
94 240	55 135	63 153
94 241	55 137	63 154
94 242	57 139	63 155
95 241	58 140	64 154
95 243	58 142	64 155
96 244	58 144	64 156
96 246	60 142	64 158
	60 143	64 160
	60 145	
	60 146	
	60 148	
	60 150	